Analytical approaches to the analysis of small samples

and

Hyphenation of fast capillary electrophoresis to other instrumental techniques

Dissertation

zur Erlangung des Doktorgrades der Naturwissenschaften (Dr. rer. nat.)

der Fakultät für Chemie und Pharmazie

der Universität Regensburg

vorgelegt von

Jonas Mark aus

Kohlberg

im Jahr 2014

Die vorgelegte Dissertation entstand in der Zeit von Juni 2010 bis April 2014 am Institut für Analytische Chemie, Chemo- und Biosensorik der naturwissenschaftlichen Fakultät IV- Chemie und Pharmazie - der Universität Regensburg.

Die Arbeit wurde angeleitet von: Prof. Dr. habil. Frank Michael-Matysik
Das Promotionsgesuch wurde eingereicht am: 11.06.2014

Termin des Kolloquiums: 17.07.2014

Dem Prüfungsausschuss saß Prof. Dr. Alkwin Slenczka vor. Erstgutachter war Prof. Dr. Frank-Michael Matysik, Zweitgutachter Prof. Dr. Otto S. Wolfbeis und Drittprüfer war PD Dr. habil. Richard Weihrich.

Ich möchte mich an dieser Stelle bei allen bedanken, die mich auf dem Wege zur Promotion unterstützt und begleitet haben.

I want to thank everyone involved in supporting and accompanying me on my way toward my doctorate.

" Wer a sagt, der muß nicht b sagen.
Er kann auch erkennen, daß a falsch war."[1]

[1] Bertholt Brecht (1898-1956), Ausgewählte Werke in sechs Bänden. Erster Band: Stücke 1. Frankfurt am Main: Suhrkamp Verlag, 1997 S. 317

Table of Contents

Curriculum vitae

Person

Full name	Jonas Mark
Date and place of birth	21st November 1984 in Weiden
Nationality	German
Spoken languages	German (native speaker), English (American University Diploma, Univ. of Kansas) Spanish (Certificado Linguistica, Univ. de Malaga) French (advanced)

Education

Degree / Occupation	Time Period	Institution
PhD	2010 – 2014	University of Regensburg Charles University Prague, CZ
American-German Dual Degree Bachelor of Science (DB.Sc)	2008 – 2009 2007 – 2008 2005 – 2007	University of Kansas, USA Universidad de Málaga, ESP University of Regensburg
Zivildienst / Civilian service	2004 – 2005	Notaufnahme Klinikum Weiden
Abitur	1995 – 2004	Kepler-Gymnasium Weiden

Scientific stays abroad

- Málaga, Spain: 8 months: Erasmus exchange at *Universidad de Málaga* during Bachelor's Program.
- Lawrence, Kansas, USA: 13 months, Atlantis exchange program at the University of Kansas (KU). Graduating to American-German Dual Bachelor's degree.
- Prague, Czech Republic: 2 months. Exchange with cooperating research group of Prof. Dr. F. Opekar at the Charles University in Prague.

Research experience

- Research assistant with Dr. Miguel Garcia in the group of Prof. Dr. Francisco Sarabia at the *Departamento de Quimica Organica* of the *Universidad de Málaga*. Research topics: Synthesis and characterization of Pirotenine.
- Research assistant with Prof. Dr. Susan Lunte at the Ralph N. Adams Institute of Bioanalytical Chemistry of the University of Kansas. Research Topics: Fabrication of microfluidic devices and electrochemical detection in combination with microchip electrophoresis.

Publications and Patents

Peer-reviewed Journal articles

Concepts and results described in this thesis have been published or are in submission in the following peer-reviewed journal articles. The patent is filed and in the application process.

Jonas Mark, Ashwini Kumar, Horst Demattio, Werner Hoffmann, Ashok Malik, Frank-Michael Matysik (2011) Combination of headspace single-drop microextraction, microchip electrophoresis and contactless conductivity detection for the determination of aliphatic amines in the biodegradation process of seafood samples. Electroanalysis 23:161–168

Jonas Mark, Pavel Coufal, Frantisek Opekar, Frank-Michael Matysik (2011) Comparison of the performance characteristics of two tubular contactless conductivity detectors with different dimensions and application in conjunction with HPLC. Anal Bioanal Chem 401:1669-1676

Jonas Mark, Rebekka Scholz, Frank-Michael Matysik (2012) Electrochemical methods in conjunction with capillary and microchip electrophoresis. J of Chromatogr A 1267:45–64

Jonas Mark, Paolo Piccinelli, Frank-Michael Matysik (2014) Very fast capillary electrophoresis with electrochemical detection for high-throughput analysis using short, vertically aligned capillaries. *Accepted* by Anal Bioanal Chem

Jonas Mark, Andrea Beutner, Marija Cindric, Frank-Michael Matysik (2014) Microanalytical study of sub-nanoliter sample volumes by capillary electrophoresis – mass spectrometry with 100% injection efficiency. *Submitted* to Microchimica Acta

Andrea Beutner, **Jonas Mark**, Sven Kochmann, Frank-Michael Matysik (2014) Comprehensive 2-dimensional ion chromatography – capillary electrophoresis with mass spectrometry detection. Manuscript *in preparation*.

Patents

Jonas Mark, Andrea Beutner, Sven Kochmann, Frank-Michael-Matysik (2014) Method and device for Two-Dimensional Separation of Ionic Species. European Patent EP 14 166 119.

Oral presentations

“Elektroanalytische Methoden in Verbindung mit elektromigrativen Trennverfahren“
Jonas Mark and Frank-Michael Matysik
Presented at the DECHEMA-Forum 2014 in Frankfurt/Main, Germany

„Instrumental aspects in CE - Fast CE with electrochemical detection”
Jonas Mark, Paolo Piccinelli and Frank-Michael Matysik
Presented at the GdCh Wissenschaftsforum 2013 in Darmstadt, Germany

“Combination of microchip electrophoresis, contactless conductivity detection and headspace single drop microextraction for the determination of aliphatic amines in seafood samples”
Jonas Mark, Ashwini Kumar and Frank-Michael Matysik
Presented at the International PhD Conference 2011 in Prague, Czech Republic

“Fast and efficient Microchip electrophoresis (MCE) with electrochemical detection”
Jonas Mark, Ashwini Kumar and Frank-Michael Matysik
Presented at Doktorandenkonferenz AK Separation Science 2011 in Hohenroda, Germany

Poster presentations

“Fast capillary electrophoresis in short, vertically aligned capillaries”
Jonas Mark, Paolo Piccinelli and Frank-Michael Matysik
Presented at CE-Forum 2013 in Jena, Germany

“Fast non-aqueous capillary electrophoresis in short capillaries with amperometric end-column detection”
Jonas Mark, Paolo Piccinelli and Frank-Michael Matysik
Presented at the ANAKON 2013 in Essen, Germany

“Fast capillary electrophoresis in short, vertically aligned capillaries”
Jonas Mark, Paolo Piccinelli and Frank-Michael Matysik
Presented at the Conference on Ion Analysis (CIA) 2013 in Berlin, Germany

“Combination of chip electrophoresis, contactless conductivity detection and headspace single drop microextraction for the determination of aliphatic amines in seafood samples”
Jonas Mark, Ashwini Kumar, Frank-Michael Matysik
Presented at the CE-Forum 2011 in Regensburg, Germany

“Microchip electrophoresis with contactless conductivity detection”
Jonas Mark, Frank-Michael Matysik
Presented at the Conference on Ion Analysis (CIA) 2011 in Berlin, Germany

Declaration of Collaborations

Most theoretical and experimental work presented in this thesis was carried out solely by the author. Some of the results, however, were obtained in collaboration with other researchers and individuals. In accordance with § 8 Abs. 1 Satz 2 Punkt 7 of the *Ordnung zum Erwerb des akademischen Grades eines Doktors der Naturwissenschaften (Dr. rer. nat.) an der Universität Regensburg vom 18. Juni 2009*, this section details the nature of these collaborations. This list is sorted by subject areas and states the sections to which each declaration refers in brackets.

Combination of Headspace Single-Drop Microextraction, Microchip Electrophoresis and Contactless Conductivity Detection for the Determination of Aliphatic Amines in the Biodegradation Process of Seafood Samples (section 5.1)

This experimental work was carried out solely by the author. Ashwini Kumar gave initial instruction, guidance and consultation on the methodology of single-drop-microextraction and the use of the microfluidic ChipGenie. The Chipgenie-prototype was given to our group by the developers Horst Demattio and Werner Hoffmann from Karlsruhe Institute of Technology.

Comparison of the performance characteristics of two tubular contactless conductivity detectors with different dimensions and application in conjunction with HPLC (section 5.2)

The experimental work was carried out solely by the author at the Institute of Analytical Chemistry of the Charles University in Prague under the supervision and guidance of Pavel Coufal and Frantisek Opekar. Model computations were done by Prof. Opekar.

Review article "Electrochemical methods in conjunction with capillary and microchip electrophoresis" (section 3.7)

The review was written under strict separation of the part written by the author and the other authors Frank-Michael Matysik and Rebekka Scholz. The author exclusively wrote and researched chapter 2 of the article. Chapter 1 was by Frank-Michael Matysik and for chapter 3 on "Hyphenation of Electrochemistry, CE and MS" was solely the co-author Rebekka Scholz responsible.

Very fast capillary electrophoresis with electrochemical detection for high-throughput analysis using short, vertically aligned capillaries (section 5.3)

The work was carried out in collaboration with Paolo Piccinelli from the University of Parma (Italy). The later method optimization with the already developed autosampling device and the application to projector pens, were done together. The actual development of the device and software was done by the author in collaboration with the mechanical and electronical workshops of the University of Regensburg. The glass parts of the electrochemical cell were produced by the glass workshop and the xy-positioner manufactured by the mechanical workshop.

Automated CE-MS (section 5.4)

This work was carried out in collaboration with Andrea Beutner. Automated CE-MS method development was done by Andrea Beutner within the scope of her research internship under the author's guidance.

Microanalytical study of sub-nanoliter sample volumes by capillary electrophoresis (section 5.5)

The experimental work on this project presented herein was solely carried out by the author, with one exception: the work on the sample pretreatment of mouse urine for real world application with the strategy of preconcentration by evaporation was done together with Andrea Beutner within the scope of her Master thesis. CE-MS method development for nucleotide compounds built upon previous method optimization by Marija Cindric.

Development of low-cost portable capillary electrophoresis apparatus with automated injection and dual electrochemical detection (section 9.1)

Initial mechanical and instrumental design, choice of components and materials, software requirements and planning of specifications and overall design were done by the author. Fabrication of the components was done by the mechanical workshop according to 3D-drawings of the author. The electrical components and circuit boards as well as software development were made by the electronical workshop under the author's guidance. All glass parts were provided by the glass workshop.

2-Dimensional IC-CE (section 5.6)

This work was done in collaboration with Sven Kochmann and Andrea Beutner. The author did the basic technical groundwork for coupling of the two methods on CE-side, the troubleshooting in the initial stages, method development and first successful IC x CE measurements. Same holds for Dr. Sven Kochmann on IC-side. Andrea Beutner joined the project and worked on the optimization of the method and also on the first successful IC x CE measurements of more complex mixtures presented within this work.

Abbreviations

AC	Alternating current
AgCl	Silver Chloride
AD	Amperometric detection
AMP	Adenosine monophosphate
BG1	Basic green 1
BGE	Background electrolyte
BV 16	Basic violet 16
cAMP	Cylcic adenosine monophosphate
CAPS	N-cyclohexyl-3-aminopropanesulfonic acid
CBI	Capillary batch injection
cCMP	Cyclic cytidine monophosphate
CD	Conductivity detection
C^4D	Capacitively coupled contactless conductivity detection
CE	Capillary electrophoresis
cGMP	cyclic guanosine monophosphate
CMP	Cytidine monophosphate
CV	Cyclic voltammetry
DC	Direct current
DEA	Diethylamine
DMA	Dimethylamine
DMSO	Dimethylsulfoxide
DVB	Divinylbenzene
ECD	Electrochemical detection
EOF	Electroosmotic flow
ESI	Electrospray ionization
FcMTMA	(Ferrocenylmethyl)trimethylammonium
GMP	Guanosine monophosphate
HDV	Hydrodynamic voltammogram
HFME	Hollow-fiber microextraction
His	Histidine
HS-SDME	Headspace single-drop microextraction
HPLC	High-pressure liquid chromatography
HV	High voltage

IC	Ion chromatography
ID	Inner diameter
ITP	Isotachophoresis
LC	Liquid chromatography
LIF	Laser-induced fluorescence
LOD	Limit of detection
LPME	Liquid phase microextraction
MA	Methylamine
MCE	Microchip electrophoresis
MEPS	Microextraction by packed sorbent
MES	2-(*N*-morpholino)ethanesulfonic acid
MinCE	Miniaturized chip electrophoresis
MS	Mass spectrometry
NACE	Non-aqueous capillary electrophoresis
NTC	Negative temperature coefficient
OD	Outer diameter
PDMS	Polydimethylsiloxane
PEEK	Polyether ether ketone
PMMA	(Poly methyl)methacrylate
ppm	Parts per million
Pt	Platinum
RE	Reference electrode
RSD	Relative standard deviation
SBSE	Stir-bar-sorptive extraction
SDME	Single-drop microextraction
SPE	Solid phase extraction
SPME	Solid phase microextraction
TAS	Total analysis system
TEA	Triethylamine
TMA	Trimethylamine
TRIS	Tris(hydroxymethyl)aminomethane
TOF-MS	Time-of-flight mass spectrometry
UV/VIS	Ultraviolet / visible light
WE	Working electrode

1. Introduction and Objectives

Two major trends could be noticed over the last decades in technology and the field of instrumental analytical chemistry. First of all, the desire for increasingly miniaturized analysis methods and equipment became evident. With progress in the downscaling of electronics and computer equipment other disciplines like chemistry soon followed [1]. The need to save resources and waste fewer reagents, materials and samples was a primary driving factor for this development. The concepts of fully miniaturized micro total-analysis-systems ("μTAS") or lab-on-a-chip devices envision the integration of various lab processes onto small-sized and portable devices [1]. Along with that comes the potential for the relocation of analytical measurements to *in-field* situations and the investigation of bioanalytical microenvironments such as mammalian cells [2]. Secondly, a rising interest towards automation and high-throughput capability of analytical methods and instruments became noticeable.

Central techniques for achieving the goals set within these movements toward miniaturization and automation are capillary electrophoresis (CE) and microchip electrophoresis (MCE) [3]. Both rely on a complementary separation principle compared to chromatographic techniques (LC). The appeal of electrophoretic techniques lies in their high separation efficiencies and capability for reaching short analysis times. However, whereas the full potential of high separation efficiency is certainly used in both modes and very fast MCE protocols were reported, to date most typically used conventional CE operations last at least 10 min or more [3]. This poses a problem when high-throughput screening or metabolomics / proteomics applications are sought after. On CE-side, a feature that is often neglected for speeding up the separation process is the actual capillary length. It was therefore one goal of this work to develop automated systems and methods based on short conventional capillaries that enable fast separation protocols for coupling CE to electrochemical detection (ECD), mass spectrometry (MS) or ion chromatography (IC).

Furthermore, the use of short separation pathways opens up the chance to create truly miniaturized and low-cost portable devices integrating various detection and injection strategies. In MCE, the use of short pathway microchannels in portable devices is already quite advanced and even reached the stage of commercial distribution [4, 5]. Indeed very small and portable devices, running totally independently from a mains power supply, have

been reported [6]. However, the overall analytical protocol usually required to perform a MCE separation cannot keep up with this high speed. Inadequate sample pretreatment and cumbersome preparation steps prolong the overall analysis time. In this work, approaches to implement better suited sample preparation techniques and speeding up MCE protocols were investigated. A further approach to tackle both challenges is the development of portable devices based on the well characterized surface chemistry of fused silica capillaries. This possibility came back into focus more recently [6, 7]. The capillaries can be easily modified in length and inner or outer diameter (ID / OD). The combination with easy-to-handle sampling units is implemented with more ease than for MCE. An additional objective of this work was the development and construction of a miniaturized CE device based on the fast separation capabilities of short pathway fused silica capillaries. It was planned to remedy some of the problems encountered with MCE, improve or complement existing portable CE devices, enable manifold detection and at the same time allow a critical first-hand comparison of the two techniques (MCE vs. CE).

Along with the progressing miniaturization of instrumentation comes the necessity to scale down the detection equipment as well as injection volumes and instruments. Well suited to miniaturization are the electrochemical detection modes like amperometric detection (AD) and capacitively coupled contactless conductivity detection (C^4D). In this work the coupling of highly sensitive AD with short-pathway CE to obtain highly efficient and very fast (< 5 s) separations of target species is presented. The technique of C^4D can be seen as an emerging but increasingly mature detection strategy for CE. Since its introduction in the late 90's of the 20^{th} century CE-C^4D has gained a lot of interest in the field of electroanalytical chemistry [8, 9]. It was a goal of this work to further investigate basic principles and potential benefits of C^4D usage for short-pathway CE and MCE. Studies concerned with the comparison of tubular and planar detection cell arrangements were undertaken as well as the application of MCE-C^4D to real-world samples.

The decreasing capillary lengths require the injection of very small sample volumes into the separation channel to conserve high separation efficiency and minimize band broadening. The traditional and to date most common injection concepts in CE are the electrokinetic and the hydrodynamic injection approach. In most commercial instruments these two modes are the predominant ways for introduction of sample into the capillary [10]. Typically utilized capillaries in CE have a length between 50 and 100 cm and inner diameters of 50 to 100 µm

[11]. Hence, the total volume of these capillaries ranges from 300 to 3000 nL and for injection plugs of 1% of the total volume, injection segments are between 3 and 30 nL. For some applications, requiring smaller ID capillaries [12-14] and shorter separation pathways [15-17], the injection volumes reach in the picoliter (pL) area. Interestingly, on the one hand, the injection volume introduced into the capillary is indeed very small. On the other hand, most commercial instruments that work with the above mentioned traditional injection modes need at least 50 µL of sample to perform the injection. This discrepancy has been critically reviewed recently and even though some homemade instruments were reported that work with volumes down to 10 µL [18], a significant mismatch of up to 3 to 5 orders of magnitude exists between the injected volume and the required sample volume to carry out the injection. Improvement of injection efficiency, as defined by the ratio of injected volume divided by required sample volume, is thus a goal for microanalytical CE determinations [19]. Apart from the trend towards green chemistry and the desire for lower reagent and sample consumption, the improvement in this area is especially relevant in cases of limited available sample. Examples include sub-cellular analysis [2] or the quantitative and repeatable measurement of limited biological fluids.

Various challenges arise from the use of very small sample volumes in the nano- or picoliter range for CE determination. Firstly, the quick evaporation of small sample amounts under room temperature conditions complicates the analysis. Secondly, the positioning of the capillary end into such small volume drops is tedious and requires special equipment. Thirdly, using flat polished capillary ends, the sample adsorption to the front-face of the capillary and its sidewalls prevents efficient measurements. A recent study showed that the geometric characteristics of the capillary tip play a crucial role for CE injections [20]. Reduction of available sample volumes pronounces these effects. Hence, it was a goal of this work to develop and construct a setup for conducting CE-MS measurements from ultrasmall sample volumes while at the same time using as short as possible separation pathways. A setup consisting of a lab-built capillary batch-injection (CBI) device [19], a thermoelectric device with cooling unit and corresponding temperature control device that enables freezing and unfreezing of very small sample volumes was developed. In combination with hair-sized sharp-tapered fused silica injection capillaries and the high-precision guiding system of the CBI-setup, handling and nearly 100% efficient injection of ultrasmall samples (down to 500 pL) into funnelled separation capillaries were enabled. The overall system was set up with the goal in mind to allow for high-throughput CE measurements from densely packed fields of

small sample drops or vials. The accomplishment of this goal lays the ground for the application of CE to the automated investigation of cell monolayers. Furthermore, by adding a microbalance to the setup, an approach to preconcentrate trace compounds by evaporation of the surrounding solvent of already small sample volumes was developed. [adapted from P5]

Often it can be a tough challenge to resolve the peaks within complex biological or environmental sample mixtures. In such instances, one individual separation technique alone does not offer high enough peak capacity. However, this problem can be solved by using 2-dimensional separation techniques. A study presented within this thesis reported the first-ever on-line coupling of CE-TOF-MS with ion chromatography (IC). This comprehensive (IC x CE) combination represents a totally novel approach to perform comprehensive 2-dimensional separations. It was found that very efficient separations of ionic analytes can be performed by coupling those two complementary strategies. The study had the goal of figuring out the technical details of the coupling and performing the very first IC x CE-MS measurements. The corresponding method optimization and results proving the potential of the technique for achievement of high peak capacities are presented herein. The new technique offers a plurality of benefits and was utilized to analyze charged molecules, like cyclic nucleotides, in a highly efficient way.

2. The author's Original Publications and Patents

Parts that were adapted from the author's publications / patents form the basis of the following chapters "Background" and "Results and Discussion" and in parts of the previous chapter "Introduction and objectives". The adapted text parts are indicated with [P1] – [P6]. This section lists the abstracts of the original publications.

[P1]

Combination of headspace single-drop microextraction, microchip electrophoresis and contactless conductivity detection for the determination of aliphatic amines in the biodegradation process of seafood samples

Jonas Mark, Ashwini Kumar, Horst Demattio, Werner Hoffmann, Ashok Malik, Frank-Michael Matysik

in *Electroanalysis* **2011** 23 (1): 161 – 168

Abstract

A new method for the efficient extraction and determination of volatile aliphatic amines by means of single-drop microextraction (SDME) in combination with microchip electrophoresis and contactless conductivity detection has been developed. An experimental approach for interfacing real world samples with chip electrophoresis is presented. The method consists of an optimized protocol for extraction via ultrasound assisted headspace SDME and the separation and determination of the target analytes with a novel microfluidic device. Five volatile, short-chained aliphatic amines, methylamine, dimethylamine, trimethylamine, diethylamine and triethylamine, were determined. The analytes were separated using a PMMA microchip with an 8.7 cm long separation channel and integrated thin-film gold electrodes for capacitively coupled contactless conductivity detection (C^4D). The determinations were carried out in a His/MES buffer (His/MES ratio of 80:20 at pH 6.6). Various parameters for the extraction and determination of the target analytes were optimized and applied to complex sample matrices like shrimp. The five analytes could be separated in less than 40 s applying a separation voltage of 3.8 kV. A linear concentration dependence was found within the range from 0.1 to 10 ppm for the ethylamine species and from 0.5 to 10 ppm for the methylamines. The limits of detection were all well below 400 ng/mL. The proposed method is simple, quick, presents low levels of waste, works with small sample quantities and is suitable to quantify aliphatic amines in seafood samples like shrimp or fish from where they are naturally developing upon biodegradation. In the present study the accelerated decay of shrimp tissue due to improper storage was monitored.

[P2]

Comparison of the performance characteristics of two tubular contactless conductivity detectors with different dimensions and application in conjunction with HPLC

Jonas Josef Peter Mark, Pavel Coufal, Frantisek Opekar, Frank-Michael Matysik

in *Analytical and Bioanalytical Chemistry* **2011** 401 (5): 1669-1676

Abstract

Two tubular capacitively coupled contactless conductivity detection (C^4D) cells with different geometric dimensions were evaluated with regard to their main analytical characteristics under non-separation and separation conditions in conjunction with liquid chromatography. A comparison of the performance of the tubular cells to a previously tested thin-layer detection cell was drawn. Additionally, using a theoretical model the experimental results were compared with sets of calculated values and partially enabled to model the complex behaviour of C^4D detection in combination with high-performance liquid chromatography (HPLC). While cell 1 is characterized by a geometric cell volume of 0.6 μL, a wall thickness of 675 μm, and an inner diameter of 125 μm, the respective values for cell 2 are 2.3 μL, 200 μm, and 250 μm. The main analytical parameters were evaluated using a potassium chloride (KCl) solution. The limits of detection were 0.4 μM KCl (5.7×10^{-6} S m−1) for cell 1 and 0.2 μM KCl (3.2×10^{-6} S m^{-1}) for cell 2, which compares well to the previously found 0.2 μM for the thin-layer cell. A pair of linear ranges was found for both cells in a concentration interval ranging from 1×10^{-6} to 1×10^{-4} M (corresponding to 1.5×10^{-5} to 1.5×10^{-3} S m^{-1}) KCl, respectively. Furthermore, the detector cells were applied to the HPLC separation of a model compound system consisting of benzoic acid, lactic acid, octanesulphonic acid, and sodium capronate. Separation of the compounds was achieved with a Biospher PSI 100 C18 column using 60% aqueous acetonitrile mobile phase. Calibration curves for the examined model system were well correlated ($r^2>0.997$), and it was found that under separation conditions the arrangement with the lower cell volume (cell 1) yields higher sensitivity and respectively lower limits of detection for all model compounds. Compared with the thin-layer cell, the tubular cells show better overall performance in regard to the determined analytical characteristics.

[P3]

Electrochemical methods in conjunction with capillary and microchip electrophoresis

Jonas Mark, Rebekka Scholz, Frank-Michael Matysik

in *Journal of Chromatography A* **2012** 1267: 45–64

Abstract

Electromigrative techniques such as capillary and microchip electrophoresis (CE and MCE) are inherently associated with various electrochemical phenomena. The electrolytic processes occurring in the buffer reservoirs have to be considered for a proper design of miniaturized electrophoretic systems and a suitable selection of buffer composition. In addition, the control of the electroosmotic flow plays a crucial role for the optimization of CE / MCE separations. Electroanalytical methods have significant importance in the field of detection in conjunction with CE / MCE. At present, amperometric detection and contactless conductivity detection are the predominating electrochemical detection methods for CE / MCE. This paper reviews the most recent trends in the field of electrochemical detection coupled to CE / MCE. The emphasis is on methodical developments and new applications that have been published over the past five years. A rather new way for the implementation of electrochemical methods into CE systems is the concept of electrochemically assisted injection which involves the electrochemical conversions of analytes during the injection step. This approach is particularly attractive in hyphenation to mass spectrometry as it widens the range of CE-MS applications. An overview of recent developments of electrochemically assisted injection coupled to CE is presented.

[P4]

Very fast capillary electrophoresis with electrochemical detection for high-throughput analysis using short, vertically aligned capillaries

Jonas Mark, Paolo Piccinelli, Frank-Michael Matysik

accepted in *Analytical and Bioanalytical Chemistry*

Abstract

We report an approach to conducting fast and efficient capillary electrophoresis (CE) measurements based on short fused silica separation capillaries in vertical alignment. Due to this special setup, the presented method enables for high-throughput analysis from small sample vials as for example from low-µL or even nL-titer plates. The system used in this study consists of a laboratory-made miniaturized autosampling unit and an electrochemical detection cell equipped with vertically aligned fused silica capillaries. The device enables a throughput of up to 200 electrophoretic separations per hour and hence a variety of samples can be analysed using minimal volumes. Due to the space-saving nature of the method it is ideally suited for applying it to the construction of truly-portable high-throughput CE-devices. Furthermore, CE separations with amperometric detection (AD) of a dye model system in capillaries of only 4 to 7.5 cm length with IDs of 10 or 15 µm could be carried out under conditions of very high electric field strengths (3.0 kV/cm) with high separation efficiency (half peak widths below 0.2 s) in less than 3 s migration time. A non-aqueous background electrolyte, consisting of ammonium acetate and acetic acid in pure acetonitrile, was used throughout the study. In this report a description of method specifications as well as details to the systematic optimization of parameters influencing the system are presented. In addition, the practical suitability of the system was evaluated by applying it to the determination of dyes in overhead projector pens

[P5]

Microanalytical study of sub-nanoliter sample volumes by capillary electrophoresis with 100% injection efficiency

Jonas Mark, Andrea Beutner, Marija Cindric, Frank-Michael Matysik

submitted to *Microchimica Acta*

Abstract

A methodology for conducting fast capillary electrophoresis (CE) from ultrasmall sample volumes (less than 10 nL) and subsequent detection of target analytes with time-of-flight mass spectrometry (TOF-MS) is presented. Furthermore, an approach to preconcentrate trace compounds by solvent evaporation of already small sample volumes is shown. Ultrasmall sample volumes of biologically important cyclic nucleotides (cyclic guanosine monophosphate, cyclic adenosine monophosphate, cyclic cytidine monophosphate) served as model compounds for CE-TOF-MS studies. Sample volumes of down to 500 pL were used to perform sample uptake and CE injections by capillary batch injection (CBI). For this protocol absolute limits of detection between 2 x 10^{-15} mol and 5 x 10^{-15} mol were obtained. The fast rate of sample evaporation prevents the operation of nano- / subnano-liter samples under room temperature conditions. A CBI-CE-TOF-MS setup that integrates a Peltier element and a corresponding temperature control device were used to enable freezing and unfreezing of very small samples. In combination with tapered fused silica injection capillaries and the high-precision guiding system of the CBI setup, nearly 100% efficient injection of ultrasmall samples into funnelled separation capillaries could be managed. The overall system allowed for high-throughput CE measurements from densely arranged sample droplets or vials with RSD of peak heights of 6 to 8 (n=5). In addition to that, CE-TOF-MS separations of mixtures of cyclic nucleotides were carried out in capillaries as short as 20 cm (25 µm ID) in less than 55 seconds with high separation efficiency. Herein, we report on the details of the setup and the optimization procedures in regard to the etching of capillaries (tapering and funnelling), sample uptake and injection of sub-nanoliter volumes as well as separation of the bioanalytically relevant compounds. Moreover, the capabilities of the experimental setup for preconcentration of target analytes by solvent evaporation are described. Preconcentration factors (PF) of up to 100 could be achieved for aqueous model samples containing cyclic nucleotides. This approach was successfully transferred to human urine samples.

[P6]

Method and device for Two-Dimensional Separation of Ionic Species

Jonas Mark, Andrea Beutner, Sven Kochmann, Frank-Michael Matysik

European Patent EP 14 166 119.9

Summary of the invention

The presented invention provides an improved method of separating ionic species and a device for use of such a method. It was surprisingly found that a highly efficient separation of ionic species is possible by coupling ion chromatography (IC) and capillary electrophoresis (CE) using a modulator as defined in the claims. The IC x CE method of the present invention is a two-dimensional separation system that allows a high orthogonality for ion separation and represents a very attractive new technology in the field of separation science. It was found that a combination of IC with retention times that are typically in the range of 5 - 30 minutes, with a CE system is possible when using the specific modulator providing a sequential injection of small volume segments in the nanoliter range into the CE system at time intervals of a few seconds. The devices and methods of the present invention allow continuous operation, i.e. IC can be coupled to CE on-line, which means that both separation methods can be operated without interruption of the basic setup. This was accomplished by the modulators of the invention used to control the transfer of the IC carrier flow to the CE system. The new system offers many advantages and can be used to separate charged molecules, like mixtures of cyclic and linear nucleotides, in an efficient manner. The method of the present invention uses IC in the first dimension and CE in the second dimension. Both methods per se are well-known in the field and the known methods and devices can be used in common manner and the optimal conditions can be found based on the species to be analyzed.

3. Background

3.1 Capillary electrophoresis

3.1.1 Basic principles

One fundamental characteristic of capillary electrophoresis (CE) is the simple instrumentation that is required to carry out measurements. The respective ends of an electrolyte-filled fused silica capillary are put into buffer reservoirs and a high voltage is applied between them. Sample is usually loaded onto the capillary by exchanging the inlet reservoir with a sample vial. A detection unit is placed at the other end of the capillary. In Figure 1 an overview of the basic scheme for CE operation is given.

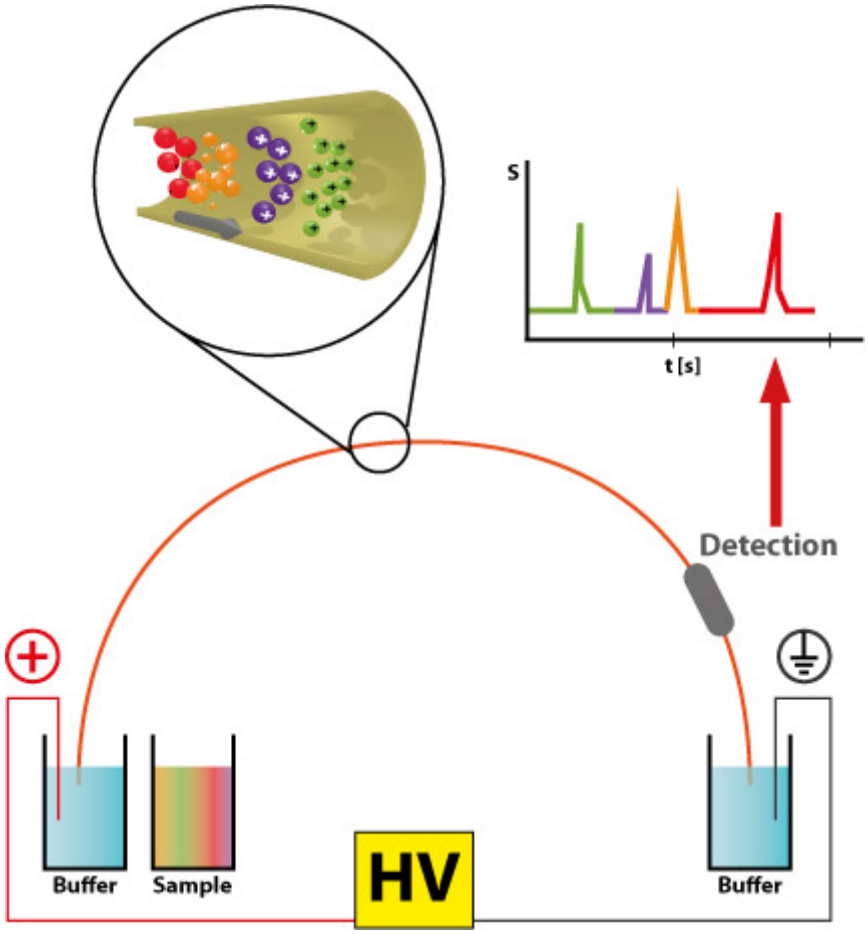

Figure 1. Basic scheme of capillary electrophoresis procedure. The capillary is immersed in an outlet and inlet buffer reservoir connected via a high voltage source. The zoom-in shows a schematic of the separation of differently charged species within the capillary. After detection the data is processed to give an electropherogram (upper right corner).

In CE, separation is achieved in narrow-bore capillaries based on the different solute velocities in an electric field. Essential requirement for an electrophoretic separation to occur is a net charge of the analyte under the given separation conditions. The velocity (*v*) at which a charged species migrates through the capillary depends on its electrophoretic mobility (μ_{el}) and the applied electric field (E).

$$v = \mu_{el} E$$

An ion in a specific medium has a characteristic mobility. The mobility depends on the electrical force that is influencing the respective ion and the frictional force in that medium. The first force is described by

$$F_{El} = qE$$

with q being the charge. The latter force (for a spherical ion) is represented by Stoke's law

$$F_{Fricl} = -6\pi\eta r v$$

with η as the solution viscosity and *r* being the ion radius in the given separation medium. Hence, after solving for *v* and then μ, the following term for electrophoretic mobility is obtained:

$$\mu_{el} = \frac{q}{6\pi\eta r}$$

It becomes clear that small and highly charged analytes possess the highest mobility values. The electrophoretic mobility is usually determined at full solute charge (α=1). This value can differ significantly from experimentally determined mobility values. Therefore the effective mobility

$$\mu_{eff} = \alpha\mu$$

is a critical factor in method development for closely migrating analytes.

A fundamental effect influencing analyte migration in CE is the electroosmotic flow (EOF). EOF is the bulk flow of liquid inside narrow-bore capillaries and is superimposed on the analytes' electrophoretic migration. The silanol (SiOH) groups of the fused silica surface become deprotonated at about pH 4. This means the interior walls of the capillaries usually

carry a surface charge under aqueous conditions. In accordance with the law of electroneutrality, layers of oppositely charged ions (solvated cations) form an electrochemical double layer very close to the interior wall. This double layer causes a potential difference, the so-termed zeta (ζ)-potential. Upon application of an electric field, a bulk flow of the solution inside the capillary towards the cathode (or in general the oppositely charged electrode) is initiated. The EOF causes a flat flow velocity profile. This is beneficial regarding separation efficiency compared to parabolic profiles which are caused by application of pressure in typical chromatographic applications. Since the zeta-potential is determined by the surface charge of the wall, it is strongly dependent on the pH of the solution. From this follows that the EOF increases under conditions of high pH as more silanol groups are deprotonated (SiO^-). As the EOF flow velocity is typically greater than the electrophoretic mobility of the charged species, even the anions migrate towards the capillary outlet and can be detected. An EOF marker, meaning a neutral species under the separation conditions, is typically added to a sample solution. The EOF can be modified by variations of pH, ionic strength and temperature or also by addition of organic modifiers or the usage of a completely non-aqueous background electrolyte. The latter is termed non-aqueous capillary electrophoresis (NACE). Apart from causing different EOF properties, the use of non-aqueous electrolytes has a number of benefits: water-insoluble compounds can be determined electrophoretically [21]. Moreover, especially acetonitrile as solvent is highly suitable for CE measurements with electrochemical detection. It offers a wide potential window (up to 6 V) and low background conductivity [22]. A variety of further literature on the CE theory introduced herein, CE instrumentation, techniques and applications is available [10, 11, 23-25].

3.1.2 Microchip electrophoresis (MCE)

Since its introduction by Manz et al. the microchip electrophoresis format has become one of the most used strategies for development of lab-on-chip devices [26, 27]. The intrinsic advantages of the technique are its low consumption of reagent and sample volumes, potential for high-throughput of samples and the possibility for development of portable devices [28]. The miniaturization of CE into the microchip format requires an injection and a separation channel connected to adequate reservoirs of sample and electrolyte solution. The most common methods to fabricate these channels for microchip electrophoresis are photolithography or micromolding techniques [29]. Typically electrophoresis microchips are made from glass, PDMS, PMMA or hybrids of glass and PDMS [30]. The advantages of the polymeric alternatives compared to glass are the significantly lower costs and the simpler fabrication process. It has to be kept in mind, that the EOF is typically much lower for the polymeric alternatives as compared to glass chips [29]. Usually chips are equipped with separation channels of 10 to 100 µm width and lengths of 3 to 40 cm [31]. As in conventional CE, liquid movement on the separation pathway is initiated via high voltage application. A major difference to CE lies in the injection concepts used. The most common formats are the electrokinetic non-pinched, pinched and gated injection [29, 31]. Apart from the laser induced fluorescence detection (LIF), the electrochemical detection modes are perfectly suited to the microchip format as electrodes and circuitry can be manufactured using the same types of photolithographic procedures used for channel fabrication [28]. Planar electrodes or electrode networks can hence be created with comparative ease onto the glass or polymer substrates. The by far most common electrochemical modes for MCE detection are amperometry and C^4D with planar electrodes outside the microchannel [31]. The benefits and challenges of coupling MCE to electrochemical detection modes are described in section 3.7.2. Even though MCE is regarded as an emerging technology compared to traditional CE, already numerous review articles and monographs describe further details on the technology [28, 29, 32-34].

3.1.3 Fast capillary electrophoresis

Since its instrumental introduction over 30 years ago, capillary electrophoresis (CE) has become an attractive and versatile separation method [35]. At the time of its introduction, some of the benefits CE possessed over the complementary HPLC methodology were the easy setup, use of cost-efficient silica capillaries and faster separation protocols. However, the speed of separation for (U)HPLC drastically improved in recent years, with separations carried out in a matter of only a few minutes [36]. The typical CE separation protocols last about 10 to 30 min [3]. In order to keep up with the enhanced speed of novel HPLC systems, new strategies for CE have to be developed and implemented. Most importantly, there is an increasing demand for high-throughput capabilities in conjunction with applications where substantially shorter separation times are essential. For example the monitoring of reaction kinetics and metabolomics are fields where fast separations are needed. Short pathway CE enables for the very fast, precise and cost-efficient analysis of a variety of samples [15]. A popular approach for using short separation pathways are the chip-based systems [37, 38]. However, contemplating the whole analytical process, these systems have a number of disadvantages. The sample preparation, handling of surface chemistry, loading of sample and buffer onto the chip, flushing of the chip and change of sample solutions are more cumbersome as with conventional CE-instrumentation. In contrast to that, the typical CE fused-silica capillaries of varying inner diameters (usually ranging from 2 to 100 µm) have been in steady use for decades and their surface properties are well studied [6]. One of the first works to couple amperometric detection with short capillaries to enable sub-minute separations was done in 1996 [39]. In this study a 5.5 cm long capillary with amperometric on-capillary detection was used to separate dopamine and hydroquinone in about 20 s. Speeding up CE separations by reducing capillary length is a challenge due to the very low amounts of injected sample required for efficient separations. A variety of injection concepts to solve this problem and systems using short capillaries in horizontal alignment were presented in the recent past [15, 19, 40, 41]. Zhang et al. [20] presented a system in which spontaneous injection into tapered capillaries resulted in very low volume (pL-range) injection into an automated high-speed CE setup. However, whilst enabling high-throughput of samples and efficient separations, this approach uses fluorescence detection, which could be a limitation for some applications. Wang et al. [42] developed a micro-electrophoresis system based on short capillaries which injects via hydrostatic pressure from slotted vials.

While this approach allows for automation and fast separations, managing high-throughput applications poses a potential problem. [partially adapted from P4]

3.1.4 Portable CE

The in-field application of portable CE instrumentation is of importance when immediate result acquirement, instable or hardly transportable samples and unavailability of benchtop devices are an issue [43]. The main requirements for a mobile CE or microchip CE instrument are small overall dimensions, low weight, vigorous construction, easy handling and as low as possible power consumption [6, 7]. Furthermore, the intrinsic advantages of CE play an important role. CE uses low sample and reagent volumes, is based on a simple basic separation setup and most parts can be easily exchanged. In addition to that, highly efficient separations even on very short pathways are possible [15]. In a portable system many of the common features of commercial instruments need modification or must be handled in a novel way. A challenge poses the implementation of a suitable detection unit. Typical CE detection strategies like UV/VIS absorption or (laser induced) fluorescence (LIF) detection cannot be implemented with ease [7]. The high power requirement of the required light sources is a potential problem for mobile devices and furthermore substances lacking a chromophore or fluorescent moiety are not suited for these detectors. Prime candidates for miniaturization are the various electrochemical detection modes, namely potentiometric, amperometric and conductometric detection. The potentiometric detection is ideally implemented in cases where high selectivity for a specific target is required and it has been used in a few portable devices [6, 7]. Amperometric detection is applicable to most electroactive species and thus many bioanalytically relevant species come into focus. Selectivity can be achieved via the regulation of the applied detection potential. Furthermore, it offers limits of detection that reach close to the ones achievable with LIF detection [11]. Many microchip or capillary based portable CE devices utilize AD as stand-alone detection mode or in combination with other detection modes. One of the first portable devices used AD in combination with potentiometric detection [44, 45]. The group that constructed this device later added conductometric detection as third detection in a single portable unit [46]. The majority of recently developed mobile CE devices utilize C^4D detection as sole or participating detector [6, 47]. Other examples include systems using optical detectors and laser induced fluorescence (LIF) detection [48, 49]. One of the smallest devices developed so far based on MCE is a device of 7.6 x 5.7 x 3.8 cm with less than 240 g weight [50]. However, maximum

separation voltage in this device is only 154 V. A number of portable CE or MCE devices have entered the stage of commercial distribution. One of the first ones based on chip electrophoresis was the so-termed ChipGenie [4, 5]. The smallest portable CE to date, which is based on conventional capillaries, weighs about 6 kg. However, a usually needed external detection unit is not counted to that weight. A complete overview of fully portable CE devices can be gained from the reviews by Macka and Lewis [6, 7]. One feature that remains mostly unused in the so far developed devices is the possibility to shorten the separation pathway and allow for variation of capillary lengths in the low-cm range (1 to 10 cm).

3.1.5 Microextraction techniques combined with CE

In many microenvironments, the analytes of interest are present in low or trace concentrations compared to possible interferents or matrix components. Hence, preconcentration steps and sample pretreatment are mandatory for achieving reliable determinations. CE can be combined with numerous either solid- or liquid-based microextraction techniques [51]. A broad (but not complete) selection of typically used microextraction techniques combined with CE is given in the following Figure 2.

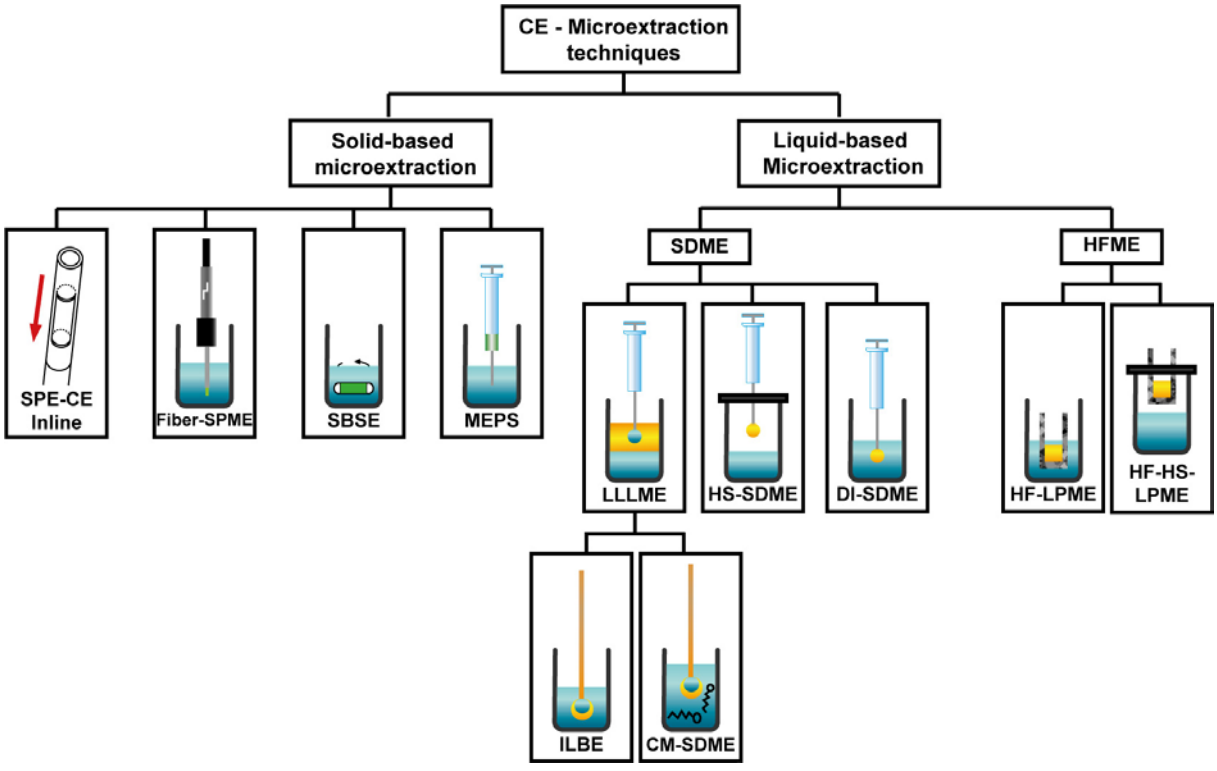

Figure 2. Selection of typical microextraction techniques combined with CE.

Developed from the experiences gained with traditional SPE, the technique of solid-phase microextraction (SPME) is receiving more and more interest [51]. A common method is the fiber-SPME, where a fiber coated with sorptive material (PDMS or PDMS/DVB) is exposed from a steel needle into the extraction solution [52]. A further approach is the stir-bar-sorptive extraction (SBSE), which was developed with the goal in mind to increase the amount of sorbent material exposed to the extraction solution [53]. A sorptive phase is coated onto a magnetic stir bar and immersed into the extractant fluid. A popular form of solid-based strategies is the microextraction by packed sorbent (MEPS) which consists of a usually 100 to 250 µL microsyringe containing up to 4 mg of a sorbent in a specifically integrated barrel [54, 55]. The technique works with volumes in the lower µL range (down to about 10 µL). MEPS has been used for a number of applications in conjunction with CE-MS and NACE-MS [56, 57]. A significant progress in terms of minaturization and sample throughput was the introduction of the on-line and in-line SPE-CE techniques. For in-line SPE-CE the sorbent material is directly integrated into the separation capillary. It has been used in various applications with CE-ESI-MS [58 - 60].

The liquid-based methods can be subdivided into single-drop microextraction (SDME) strategies and hollow-fiber microextraction techniques (HFME). In HFME a hollow polymeric fiber (often polypropylene with ID of 200 µm) acts as support material for the extraction analytes [61]. Two common forms are the hollow-fiber liquid phase microextraction (HF-LPME) and the headspace (HS-)HF-LPME [62, 63]. Frequently used are the techniques derived from SDME. The concept was introduced in the year 1997 by Jeannot and He [64, 65]. A 1 µL drop of n-octane hanging from microsyringe-tip was directly immersed into a stirred aqueous sample (see Figure 2, DI-SDME). SDME, however, often lacks in repeatability and has a low recovery rate. Furthermore, especially for CE, the drops have to be diluted again to obtain enough sample volume to perform an injection. In 2001 a concept aimed at extraction of volatile compounds was introduced and called headspace-single-drop microextraction (HS-SDME) [66]. In this setup a drop of liquid is exposed to the gaseous phase above the extraction solution. The advantages are that higher stirring rates can be applied and that interferences from non-volatile matrix constituents are drastically reduced. It has been used with CE and MCE in the past [67, 68]. A detailed scheme of the processes occurring during extraction of basic volatile amines is depicted in Figure 3.

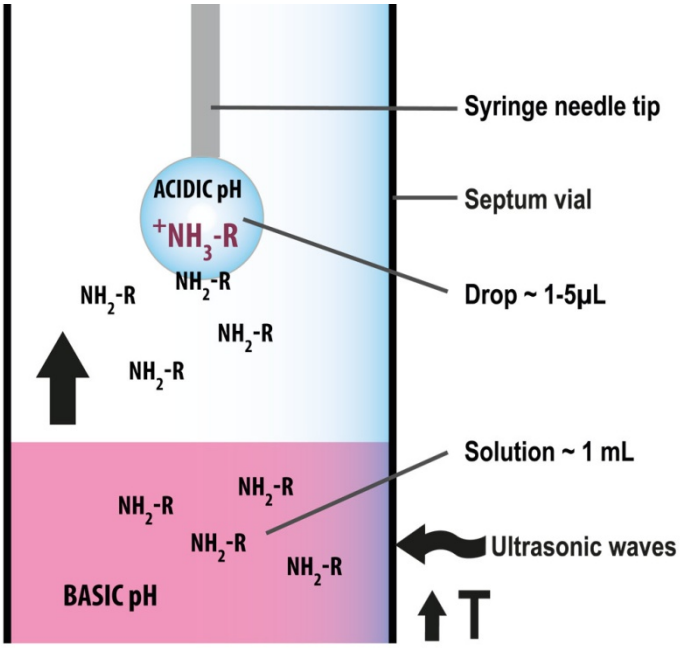

Figure 3. Scheme of HS-SDME principle for the extraction of volatile basic amines into a µL-drop (blue drop) suspended in the gaseous phase above the sample solution (pink) in the mL-range.

A recent study showed that liquid-based inline-back extraction (ILBE) reduces the volume of organic extractant to 13 nL [69]. Nevertheless, the actually needed sample volume is with 1.4 mL comparatively large. Other forms of single-drop techniques like carrier mediated SDME (CM-SDME), or directly suspended droplet microextraction (DSDME) also work with sample volumes not smaller than the µL-range [70, 71].

3.2 Injection concepts for CE

The introduction of sample is one of the most critical steps for CE instrumentation, especially when short separation capillaries (<20 cm) are utilized [72]. Besides the established methods of hydrodynamic and electrokinetic injection [11] a number of highly different, alternative methods has been proposed. These non-conventional approaches follow various goals: reduction of LOD, fast separations, online-sample preparation, reaction monitoring and minimization of injection volume [72]. In recent years, some studies addressed the use of shorter separation pathways and the corresponding reduction of the injection volume [15, 72, 73]. Nevertheless, although the reported approaches represent interesting ways to further minimize injection volumes and improve injection precision, they still require comparatively large amounts of initial sample [18]. Andrew Ewing's work with injection from single mammalian cells represents the lowest-volume approach to inject from small sample volumes into CE capillaries [74]. However, even though it represents an impressive milestone in CE bioanalysis, the methodology required dexterity, specialized equipment and capillaries with an ID of only 770 nanometers. Furthermore, it was not developed for the purpose of exchanging different samples and targeting samples other than single cells. Inside the cells the liquid is fixed in position and tightly closed against the environment (making evaporation a negligible issue). A further disadvantage of most alternative injection concepts is the limited compatibility with short capillary CE-MS measurements. [partially adapted from P5]

3.3 Capillary batch injection

An injection strategy for CE that is well-suited for coupling with ESI-MS and the usage of short capillaries is the so-termed capillary batch injection (CBI) [75, 76]. One end of an additional injection capillary is directed towards the inlet of the actual CE separation capillary. The other end of the injection capillary is connected to a microsyringe inside a micropump. Microprocessor control of the pump allows dispensing of well-defined amounts of sample volume from the injection capillary onto the separation capillary. The actual injection occurs in an electrolyte filled cell, either hydrodynamically or electrokinetically. Furthermore the approach allows the uptake of very small sample volumes and subsequent highly efficient injection into the CE system.

The ID of the injection capillary can be easily varied and a number of different capillary combinations tried in method development. As the separation capillary is spatially fixed and does not move during the injection process, the danger of air bubble introduction is drastically minimized compared to conventional injection procedures. CBI has been successfully employed for CE with electrochemical detection [77] and more recently for fast CE-MS applications [78, 79]. Capillaries as short as 15 cm, leading to migration times of less than 15 s for cationic species, have been utilized [19].

3.4 Mass spectrometry

3.4.1 General background

Mass spectrometry (MS) is a powerful tool for obtaining structural, quantitative and qualitative information on a broad range of substances. The main processes taking place in the mass spectrometer are the following: transfer into the gas phase and ionization of the analytes, separation of analytes according to their mass-to-charge (m/z) ratio in a mass analyzer and subsequent detection of the analytes. The primary mode of ionization used in this work (electrospray ionization) will be presented in the next section 3.4.2 in more detail. After ionization, the mass analyzer splits up the species in the order of their m/z ratios. The mass analyzer operates under high vacuum conditions. A number of different mass analyzers are available nowadays: ion trap, orbitrap, quadrupole, sector field and the time-of-flight (TOF) mass analyzer [80]. The latter is the preferential technique for the investigation of large biomolecules with high m/z-values and in cases where high mass precision is desired. For detection usually the individual m/z portions are counted upon their impact onto the detector. The principle behind the detection is the generation of secondary electrons initiated by the impact of the different analyte ions. Typical commercially available detectors are the dynode electron multiplier or multi channel electron multiplier [80]. The detector used in the course of the studies presented herein was an electron multiplication-based microchannel plate detection unit.

3.4.2 Electrospray ionization (ESI)

The electrospray ionization mode was the preferred technique used in the projects on CE-MS presented in this work. ESI represents a mild ionization mode with no or little fragmentation processes taking place [24]. The concept of the tri-axial sprayer has become the standard and most robust method to generate the electrospray needed for ionization [81]. In the sheath-flow-interface, the CE capillary is the most inner fluid channel. In the next layer / tube the sheath liquid is delivered and contact to the CE background electrolyte is established. The metallic tube delivering the sheath liquid is put to ground potential. The sheath liquid is fed to the interface from a pump at rates from typically 1 to 10 µL/min [24]. It does not only establish the electrical contact, but also facilitates the ion formation processes. The nebulizing gas (usually N_2) is fed through the third channel and supports stable spray generation. A detailed overview of the processes leading to spray formation in a tri-axial capillary sprayer is given in Figure 4.

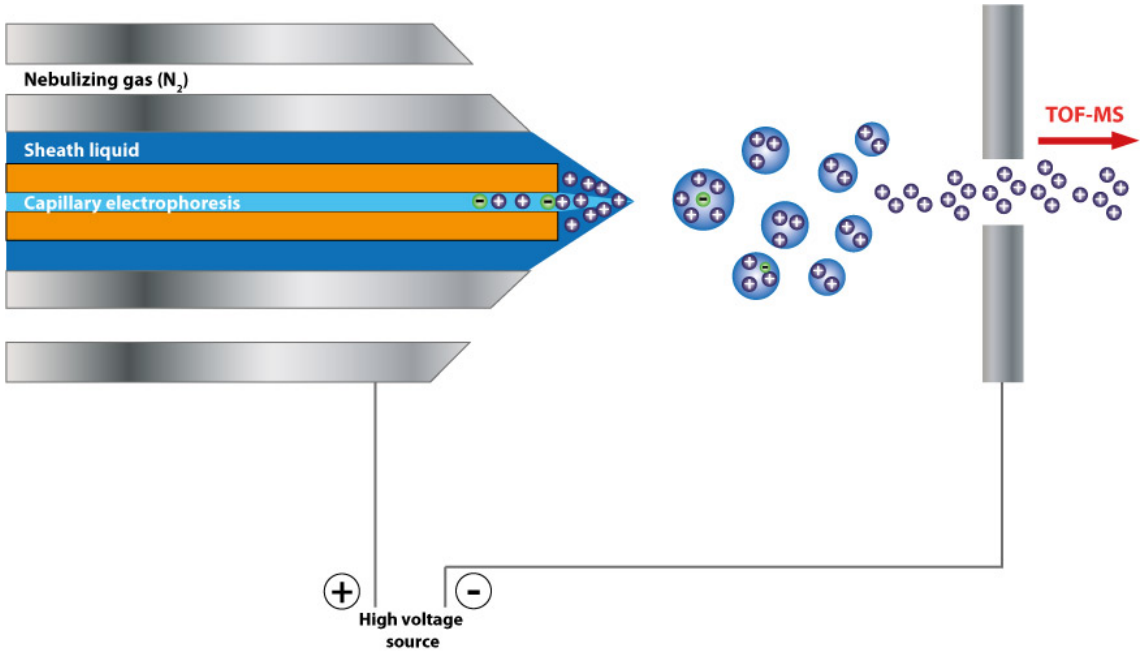

Figure 4. ESI-interface principle. Formation of Taylor cone and evolution of increasingly smaller droplets. At a certain point, when repulsion between ions is high enough, Coulomb explosions occur. This leaves individual ions for analysis in the mass spectrometer. The CE capillary, located in the center is protruding slightly and sheath liquid and nebulizing gas support in the formation of a stable spray while an ESI high-voltage is applied.

Under the influence of an applied high voltage between the sprayer tip and the aperture plate of the MS a Taylor cone is formed at the needle outlet. The resulting, rather large droplets leaving the tip carry an excessive surface charge. Under support of the heated drying gas streaming out from the MS device (see also Figure 5) the neutral solvent molecules quickly evaporate and surface charge rises even more. At a certain point Coulomb explosions occur, forming increasingly smaller droplets until gaseous ions are left [24]. They are guided into the inlet of the MS. The molecules can carry more than one charge and have a decreased m/z ratio which allows analysis within the limited mass window of the analyzers [82].

3.5 Hyphenation of CE and MS

The utilization of MS as detection system following CE separations has gained a lot of attention since the first reports on that technique emerged [83]. A significant challenge is the proper coupling of the two high voltage circuits involved. The electrical field applied in the CE system has to be effectively separated from the electrospray high-voltage inside the ESI chamber [82]. The electrophoretic currents generated in the CE capillary (µA to mA) can be several orders of magnitude higher than the ESI currents (~ nA). The possible danger with this arrangement lies in an eventual damage of the ESI power supply. One way to solve this problem is to use the sprayer needle as a common ground. To measure in the positive (negative) ion mode a negative (positive) ESI high voltage is applied to the aperture where ions enter the MS transfer capillary. A scheme of ESI-CE-MS with the respective electrical circuits is given in Figure 5.

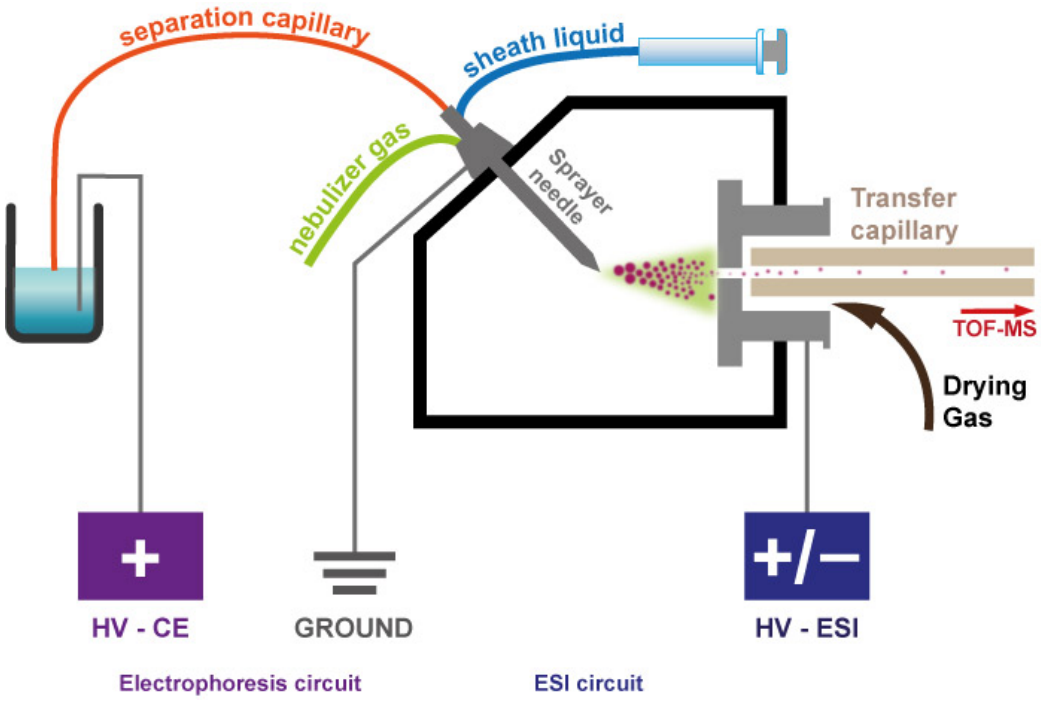

Figure 5. Scheme of the principal ESI-CE-MS setup used in this work.

The contact between capillary and sprayer needle tip can either be established with a conductive sheath liquid support (see section 3.4.2) or various sheathless approaches [82]. The background electrolytes employed for CE-ESI-MS operation should be volatile and not be prone to disturb ion formation processes. Often used buffers for CE combined with other detection modes are hence not suitable for CE-MS. Well-suited buffer types are formic acid, acetic acid and acetates.

3.6 Two-dimensional separation techniques

It is often a challenge to analyze complex bioanalytical or environmental sample probes. In cases where the peak capacity (defined as the number of resolved signals of the analytical separation in a specified time slot) of one-dimensional separation methods is not sufficient to resolve all substances, the multi- or two-dimensional (2D) approaches can help to analyze highly complex samples. The requirements for multi- or two-dimensionality are (1) different or even orthogonal separation mechanisms of the involved methods and (2) a conversion of all sample components from the first dimension separation to the next dimension. The aim is to use the orthogonality of different techniques or separation conditions to obtain more information on a specific analytical problem. Some efforts have been undertaken in the past to (comprehensively) couple separation methods. One example is the 2D-gel electrophoresis that has been for long a frequently used two-dimensional electrophoretic separation mode [84]. Two-dimensional separation systems involving CE in either one or both dimensions have been reported in the literature. Recently, the coupling of isotachophoresis (ITP) with CE-MS showed the potential of 2D-electrophoretic separations for applications in metabolomics and proteomics [85]. Another group reported on the coupling of UPLC with CE for the fast and time-efficient analysis of multifaceted peptide mixtures [86]. The probably most elaborate and important 2D-technique is the comprehensive GCxGC-coupling. Usually, a comparatively long apolar column is coupled to a short and narrow polar column. A suitable modulator handles the transfer of analytes between the 2 dimensions [87].

3.7 Electroanalytical chemistry

3.7.1 General principles

Amperometry

Amperometry is the application of a fixed potential to a working electrode in a solution of electroactive analytes. Upon reduction or oxidation of the species a concentration-dependent faradaic current is generated and measured over time (I-t curves) via a data acquisition system. The potential must be set to a value where the analytes of interest are oxidized or reduced. Usually, a three electrode setup consisting of working electrode (WE), reference electrode (RE) and counter electrode is used. A two-electrode setup without an additional counter electrode is applicable if the generated faradaic currents are rather small (below the microampere range) and hence the voltage drop between WE and RE remains small enough (around 1 mV or lower). The WE can be made from a variety of materials ranging from metals (Au, Ag or Cu) to boron-doped diamond or rods made from nanotubes [31]. The properties of the target analytes are usually the decisive factor in the choice of WE material. Via the RE potential, control of the system is enabled. In the ideal case a RE does not change its potential upon passage of a current. The counter electrode enables a current flow that is not passing through the RE. It is usually a stainless steel needle or platinum wire.

(Contactless) Conductivity detection

The principal characteristic of conductometric detection methods is the (almost) universal applicability to charged species. Basically, the conductivity in a certain solution volume between two electrodes is measured. It is either done in a contact or contactless mode. In direct contact mode the electrodes are immersed in the solution and hence disadvantageous effects like undesired redox reactions or gas bubble formation can take place [29]. In contactless mode the electrodes are well separated from the solution. In capacitively coupled contactless conductivity detection (C^4D) a dielectric layer (for example the capillary wall) enables the separation of charges and hence a capacitance is created. A high-frequency AC is applied to a receiver electrode and conductometric signals are recorded by the second pick-up electrode. Upon change of the conductivity between the two electrodes signal change is detected.

3.7.2 Electroanalytical methods in combination with capillary and microchip electrophoresis

Electroanalytical methods are important detection strategies for CE and MCE. Due to the small dimensions of CE and MCE, powerful detection schemes are required. At present, amperometric detection and contactless conductivity detection are the predominating electrochemical detection methods for CE / MCE [31].

Amperometric detection

A traditional field of electroanalytical chemistry is amperometric detection (AD) which was first applied in combination with CE by Ewing´s group in 1987 [88]. The main challenge of coupling CE or MCE with AD is to manage highly sensitive amperometric measurements in the presence of a high-voltage electrical field. There are two established concepts to perform CE / MCE – AD experiments. The first approach is "off-column" detection [31] involving an electrical-field decoupler near to the capillary end through which the electrophoretic current is led to ground. On the other hand, the "end-column" approach avoids the implementation of a decoupler and is based on the positioning of the sensing electrode close to the capillary / channel outlet [89]. The advantage of off-column mode is that analytes flow right over the electrode and no significant band broadening occurs. In end-column mode the zones have to flow over the gap outside the capillary and hence band broadening occurs. However, implementation and handling are much more facile than the off-column mode. A third mode that has been recently reported, specifically for MCE, is the in-channel approach which works with an isolated potentiostat and the electrode being placed right into the separation channel [31].[adapted from P3]

Capactively Coupled Contactless Conductivity Detection (C^4D)

In contrast to AD or direct contact conductivity detection, there is no direct contact between the sensing electrodes and the electrolyte solution inside the CE capillary. Thus, problems concerning interference of the high-voltage electrical field with the detection circuit and fouling of the electrodes can be eliminated [8]. The separation voltage is decoupled from the conductivity signal via the applied AC field. The BGE itself creates a background signal and the higher charged the BGE the higher is the background signal. This means that the choice of electrophoresis buffers is somewhat limited and has to meet a compromise between separation and detection aspects. Often used buffers for CE-C^4D are MES-His systems or

CAPS or TRIS [9]. The commercial availability of C^4D devices and the ease of implementation have greatly stimulated the widespread use of this detection mode. However, the limits of detection obtained on the basis of C^4D are usually not as low as for AD [24]. Whereas in C^4D for conventional capillaries the tubular electrode arrangement is most common, this approach is not suitable for chip applications. Therefore, mostly planar electrodes are utilized due to the more compatible fabrication process [10]. The C^4D electrodes are either placed externally to the device or they are directly integrated into the microchip or attached to it by placing it on top or below the device. The fabrication processes for the electrodes range from screen-printing approaches (for an example see [88]), metal evaporation techniques and photolithographic pattering to the utilization of aluminium foil strips or silver varnishes. [adapted from P3]

3.7.3 Applications of electroanalytical methods in CE

Amperometric detection

A number of applications for capillary electrophoresis with amperometric detection has been reported in the recent past. Coupling the capability of CE techniques to separate difficult samples with the selectivity of amperometric detection enables a system for a broad spectrum of analytical applications. Furthermore, the requirement of only low sample volumes is advantageous, as it makes single cell analysis, determination of small amounts of natural products and microdialysis possible. Most studies worked with the oxidative mode, as the reductive mode has the disadvantage of oxygen interference. CE-AD was successfully applied to carbohydrates, phenolic compounds, various drugs and pharmaceuticals, biogenic amines and amino acids. Traditionally, amperometric detection of amino acids was carried out by carbon and in fewer instances with amalgamated gold or copper electrodes. Various neurotransmitters were determined with novel, modified electrodes like boron-doped diamond [91] or enzyme modified electrodes [92]. A variety of textile dyes were determined by non-aqueous capillary electrophoresis (NACE) coupled with end-column amperometric detection [93]. Another ongoing trend is the drug-screening via CE-AD. Accordingly the active agents of many pharmaceutical formulations have been investigated and quantified by AD with different electrode materials. [94-99]. Carbohydrates are usually detected amperometrically with copper electrodes under basic conditions [100, 101].

The most common fields of application for MCE-AD have been in neurochemistry, environmental and food analysis as well as in biochemical studies. In the area of

neurochemistry the behaviour of neurotransmitters and nitric oxide and its degradation products have been studied [102-107]. The interest in the supervision of food materials and monitoring of explosive materials remains on a high level [108, 109].

Contactless Conductivity Detection

Traditionally, in CE applications, C^4D has been the typical detection mode for inorganic ions and other typically non-UV absorbing species. Using C^4D, not only the low-sensitivity indirect optical methods can be circumvented, but also the high differences between high-conductive inorganic ions and weakly conductive BGE's offer high sensitivity levels [110]. Recent bioanalytical examples include the determination of inorganic cations in bodily fluids like human saliva [111] and plasma, serum and whole blood [112]. The importance of C^4D for the detection of other species, such as organic ions, is increasing. However, one needs to keep in mind, that due to the lower charge-to-size ratios of organic ions sensitivity is somewhat reduced compared to the inorganic ion determination. The range of examined substance classes includes drugs, drugs of abuse, antibiotics, amino acids, clinically relevant species and carbohydrates / sugars [113-115]. The existence of a variety of illegal doping substances like amphetamine or norephedrine in the urine of athletes was demonstrated in a recent study using CE-C^4D [116]. The C^4D-technology enables the detection of amino acids, proteins and peptides without the need for any derivatization steps. Exposing those analytes to an acidic environment renders them in their cationic form and thus makes them measurable with the "universal" C^4D approach [117]. In contrast to that, another important class of analytes, namely the carbohydrate-sugars, form anionic species under strongly alkaline media and can be detected in such environments using C^4D-CE [118]. An important application field is the quantitative determination of (often non-absorbing) active agents in pharmaceutical formulations / drugs [119-123].

The field of MCE-C^4D is reaching a point where an increase in applied studies can be observed. Fundamental basics and groundbreaking studies have been carried out over the turn of the last two decades and some mature techniques are finding their way into complex applications. An on-chip enzymatic reaction was used to monitor and quantify the ammonium produced in the conversion of urea with urease [124]. Such methods allow the study of the mechanism of enzymatic reactions without having to rely on indirect approaches. As it is the case in conventional CE with C^4D detection, the determination of inorganic ions was the main application field in the past years [125-128]. [parts adapted from P3]

4. Experimental

4.1. Chemicals, Materials and Model systems

In this section an overview is given of the materials and reagents used to carry out the work presented in this thesis. Furthermore, the model systems and background electrolytes (BGE) used in the different studies are listed.

4.1.1 General

Fused silica capillaries of 360 µm outer diameter (OD) and 100, 75, 50, 25, 15, 10 and 5 µm inner diameter (ID) were obtained from Polymicro Technologies (Phoenix, AZ, USA). Water purified with an Astacus system (MembraPure, Bodenheim, Germany) and HPLC-MS grade isopropanol (Carl Roth, Karlsruhe, Germany) were used for the TOF-MS studies. Formic acid and ammonia for preparation of the respective sheath liquids were purchased from Merck (Darmstadt, Germany). TOF-MS calibration was done with a 10 mM sodium formate solution for the lower mass range of 50 m/z to 300 m/z. The calibration solution was made by diluting 10 µL of 1 M NaOH in 990 µL of solvent containing H_2O/Isopropanol (50/50, v/v) and 0.1% formic acid. For etching procedures 48% hydrofluoric acid from Sigma Aldrich (St. Louis, MO, USA) was used. Furthermore, oils (either sesame or olive oil) obtained from local grocery stores, desiccator grease (Merck) and octylsilane (Sigma Aldrich) for hydrophobization were used. Thermal conductivity paste was purchased from Conrad Electronics (Hirschau, Germany).

4.1.2 Model systems and background electrolytes

4.1.2.1 HPLC-C^4D

The applicability of the C^4D detection cells to HPLC was evaluated using a model mixture of the following ionic substances: benzoic acid, lactic acid, octanesulphonic acid, and sodium capronate (all Sigma Aldrich, St. Louis, MO, USA).

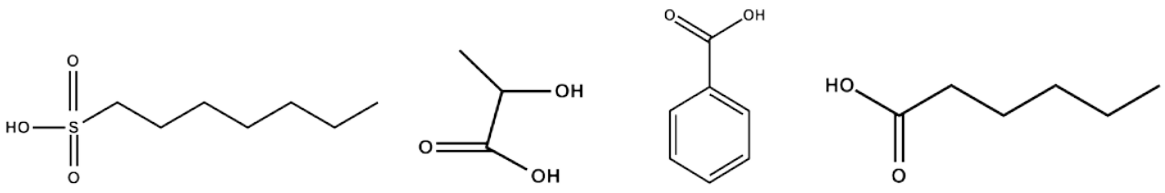

Octanesulphonic acid Lactic acid Benzoic acid Caproic acid

Figure 6. Structures of the model species used in HPLC-C^4D experiments.

4.1.2.2 Aliphatic amines

Aliphatic amines methylamine (MA), dimethylamine (DMA), trimethylamine (TMA), diethylamine (DEA) and triethylamine (TEA) were obtained from Sigma-Aldrich (St. Louis, MO, USA). The amines were used without any further purification. Aqueous stock solutions with a concentration of 500 mg/L were prepared and subsequent dilutions of these solutions were used to perform the measurements.

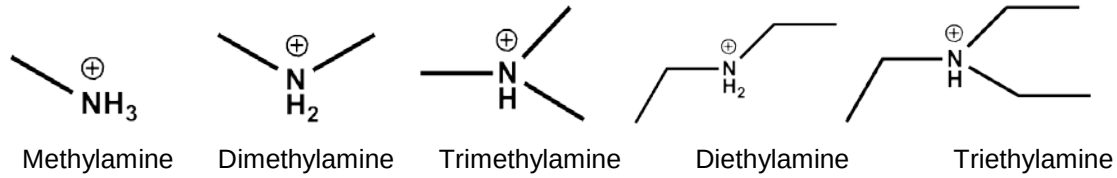

Figure 7. Structures of the aliphatic amines employed. Charge states for the conditions of the histidine/MES (pH 6.6) background electrolyte are given.

For preparation of the background electrolyte, histidine from Merck (Darmstadt, Germany) and 2-(N-morpholino)-ethanesulfonic (MES) acid monohydrate from Fluka (Buchs, Switzerland) were purchased. For the 20:80 buffer composition that was used throughout the study after optimization the sufficient amounts of l-histidine and MES were weighed and dissolved in 20 mL of Millipore water. The buffer solutions were stored in glass vials in a refrigerator. [partially adapted from P1]

4.1.2.3 Non-aqueous CE of dyes

Acetonitrile, acetic acid (100%) and ammonium acetate were obtained from Merck KGaA (Darmstadt, Germany). The textile dye compounds used were basic green 1, obtained from Schwan Stabilo (Heroldsberg, Germany), sandocryl red (basic violet 16) and basic red 28 provided by Clariant (Mexico) and methylene blue, which was obtained from Riedel-de-Haen (Saelze, Germany). Overhead projector pens were from Faber-Castell. (Ferrocenylmethyl)trimethylammonium (FcMTMA) acetate was prepared from the corresponding iodide salt (Lancaster Synthesis GmbH, Mühlheim, Germany) with the help of an anion exchanger. Purification was done by recrystallization from methanol / water. The water used to prepare solutions was doubly distilled. Stock solutions of samples (1 M) were prepared fresh. The respective standard solutions were prepared by dilution with the corresponding amount of running buffer. [adapted from P4]

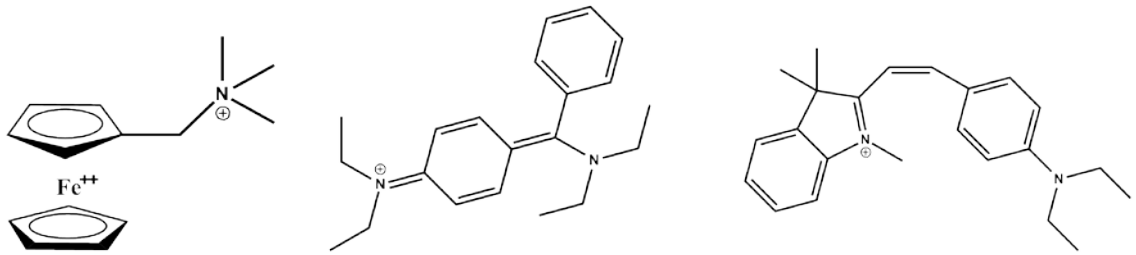

Figure 8. Structures of 3 model substances used in the NACE-AD study. Charge states given for conditions of the background electrolyte used.

4.1.2.4 Biogenic amines

For automated high-throughput CE-MS experiments norepinephrine hydrochloride and epinephrine were purchased from Sigma Aldrich (St. Louis, MO, USA) and histidine and dimethyl sulfoxide (DMSO) from Merck. Solutions of different concentrations in either BGE or pure water were prepared freshly. As background electrolyte served 100 mM formic acid which was prepared by dilution from 98-100% formic acid (Merck, Darmstadt, Germany). The solution was degassed by ultrasonification and filtered with Milliex-GP 0.2 µm filters.

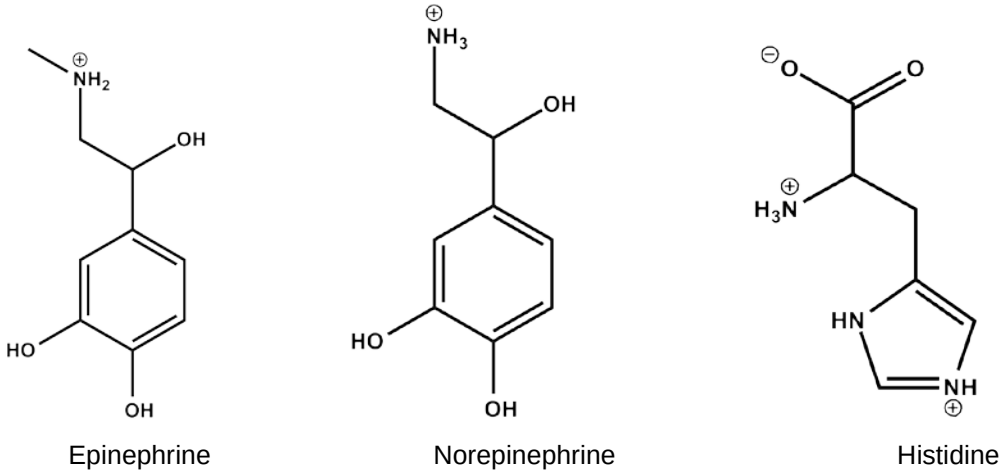

Figure 9. Structures of the analytes employed in the CE-MS study. Charge states given for conditions of the background electrolyte used.

4.1.2.5 (Cyclic) Nucleotides for CBI-CE-MS and 2-dimensional IC x CE studies

The cyclic nucleotides, cyclic adenosine monophosphate (cAMP), cyclic cytidine monophosphate (cCMP) and cyclic guanosine monophosphate (cGMP) were obtained from BioLog (Bremen, Germany) and served as model analytes for the CBI-CE-MS studies. The adenosine monophosphate (AMP), cytidine monophosphate (CMP) and guanosine monophosphate were obtained from Sigma Aldrich (St. Louis, MO, USA) and EOF marker dimethylsulfoxide (DMSO) from Merck. Stock solutions of the analytes of 50 mM were prepared in pure water and subsequently diluted in buffer to the desired concentrations. Ammonium acetate, ammonia solution and formic acid were obtained from Merck. CE runs were conducted in 25 to 50 mM ammonium acetate / ammonia (NH_4OAc / NH_3) buffer solutions at pH 9.25. The ammonium acetate BGE solutions were prepared freshly from an ammonium acetate solution of known concentration, pH adjusted with the ammonia and filtered through 0.2 µm Milliex-GP syringe filters (Millipore, Cork, Ireland). [adapted from P5]

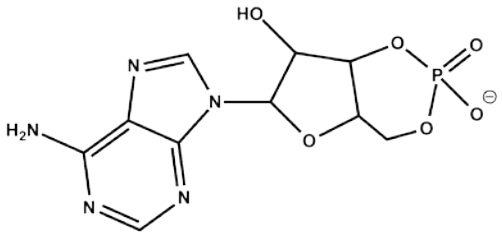

Cyclic adenosine monophosphate (cAMP)

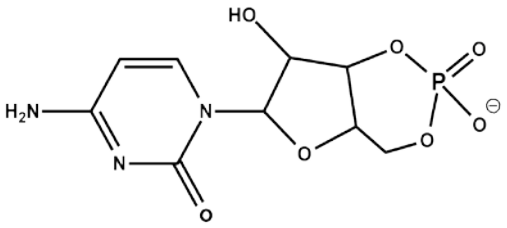

cyclic cytidine monophosphate (cCMP)

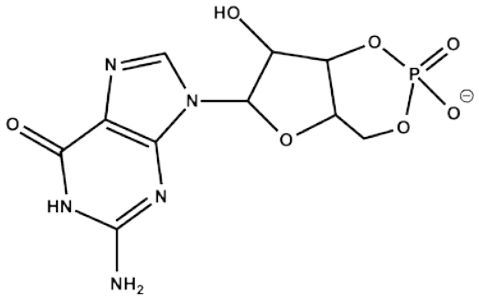

Cylic guanosine monophosphate (cGMP)

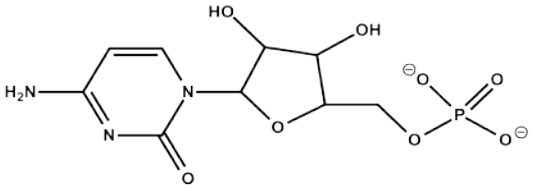

cytidine monophosphate (CMP)

Figure 10. Structures of 4 of the (cyclic) nucleotides used in the CBI-MS and IC x CE-MS studies. Charge states given for conditions of the background electrolyte used.

4. 2. Instrumentation

This section gives an overview of the main components used for the experiments presented in this work.

4.2.1 Liquid-chromatography system and C^4D cells

Two tubular PTFE detection cells, differing in their wall thickness, inner diameter and geometric cell volume were tested and evaluated under the same experimental conditions as those used for previous cell determinations [129]. The detection cells were manufactured by tightly inserting PTFE-tubes into cylindrical electrodes made of 5 mm long sections of stainless steel needles. Cell 1 was made from standard PTFE tubing, OD 1/16", ID 0.01". Cell 2 was constructed using a 10 mm long piece of thin-walled PTFE tubing. Both ends of this tubing were tightly inserted into standard PTFE tubing, the same as that of cell 1, with the internal diameter widened by heating. The length of the PTFE tubing between the column (sampling valve) and the individual detection cells were identical 16 cm (18 cm) for both arrangements. The scheme of the detection cells is illustrated in Figures 11 A and B, and their geometric parameters (in metric units) are summarized in Table 1. The tubes with the detection cells were connected to the sampling valve (non-separation conditions) or to the column (separation conditions) using standard PEEK fittings. A generally accepted simplified electronic equivalent circuit of the C^4D cell [130, 131], see Figure 11 C, was used for modelling the cell performance.

Table 1 Geometric parameters of the tested tubular cells and parameters used for model computations (for explanation of some parameters see Figure 11)

Parameter	Tubular cell 1	Tubular cell 2
Insulator (dielectric) material	PTFE	
Insulator relative permittivity, ε_r	2.1	
Geometric cell length, L [m]	11.5×10^{-3}	11.5×10^{-3}
Cross-section area, a [m^2]	4.9×10^{-8}	2×10^{-7}
Geometric volume, V [μL]	0.6	2.3
Internal radius, r [m]	1.25×10^{-4}	2.5×10^{-4}
Outer radius, ρ [m]	8×10^{-4}	4.5×10^{-4}
Tube wall thickness, t [m]	6.75×10^{-4}	2×10^{-4}
Geometric electrode width, w [m]	5×10^{-3}	5×10^{-3}
Gap between electrodes, d [m]	1.5×10^{-3}	1.5×10^{-3}
Specific conductivity of water [S m^{-1}]	1.0×10^{-6}	
Specific conductivity of KCl solutions, κ [S m^{-1}]	from 1.5×10^{-5} to 1.5×10^{-3}	
Input a. c. voltage frequency, f [Hz]	100 000	
Input a. c. voltage amplitude, U [V]	± 10	
Stray capacitance, C_x [F]	1×10^{-13} (estimated)*	
Permittivity of vacuum, ε_0 [F m^{-1}]	8.85×10^{-12}	

*) For this value the best agreement between experimental and modelled data has been obtained.

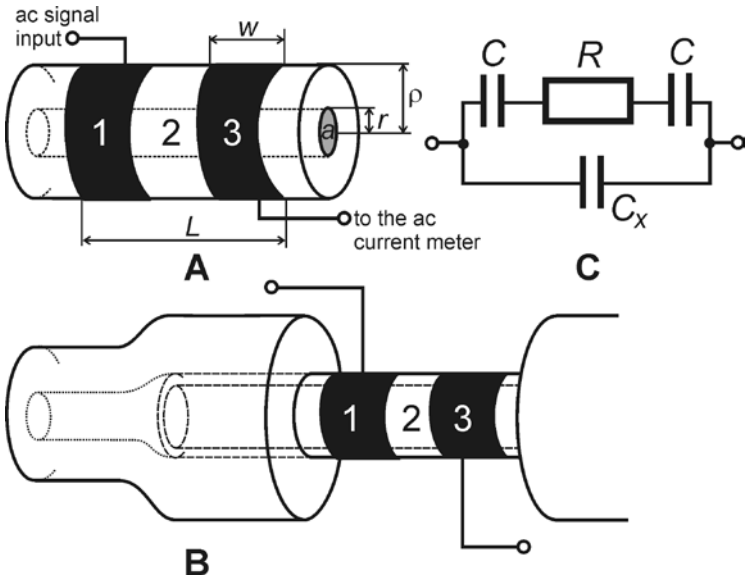

Figure 11. Geometric arrangement of the tubular contactless conductivity cell 1 (A), cell 2 (B) (dimensions are not in scale) and their simplified electric equivalent circuit (C). 1 - stainless steel actuator electrode, 2 - electrode gap, 3 - pick-up electrode, C - electrode/tube wall/solution interface capacitance, R - solution resistance, C_x - parasitic stray capacitance

The respective detection cell was connected to the laboratory-made electronic circuitry based on the scheme in [132]. A sine-wave AC signal with a frequency of 100 kHz and amplitude of ±10 V was applied to the actuator electrode from a FG 503 generator (Motech Industries Inc., Taiwan). The AC current passing through the cell was taken from the pick-up electrode and after rectification and amplification it was recorded by a computer which was equipped with a Clarity (DataApex, Czech Republic) data acquisition system. [adapted from P2]

4.2.2 Microchip electrophoresis device Chipgenie

The MCE-HS-SDME study was carried out using the prototype of the ChipGenie edition E [4, 5]. This miniaturized chip electrophoresis (MinCE) system integrated both the separation and the detection electronics in a portable compact device. The size of the MinCE system is 18 cm in length, 12 cm in width and 9 cm in height. The top cover is equipped with the high voltage source for the electrophoretic injection and separation processes. It can deliver up to 4 kV injection or separation voltage. Four platinum electrodes fixed to a polymeric holder were responsible for feeding the HV to the reservoirs of the chip. In the bottom part of the device, the C^4D detection electronics were attached including a high frequency emitter and the corresponding receiver. Via gold spring contacts the thin-film gold electrodes sputtered on the chip were connected to the device. The frequency applied to the detection unit is 3.6

MHz. (In Figure 12 an illustration of the miniaturized microchip electrophoresis device is shown.

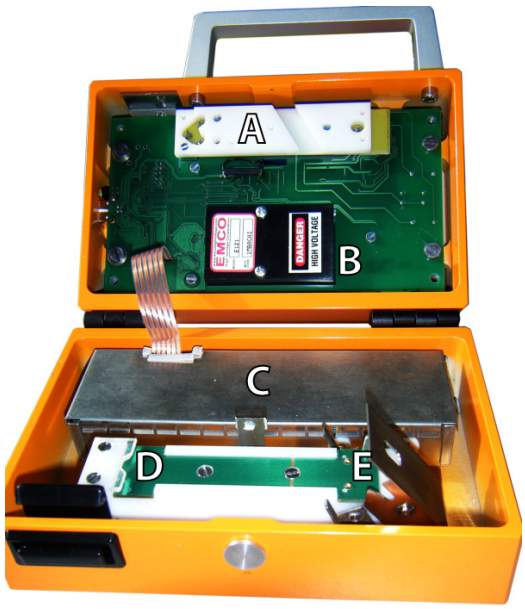

Figure 12. Chipgenie Prototype used in this work. **A** high voltage electrodes **B** high voltage source **C** C^4D detection circuitry **D** chip holder **E** C^4D gold spring contacts

The microfluidic chips were obtained from the Microfluidic ChipShop GmbH (Jena, Germany). Thin-film gold electrodes are sputtered on the cover foil of the chips. The channel structure is arranged in a cross-like manner with two microchannels of different length for electrokinetic injection and subsequent separation. The dimensions of the channels on the chip are as follows: channel depth is 50 µm, channel width is 50 µm and length of the separation channel is 8.7 cm. Injection of samples occurred along the shorter injection channel (1 cm) and usually lasted 5 s at 0.5 kV injection voltage. [in parts adapted from P1]

4.2.3 Potentiostat for CE-AD

The PalmSens potentiostat (PalmSens BV, Utrecht, The Netherlands) is a portable and battery-powered potentiostat which is connected via USB to a computer. The device enables current measurements in a range from 1 nA to 100 µA within a selectable potential range from -2 V to + 2 V. It is capable of running a number of electrochemical measurement techniques. The amperometric detection mode was used for measuring the I-t curves and the cyclic voltammetry (CV) mode for the basic studies of the substances to be investigated.

Suitable adaptor clamps and a specific connection cable for connection to the 3-electrode setup of the electrochemical cell were developed.

4.2.4 Compact C^4D detector

The contactless conductivity detector (see Figure 13) was obtained from our cooperating partner Prof. do Lago from the *Universidade de Sao Paulo* (Sao Paulo, Brazil). The highly compact (6.5 cm^3) and versatile detection unit features two detection electrodes made of stainless steel needles wrapped with copper wire through which the capillary can be guided [132]. It works with a local oscillator at 1.1 MHz, a low-noise circuitry and an analog-to-digital converter (ADC, 21 bits). An ATMEGA168 microcontroller (Atmel, San Jose, CA) was developed via Arduino (www.arduino.cc) and the software control interface was developed in LabView 8 (National Instruments, Austin, TX) [133].

Figure 13. Photograph of the C^4D detector used in the portable CE system (see section 9.1) and for experiments with the CBI setup.

4.2.5 Automated capillary batch injection

This CBI injection device [19] is firstly composed of an injection cell (Figure 14 (E)) made of glass which is equipped with motorized stirrer (I), xy-positioning unit (D) and high-voltage electrode (F). The separation capillary (H) is vertically fixed into the base plate of the injection cell using a PEEK-fitting (390 µm ID). The injection capillary is fixed in a holder (C) and is directed into the cell from the top through a 380 µm ID glass tube (Hilgenberg, Malsfeld, Germany) which is located in a manual xy-positioning unit (D). Hence, the injection capillary can be positioned precisely towards the separation capillary. Vertical movements are done by a 1.8° stepper motor (B) with precision leadscrew. It allows for a step precision of 1 µm/step. A second stepper motor (A) provides the horizontal movement. The liquid inside the injection capillary is controlled by a 10 µL Nanofil microsyringe (WPI, USA). The syringe is clamped into a UMP3 syringe pump (WPI, USA) which is controlled by a microcontrol system (WPI, USA). The initial alignment of the two capillaries and control of the injection process are accomplished visually with a modified microscopic video camera (DNT, Dietzenbach, Germany). Specific precautions for avoiding high-voltage

flashovers, like extra shielding of certain components, were taken during the course of the study. A lab-built CE setup served as high voltage source (see section 4.2.8). [adapted from P5]

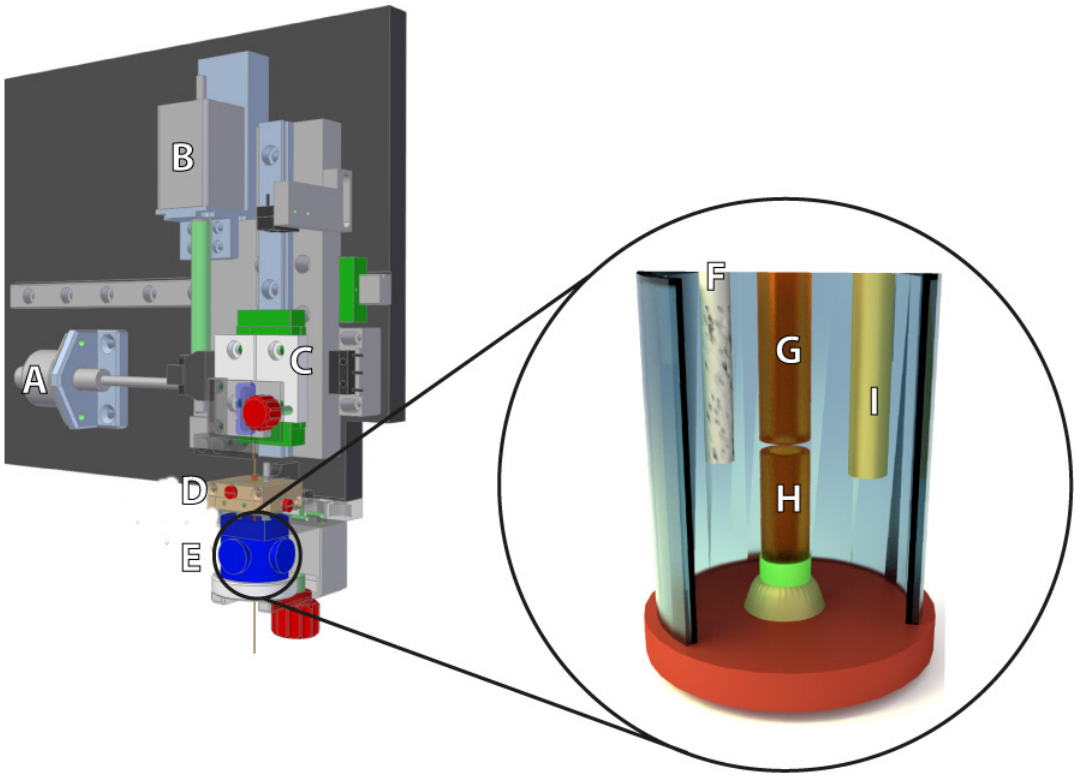

Figure 14. Automated capillary batch injection (CBI) setup with close-up of injection cell. **A** x-direction motor **B** z-direction motor **C** fixation for injection capillary **D** positioning unit for injection capillary **E** injection cell filled with background electrolyte **F** high-voltage electrode **G** injection capillary **H** separation capillary

4.2.6 Time-of-flight Mass Spectrometer

For CE-MS experiments a Bruker MicroOTOF (Bruker Daltonics, Bremen, Germany) time-of-flight mass spectrometer (TOF-MS) with an electrospray ion source (ESI) was used. The mass analyzer of the TOF-MS enables data acquisition in positive or negative ion mode within an m/z window of either 50 to 3000 m/z or in the extended mode from 50 to 20000 m/z [134].

4.2.7 Electrospray ionization (ESI) interface

With a grounded coaxial sheath liquid sprayer interface (Agilent, Waldbronn, Germany) direct introduction of the CE capillary into the mass spectrometer was accomplished. Under addition of a sheath liquid and a nitrogen nebulizer gas stream the CE eluents formed a stable electrospray. One end of the separation capillary was guided into the ESI-interface and the protrusion of the capillary from the sprayer tip was adjusted under video monitoring. The ESI-interface chamber of the TOF-MS was modified in our lab in a way that the introduction of a purpose made microscopic camera was possible (see section 4.5.5) to monitor spray formation. The sheath-liquid was fed to the interface with a syringe pump model 601553 from kd Scientific (Holliston, MA, USA).

4.2.8 Lab-built capillary electrophoresis setup

For CBI-CE-MS measurements a high voltage power supply (model HCN 7E-35000, F. u. G. Elektronik, Rosenheim-Langenpfunzen, Germany) provided potentials of up to + 35 kV. As a safety measurement the anodic high voltage end and the ground wire were led into a Plexiglas box with magnetic HV interrupt.

4.2.9 Ion chromatograph

The ion chromatograph that was coupled to the CBI-CE-MS setup was a Dionex ICS-5000 HPIC device (Thermo Scientific Dionex, Munich, Germany) equipped with an Ion-Swift MAX-200 (0.25 x 250 mm) anion-exchange column with suitable guard column (0.25 mm x 50 mm), which were both operated at 35 °C. Furthermore, it features two conductivity detection (CD) modules. Eluent concentration was kept constant at 40 mM hydroxide (KOH). The system included a suppressor which allowed to obtain an effluent composed of highly pure water.

4. 3. Instrumental developments

This section lists own instrumental developments that were carried out during this work.

4.3.1 Electrochemical cell and end-column detection

The electrochemical cell consisted of a glass cylinder (12 mm inner diameter, 10 mm height) equipped with two perpendicularly arranged glass windows to enable video monitoring of the electrode-to-capillary alignment. The cell's bottom part was closed against its surroundings with a PTFE plate through which the separation capillary was guided via PEEK tubing. On top of the cell a homemade micromachined xy-positioning unit was tightly fit to the glass body. The xy-positioning contained narrowly spaced three electrodes: an Ag/AgCl reference electrode, platinum counter electrode and the Pt-microdisk working electrode with fine-thread for aligning the electrode in z-direction. A digital microscope camera was used for the alignment of the working electrode with the capillary end. The alignment could be monitored from two sides of the cell. All measurements were done using a PalmSens portable potentiostat (Palm Instruments B.V., Houten, Netherlands) through the software PTSense. [adapted from P4]

4.3.2 Lab-built CE autosampling unit

The CE system depicted in Figure 15 consisted of a laboratory-made autosampling device which was developed and constructed in our group.

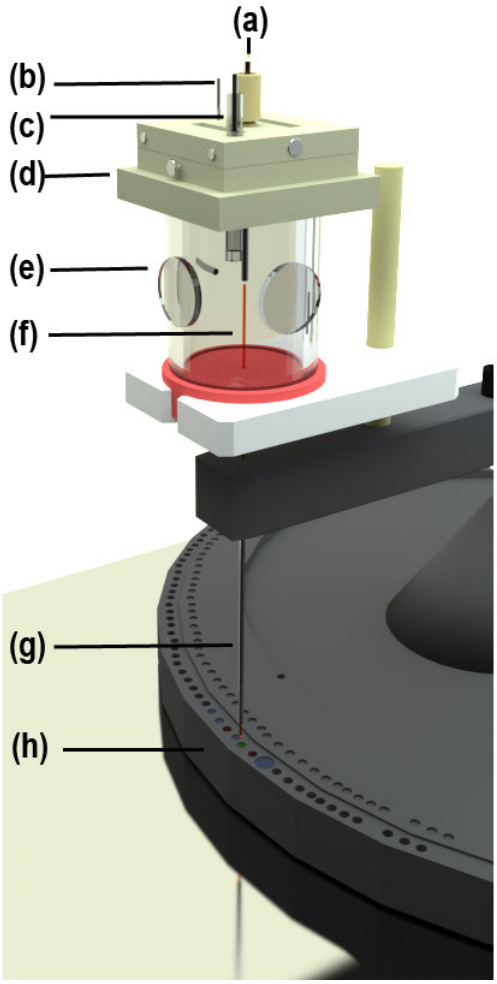

Figure 15. Overview of the CE-AD setup. **(a)** working electrode embedded in screw for z-positioning **(b)** auxiliary electrode **(c)** Ag/AgCl reference electrode **(d)** xy-positioner for working electrode **(e)** cell window for video monitoring **(f)** separation capillary threaded through **(g)** HV-voltage stainless steel needle **(h)** autosampler tray

Parts from a Hewlett Packard HPLC device were used to construct the miniaturized autosampling unit. A LabView based software (see section 4.4.2) was developed to control the autosampler and the injection process. A ±30 kV high voltage dc supply (ISEG GmbH, Dresden, Germany) was used to apply high voltage between the capillary ends. The inlet end of the capillary was held at positive potential whereas the buffer-filled electrochemical cell (see section 4.3.1) was grounded. Injection times as short as 0.1 s could be applied and the stainless steel needle was acting as high voltage electrode for electrokinetic injection. The overall setup was placed into a Plexiglas box for safety reasons. Based on the described setup an own, portable CE device was constructed (see section 9.1). [partially adapted from P4]

4.3.3 Autosampler modifications for CE-MS

The setup described in section 4.3.2 could be used with a few modifications also for high-throughput CE-MS measurements with short separation pathway capillaries. One specialty in this setup was that injection could be accomplished hydrodynamically under aid of the vacuum suction pressure from the TOF-MS. In Figure 16 the autosampler setup coupled to the TOF-MS is shown (in this instance with the large sampling tray).

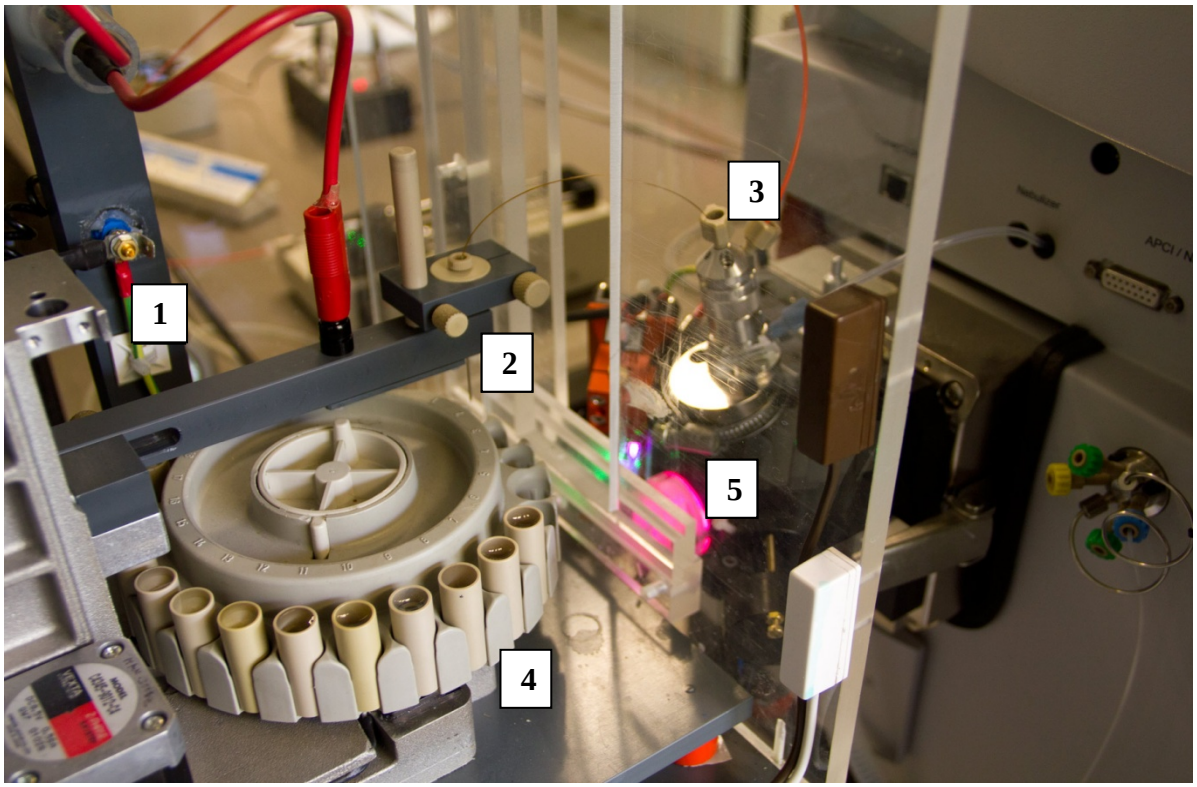

Figure 16. Experimental setup for automated fast CE-MS. 1: high-voltage, 2: fixation of capillary, 3: ESI-interface with sheath-liquid and nebulizer gas, 4: Sample tray, 5: microscopic camera

The injection end of the capillary was guided through a purpose made fixation unit to keep it plane with the end of the stainless steel needle. The high voltage ground was clamped to the ESI-interface at the TOF-MS device.

4.3.4 Thermoelectric device

For CBI-CE-MS experiments with very small sample drops it was necessary to control the temperature of the sample drops and freeze / unfreeze them. For precise control of the temperature conditions of the drops a control unit for Peltier elements was developed and built within our group. The following elements were purchased from Conrad Electronics (Hirschau, Germany) and then assembled to a compact control device: Peltier controller 12 V, display for Peltier controller, standard Peltier element (44 x 44 mm) and a NTC temperature sensor 833. The thermoelectric element basically worked as a thermal pump between its two surfaces and one side becomes excessively hot while the other is cooled down. Achievement of low temperatures on the upper layer required substantial cooling of the other side. The refrigeration of the bottom side was accomplished under aid of a modified ventilation unit from a personal computer.

4.4. Software

This section names in 4.4.1 freeware and commercial software that was used for different purposes in the course of this work. In 4.4.2 and 9.1.2 own software developments used to run the autosampling unit and the portable CE are described.

4.4.1 General

Chipgenie. A LabView based software (Version 8, National Instruments, USA) was used to control all the parameters relating to microchip electrophoresis separations with the Chipgenie.

PalmSens. The user software PSLite (PalmSens BV, The Netherlands) in either version 2.0 or version 3.0 offered amperometric detection and a range of voltammetric methodologies (cyclic-, square wave-, differential pulse-, linear sweep voltammetry).

C^4D detector. The open C^4D LITE Software for the C^4D detector was developed in LabView 8 in the group of Prof. Dr. Claudimir do Lago (Universidade de Sao Paulo, Brazil).

CBI system. The control software CBI-Control for the CBI setup was fully designed and developed within our group and written in Microsoft Visual Basic 2010 Express.

TOF-MS. The TOF-MS control with data acquisition was achieved with the micrOTOF control version 2.3 from Bruker Daltonik. For data analysis the Compass Data Analysis software version 4.0 SP1 from Bruker Daltonik was used. For data representation Origin (Version 6.0) was used.

Graphics and Illustration. 3-D Graphics and animations were done with Blender 2.68 (Blender Foundation, The Netherlands). Vector-based graphics and schemes were designed with Illustrator 5.5 (Adobe, San Jose, CA, USA). Video recording was done with VirtualDub and videos were edited using Sony Vegas (Sony Corp., Tokyo, Japan).

CAD-software. The design and construction drawings for the portable CE device were made with Solid Edge Version 12.

MicrosamplerSoftware. For the software of the lab-built portable CE device, see Chapter 9 “Appendix”.

4.4.2 Autosampler Control software

The automated injection device was computer-controlled from a graphical user interface, which allowed full control over all the details governing the injection process with either CE-

AD or CE-MS setup. The software to control the autosampling unit together with the high voltage source was designed and developed in LabView 8. General design and structural components of the software are described in the following.

User interface

The user interaction occured via the main interface shown in Figure 17. It consists of a detailed overview of the motor position status as well as status of the voltage source (A). Upon start of the software the choice of the desired sampling tray is requested (B). The sampler was programmed to enable measurements from three different sample trays. One is the original full round on the HPLC sample tray with the larger vials (400 µL, 21 positions). Secondly, it can run from a smaller segment of either 10 vials of 100 µL size or thirdly from 21 vials with 10 µL capacity. The processor load and job execution status can be monitored in (C). A variety of parameters regarding the machine control can be adjusted via various tabs in the lower right corner of the interface (D). Most importantly the injection depth and motor null positions can be adjusted there. Initially, the main control buttons for the system are shown (E) and via the tab selection (F) switching between machine controls and the job list can be managed. The “Prepare Autosampler” button initializes the sampler and lets it find the respective starting positions depending on the choice in (B). The “loop” button enables unattended repeat runs of the measurement cycle ordered in the job list.

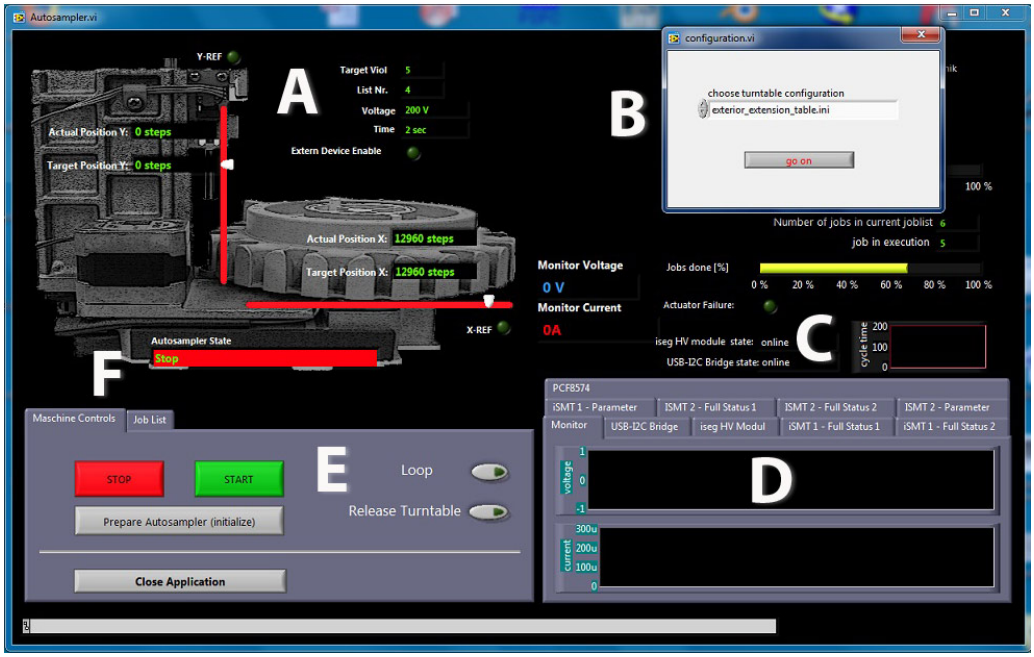

Figure 17. Main form of Autosampler software upon system start **A** Position status of the motors **B** Initial query for the choice of sampling tray **C** System and job status. **D** Various tabs for parameter control **E** Machine control buttons **F** Selection tabs

Job list and execution of measurements

All relevant measurement and injection parameters can be adjusted in the “Job list” tab (see Figure 18). In a list consisting of 7 columns and theoretically 999 rows, the sequence of events for a measurement session can be managed. Furthermore, different tabs for parameter handling are offered to the right of the job list. The COM-Ports for the attached motor and ISEG HV Modul can be set and also injection depth into the respective vials of the different sample trays can be adjusted in this section. Manual control of the z-positioning is possible via the “Drive to null” and “Drive to injection” buttons. In addition to that different system management functions can be found in this section. Table 2 lists the respective functions.

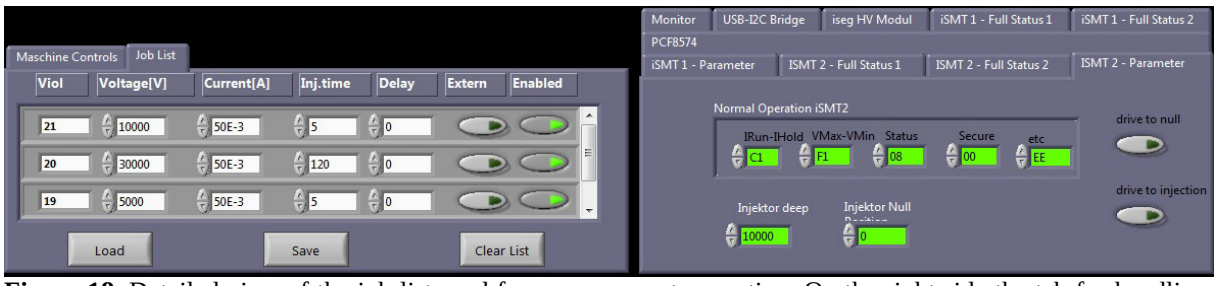

Figure 18. Detailed view of the job list used for measurement execution. On the right side the tab for handling of the limiting values for the z-movement of the motor.

Table 2. Functions of the job list’s columns

Column	Function
Vial	Position of the respective vial for the executed step
Voltage	Voltage application for injection or separation (0 to 30000 V)
Current	Allowed current limit for the respective step
Inj. time	Chosen length of injection and also duration of separation steps
Delay	Time period between transfer from one to another vial
Extern	Enable / Disable detection unit (Potentiostat or TOF-MS)
Enabled	Activates / Deactivates the respective row

4.5 General methods

4.5.1 Sample collection and preparation

Microchip electrophoresis. The shrimp samples were obtained from grocery stores, one of them Lidl (Lidl Dienstleistung GmbH & Co. KG, Neckarsulm, Germany) and the other Netto Marken-Discount AG & Co. KG (Maxhütte-Haidhof, Germany). The investigated shrimp were captured in the Pacific Ocean either at the coast of Thailand or the waters around Indonesia and in the Atlantic Ocean close to Canada. [adapted from P1]

Nonaqueous CE of dyes. Different-colour (green, blue and red) overhead projector pens from Faber-Castell were investigated for their content in methylene blue, basic green 1 and basic red 28. In order to do this, lines of certain length and width were drawn on a glass plate and then dissolved in 1 mL of non-aqueous buffer solution. Furthermore, the high-throughput capability for real samples was evaluated. A number of different lines were drawn on the glass plates and then dissolved in the buffer. [adapted from P4]

CBI-CE-MS. The urine for preconcentration experiments was obtained from a healthy volunteer the same day and subsequently spiked with the respective amount of cGMP.

4.5.2 Capillary treatment

Prior to use, fresh capillaries were cut to the proper length, polished or etched at the ends and prepared according to the following protocol: flushing for 2 to 5 min with pure water, followed by a 5 min flush with 100 mM NaOH and again a few minutes with water. Finally it was usually rinsed for about 20 to 30 min with respective buffer solution. Between runs, the capillary was flushed with buffer solution. After use, capillaries were flushed with the respective buffer and kept overnight in vials containing separation buffer. Capillary polishing for flat end capillaries was either done manually after standard procedures or for more precise polishing a disc-type sander was used. It was developed within our group to enable a fixed positioning of the material to be ground within a micro-positioning unit. Via a knurl polishing angles of 0° to 90° could be adjusted. A controllable DC motor drove the sanding disc at adjustable speeds. [partially adapted from P5]

4.5.3 Electrode fabrication

The working electrodes for CE-AD measurements were made from 25 and 50 µm diameter platinum wires (Goodfellow GmbH, Bad Nauheim, Germany). A 3-cm long piece of the wire was threaded into a narrow bore glass capillary (ID of 100 µm) under a light microscope. The protruding end of the platinum wire was molten into the glass and polished flat until a platinum disk was exposed. The other end was inserted into a copper tube, the Pt wire threaded through the tube and soldered to the other end. This assembly was then placed into a fine-thread screw and inserted into the xy-positioner. After certain time periods the electrode was polished and pre-treated with 50 CV scans in 1 M sulphuric acid solutions. [partially adapted from P4]

4.5.4 End-column amperometric detection

The proper alignment of the capillary towards the end of the separation capillary was of importance for repeatable and sensitive amperometric detection. In the so called end-column detection the surface of the electrode was exposed perpendicularly to the capillary outlet stream in a suitable distance. In initial setups this was done via fixed guiding systems and only the z-direction needed adjustment. However, geometrical irregularities and deviations from the desired direction led to unsatisfactory results in the process of electrode alignment. Therefore, the xy-positioning unit (see section 4.5.1) was constructed in order to have more precise control over the end-column detection arrangement.

4.5.5 Electrospray visualization

The generated electrospray was of particular importance for CE-MS method development. The spray affects peak quality as well as signal intensities. It was found that a correlation exists between the visually observed stability of the spray and the total ion count or peak shapes. In order to check the spray stability, a modified microscope camera (DigiMicro 1.3, DNT, Dietzenbach, Germany) was inserted into the ESI-spray chamber of the TOF-MS device. In order to make the spray visible, specialized illumination was needed. Therefore, a green laser beam (532 nm) from a laser diode (Roithner, Vienna, Austria) was directed via a mirror into the spray chamber. Moving the mirror allowed for precise direction of the beam onto the tip of the sprayer and with the right tuning it was possible to visualize the spray. A variety of different LEDs implemented into the illumination setup in the spray chamber

provided sufficient background illumination for video monitoring. A purpose-built control unit was used for control of the different illumination options.

4.5.6 HF-etching of capillaries

Tapered Tips. The preparation of the tapered injection capillaries, with outer diameters at the tip reaching the respective inner diameters, required a multi-step etching procedure (see Figure 19).

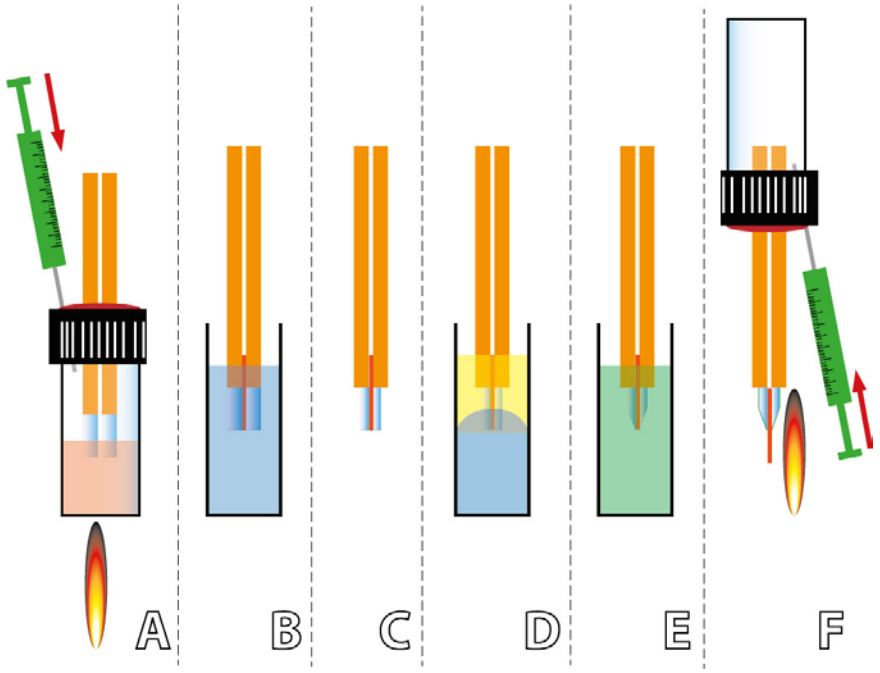

Figure 19. Etching procedure for preparation of sharply tapered, hydrophobized injection capillary tips. **A** filling of tip with hot desiccator grease **B** etching in 48% HF **C** result of first etching step **D** etching at oil / HF – meniscus (oil is upper layer) **E** hydrophobization with octylsilane **F** removing grease

First of all, the chosen capillary was cut at appropriate length with a ceramic-blade knife and the polyimide coating was burnt off from its end (carefully remove remaining combustion material). Next this capillary end was guided into a septum vial (4 mL) and closed tightly against its environment. In it, standard desiccator grease (melting point between 45 and 60° C) was liquefied with a heat gun. Next, pressure was applied and the capillary was dipped for a few seconds into the hot grease to fill the first millimetres of the capillary. Then, the capillary end was placed into a Plexiglas cuvette containing 48% hydrofluoric acid (HF). The progression of the etching was monitored via a microscopic video camera. At this point the capillary was left inside the pure HF until about 90% of the capillary wall's circumference was etched away. The capillary was then washed with calcium chloride solution and membrapure water. To obtain a sharp tip, the capillary was placed in another Plexiglas cuvette, which contained 1:1 48% HF and oil (olive or sesame oil). A convex meniscus was

forming at the border between the upper oil layer and the bottom HF-layer. Placing the end right into the meniscus etched the capillary down to a tip-shape end. After another washing step the capillary was then placed for about 30 min into a vial containing 5% octylsilane in toluene for hydrophobization. In the final step, the grease was removed from the capillary by carefully heating it in a drying oven to about 60-70° C under application of pressure.

Funnelled ends. In contrast to the tapered tips, the etching of a funnelled separation capillary end was comparatively straightforward. The pre-cut capillary was placed into a vial containing hydrofluoric acid until the desired result was obtained. The width and depth of the funnel could be controlled by applying varying pressure from the other end of the capillary. The different air streams at the capillary outlet lead to a variety of different funnels. Lower or no pressure resulted in more drawn out funnels whereas high pressure gave short and wide funnels. [adapted from P5]

4.6 Method development

4.6.1 HPLC-C^4D method for comparison of detection cell

Non-separation conditions. For basic testing, the model KCl solutions were injected directly into a flow stream of deionized water (Milli-Q Plus, Millipore, USA). Solutions with concentrations ranging from $1x10^{-6}$ to $1x10^{-4}$ mol L^{-1}, corresponding to an electrical conductance range from $1.5x10^{-5}$ to $1.5x10^{-3}$ S m^{-1}, were used. To obtain stationary response, a long zone of KCl solution was injected using a BETA 10 plus gradient pump (Ecom, Czech Republic) and a sampling valve equipped with a 500 µL sampling loop directly in the flow of mobile phase was used. The mobile phase (deionized water) was degassed using the Vacuum Degasser 3014 (Ecom, Czech Republic). No significant dependence of the detector response on the mobile phase flow rate within a test interval from 0.1 – 1 mL min^{-1} was observed. Therefore, the flow rate of 0.5 mL min^{-1} was used throughout the non-separation measurements.

Separation conditions. The applicability of the system for detection in conjunction with HPLC was evaluated using the described model system (see section 4.1.2.1). These substances were used to ensure comparability to the previous study with the thin-layer cell [129]. The setup comprised the above mentioned components, except that the sampling valve was equipped with a 10 µL loop and a 4.6 mm x 150 mm column packed with Biospher PSI 100 C18, 5 µm particles (Labio a.s., Czech Republic), was used. The flow rate was increased to 0.8 mL min^{-1} and a 60:40 (v/v) acetonitrile / water solution was applied instead of deionized water as the mobile phase. [adapted from P2]

4.6.2 HS-SDME method

In order to take advantage of the volatile nature of the aliphatic amines and reduce interferences with the complex matrices the HS-SDME technique was used. A 50mL syringe from ILS Innovative Labor Systeme GmbH (Stuetzerbach, Germany) was used for exposing extraction drops. The analyte solution was filled into 4 mL septum vials with corresponding screw cap (Carl Roth GmbH, Karlsruhe, Germany). Ultrasonification for extraction purposes was accomplished with an Elmasonic S30 ultrasonic unit from Elma Hans Schmidbauer GmbH & Co. KG (Stingen, Germany). The pH determinations were done with a pH glass electrode from Radiometer Analytical S.A. (Lyon, France). The vials were fixed in the ultrasonic bath with conventional clamp patches. An amount of 1 mL of analyte solution was

pipetted into the vial and diluted to a total of 2 mL with 50% NaOH. The next step consisted in penetrating the septum with the syringe and exposing a 5 µL drop of the His/MES electrolyte solution (pH 6.6). This step required careful handling as the drop might fall into the solution if not executed properly. After the extraction by ultrasonic irradiation was finished the drop could safely be retracted into the syringe. The 5 µL drop was afterwards filled into the sample reservoir of the chip and diluted 10-fold with His/MES buffer. [adapted from P1]

4.6.3 Microchip electrophoresis procedure

Prior to use, the microchips had to be prepared for measurements. All solutions used in the studies were filtered with a membrane Minisart RC (PTFE, 0.45 mm pore size, Carl Roth GmbH, Karlsruhe, Germany) to avoid channel clogging. Next, the microchannels were rinsed for 2 to 3 minutes with distilled water. In order to accomplish that the channels were filled with buffer (or water) the 3 upper reservoirs were filled with distilled water and a vacuum was applied to the outlet reservoir (under aid of homemade suction tubing). Following this step, the respective sample could be pipetted into the sample reservoir, while the other reservoirs remained filled with electrolyte. Each reservoir was filled with 50 µL of fluid and subsequently the chip was inserted into the microfluidic analysis system and put in place via the chip holder. Prior to any separations, daily baseline checks with the background electrolyte were carried out. Once the baseline was stable, the separation measurements could begin. Applying the predetermined injection voltage to the shorter microchannel resulted in electrokinetic injection into the intersection area. The separation voltage was applied along the longer channel and thus electrophoretic separation occured. After use the channels of the chips were rinsed with distilled water for 5 minutes and wrapped up in Parafilm-foil to prevent clogging by particles during the storage. [adapted from P1]

4.6.4 Non-aqueous CE-AD method

Before measurements capillaries were conditioned with 0.1 M sodium hydroxide, water, acetonitrile and acetonitrile buffer. The detection cell was filled with electrolyte solution. The sample was injected from special sample vials placed right underneath the electrochemical cell. To inject from another vial the autosampling unit rotated while the detection cell was lifted. It was possible to set a delay time between the introduction into the separation buffer and injection of the next sample when several measurements in a row were done. Injection

depths and lift of the cell were set as short as possible in order to minimize the time in which the capillary was outside a vial. The high-voltage ground was permanently integrated into the electrochemical cell. The interval time of current measurements for amperometric recording was 0.05 s. The pretreatment of the electrode before each run was done by applying a 3 s cathodic pulse of -1.0 V and a 3 s anodic pulse of +2.0 V. The electropherograms were normally obtained at a detection potential of +1.3 V against an Ag/AgCl reference electrode in NACE buffer solution. [adapted from P4]

4.6.5 Method for high-throughput CE-MS

CE-Method. On CE side, the method optimization essentially required the choice of the right background electrolyte, the proper capillary lengths and IDs. A 100 µM formic acid solution was used as BGE to ensure compatibility with the TOF-MS. For CE-MS with an ESI-interface it was found to be beneficial to work with rather volatile BGE components to ensure higher ionization rates of the analytes. Before each measurement the values for separation voltage, duration of voltage application, positions of vials and duration of injection were adjusted. Injection was carried out either electrokinetically or by hydrodynamic suction pressure deriving from the TOF-MS vacuum. After an injection the capillary is transferred to the background electrolyte vial and the separation was started. The sequence of injection, separation and time in the intermediate buffer represented one measurement cycle. The following ion traces were extracted: histidine: 156.08 ± 0.5; adrenaline: 137.07 ± 0.5; 154.09 ± 0.5; noradrenaline: 152.08 ± 0.5; 170.09 ± 0.5. A manual injection method for the catecholamines delivered relative standard deviations of the peak heights of more than 10% [19]. The automated system was developed with the goal in mind to improve the reproducibility and throughput of fast CE-MS measurements. The sampler was programmed to run at least 5 measurement cycles under varying conditions regarding separation voltage and vial positions.

MS-method optimization. For the model system used a previously optimized set of MS parameters was in large part adapted [19]. Mainly, the nebulizer gas pressure and the sheath-liquid flow rate were varied compared to this strategy. In Table 5 in the following section 4.6.6 an overview of the optimized MS-detection parameters is given.

Voltage and injection vial variation. The autosampler was programmed to run a sequence of 5 cycles with a differing injection vial for each run (see Table 3). Furthermore, the voltage was varied. A 25 µm separation capillary was used for these determinations**.**

Table 3. Parameters of measurements of a sequence of 5 cycles with injections from differing vials. The measurements were carried out at 20, 25 and 30 kV separation voltage, respectively.

Step	Vial position	Voltage [kV]	Time
Injection	20, 16, 12, 8 ,4	0	30 s
Separation	21	20, 25 and 30	120 s

Increase of measurement cycles. In addition to the above measurements, repeatability was evaluated for an increasing number of measurement cycles. One time, 8 consecutive measurement cycles were carried out and the other time 15 cycles were run. Injection occurred in both instances from differing injection vials in the sample tray. All runs were carried out at 30 kV separation voltage.

4.6.6 CBI-CE-MS method for handling of very small samples

Experimental setup. The experimental setup consisted of a home-made Peltier control unit, a Peltier element with temperature sensor (Conrad Electronics, Hirschau, Germany) placed onto a cooling device, a purpose-built capillary batch-injection (CBI) system, a high-voltage supply and control unit, a coaxial sheath liquid interface (Agilent Technologies) and a microTOF-MS (Bruker Daltonik). In Figure 20 the setup details for the handling of small sample volumes are illustrated (details to the preconcentration are in section 4.6.7). The sheath liquid standard flow rate for electrospray ionization (ESI)-MS was set to 0.48 mL/h. The nebulizer gas pressure was set between 1.0 and 1.4 bar. [adapted from P5]

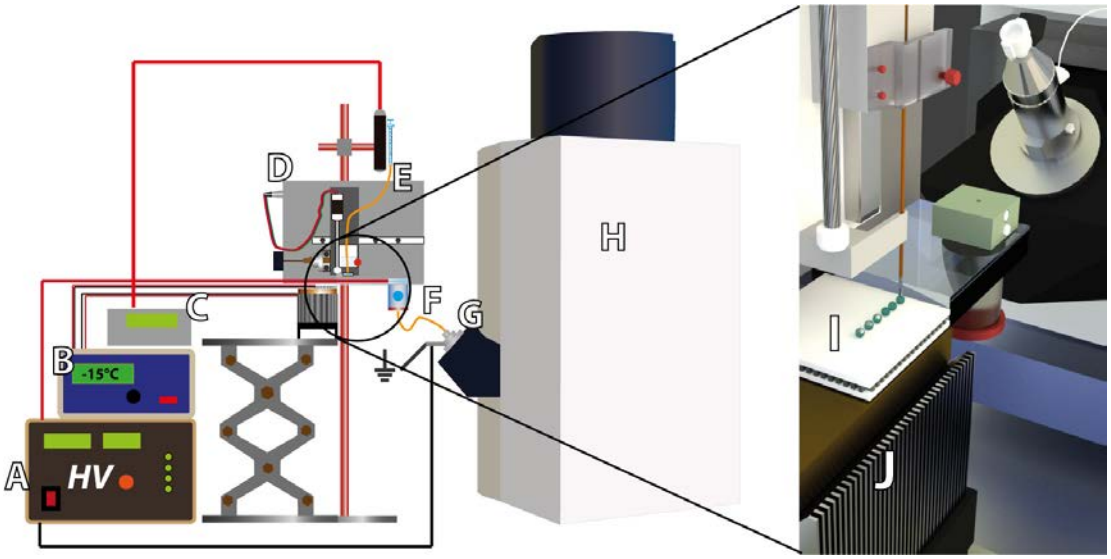

Figure 20. Scheme of the experimental setup for CE-TOF-MS measurements of nL-/pL-sized sample volumes. Left side: overview of the whole setup. Right side: close-up of the area where sample uptake occurs. The setup consists of **A** high voltage source **B** Peltier-control unit **C** microcontroller for micropump **D** CBI unit **E** micropump with microsyringe and injection capillary **F** injection cell **G** ESI-interface **H** TOF-MS **I** Peltier element with frozen drops **J** cooling unit for Peltier element.

CE-method optimization. The details of the injection process for a small sample volume under utilization of the Peltier-element is described and illustrated in Table 4.

Table 4. Overview of an optimized injection protocol for very small sample volumes

Step	Description	Parameters	Instrument
1	Align inj. capillary into funnelled sep. capillary	manually	Microscope camera
2	Take up sample solution	1 to 100 nL	Microcontrolled syringe
3	Move to sample position in x and z	x- & z-sample pos.	x- & z-motors
4	1st cool down of Peltier element	-2 to -5 °C	Peltier controller &element
5	Placing drop onto Peltier surface	~500 pL to 50 nL	Microcontrolled syringe
6	2nd cool down to -20°C	-20°C	Peltier controller
7	Flushing injection capillary	100 – 250 nL	Syringe pump
8	Move to water reservoir	go to x-position 1	x-motor
9	Take in water and reverse plunger	-100nL, 20 nL/s	Syringe pump
10	Move back to sample position	x- & z-sample pos.	x- & z-motors
11	Carefully guide capillary on top of frozen drop	on demand	z-motor
12	Reduce cooling to 0°C	0°C	Peltier controller
13	Guide capillary further into drop	on demand	z-motor
14	Switch-off cooling	>10°C	Peltier controller
15	Withdraw (simultaneously with 13) sample	varying	Syringe pump
16	Reverse plunger direction	35 nL, 20 nL/s	Syringe pump
17	Go to position “up”		z-motor
18	Go to injection position in x and z-direction		x- and z-motors
19	Expel sample	varying	Syringe pump
20	Start of separation and data acquisition	30 kV	HV-source / TOF-MS
21	Move inj. capillary out of cell	“Up”-position	z-motor

MS-Method. The optimized MS settings found over the course of this work are summarized in Table 5. The values for the automated CE-MS method described in section 4.6.5 can be found there as well (column *Biogenic Amines*)

Table 5. Overview of the optimized CE-MS values for the two model systems used (see 4.1.2.4 and 4.1.2.5)

Parameters	Unit	Biogenic amines	Cyclic nucleotides
Mass range lower limit	m/z	50	50
Mass range upper limit	m/z	300	500
Nebulizer gas pressure	Bar	1.4	1.0
Capillary exit	V	75	-100
Dry Gas Flow	L/min	4	4
Dry Gas Temperature	°C	200	200
End plate offset	V	-500	-500
Capillary	V	-4000	4000
Polarity	-	positive	negative

4.6.7 Preconcentration of small samples by solvent evaporation

A semi-microbalance R160 P from Sartorius (Göttingen, Germany) was used to weigh in the drops in the preconcentration experiments. The whole CBI unit was placed carefully via a system of purpose-made fittings right into the balance. Special care and insulation around the high-voltage lead is of utmost importance and was accomplished by two thick layers of silicone tubing. The micropump was placed above the balance. Drop placement occurred via 0.5, 1 or 2 µL microsyringes (ILS, Germany). A scheme of the setup can be seen in Figure 21. [adapted from P5]

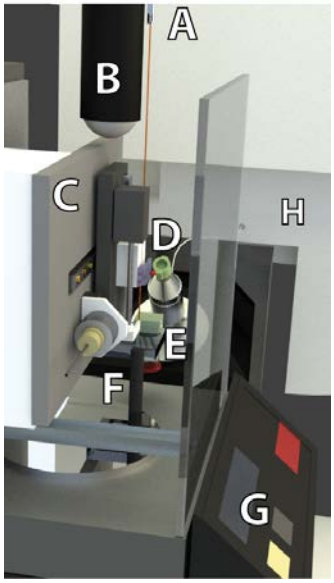

Figure 21. 3D-graphic of the sample uptake zone for preconcentration by evaporation experiments. **A** microsyringe with injection capillary **B** micropump **C** CBI unit inside the balance **D** ESI-Interface **E** injection cell **F** adapter piece for drop placement **G** microbalance display **H** TOF-MS

4.6.8 Two-Dimensional IC x CE with TOF-MS detection

For the on-line 2D coupling of IC and CE, the CBI control system (see 4.2.5 for details) acted as the modulator between the two separation dimensions with the IC being the first one and the CE being the second dimension. In combination with the TOF-MS a complex and highly orthogonal separation system integrating various colluding components was created to give an HPIC-CD-(CBI-modulator)-CE-ESI-TOF-MS setup. The micropump and the syringe equipment were removed from the modulating CBI unit and instead the outlet capillary (L= 60cm, ID= 75 µm) of a Thermo Scientific HP-Ion Chromatography system was fixed into the capillary holder and inserted into the injection cell. The BGE-filled (25 mM ammonium acetate at pH 9.15) CBI injection cell ((3) in Figure 22) was used as meeting point of IC carrier stream and CE separation capillary. Integrated into the cell were also the stirrer (5) and the high-voltage electrode (6). First step for a measurement was the perpendicular

alignment of IC capillary (2) and the CE separation capillary (4) via the xy-positioner (see 4.2.5 for the details) of the modulator. Next the alignment in z-direction and definition of the injection position (about 10 to 50 µm distance between the capillaries, see Figure 22 B) were accomplished. Measurement was started with injection of 0.4 µL sample into the injection loop and after the first analyte had passed the conductivity detector of the IC, the modulation was started and high-voltage turned on permanently. The modulator regulated the actual injection process: the IC capillary was brought for a certain time period close to the separation capillary (injection position) and was then withdrawn for a pre-set time period to a z-position far enough away from the CE capillary inlet to avoid further sample introduction (preinjection position, > 0.2 mm distance). This cycle was repeated over and over again during the turn of a measurement, i.e. until all components from the IC arrived at the MS detector. A stirrer (5) was modified for the IC x CE measurements with additional agitators to give a higher convection rate around the injection point. Further instruments required for the setup were the digital microscope camera for monitoring of the spray and the alignment of the capillaries. A scheme of the IC x CE system is shown in Figure 22.

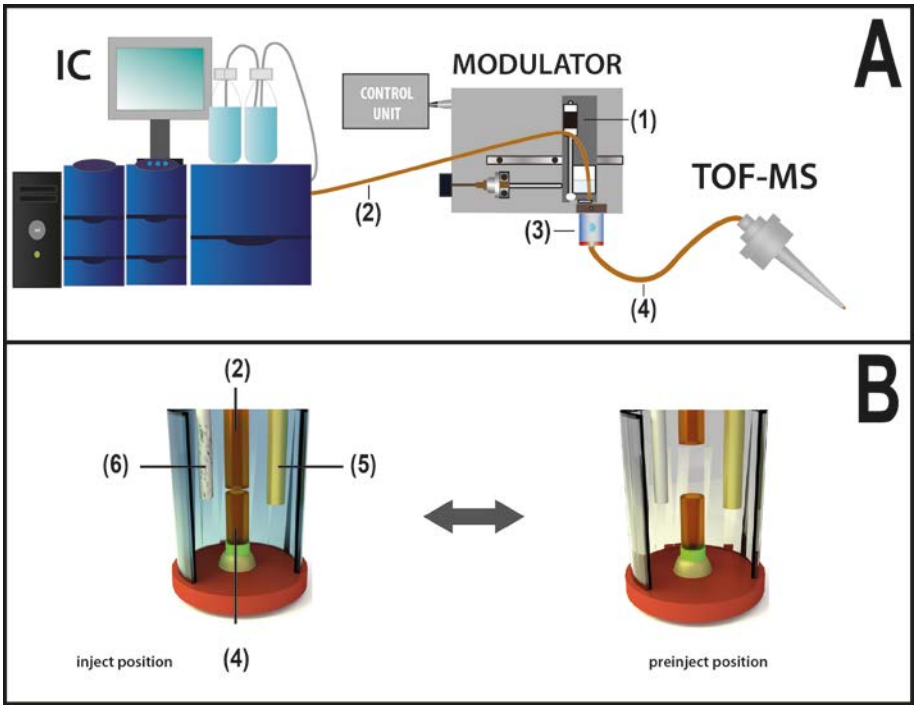

Figure 22. Coupling of IC and CE-MS. **A** The modulation unit (1) interfaces IC and CE-MS. The modulator allows precise positioning of the IC outflow capillary (2) towards the CE separation capillary (4) inside the injection cell (3). In **B** the injection cell with HV stirrer (5) and high-voltage (**6**) is illustrated. The injection in the proposed manner occurs as a repeated and timed cycle of *up-and- down* movements of the IC-capillary between inject position and preinject position.

5. Results and Discussion

5.1 HS-SDME combined with fast MCE-C^4D for Determination of Aliphatic Amines in the Biodegradation Process of Seafood Samples

5.1.1 Optimization of the microfluidic parameters

pH-optimization

Proper adjustment of the pH value is crucial for ionizing the amines and detecting them as cations. The pK_a values of these compounds are all over 9 and hence the species are present in protonated form in neutral and acidic solutions. In order to avoid high background noise and baseline unsteadiness it is ideal to choose buffers with a low conductivity. Owing to its beneficial properties, the His/MES buffer is often the first choice for C^4D measurements in CE. In order to determine the optimal pH for measurements of the aliphatic amines, 8 different buffer compositions were tested for their suitability. The pH ranged from 5.1 to 6.9 and the following His/MES ratios were used: 90 mM MES/10 mM His; 75/25; 60/40; 50/50; 40/60; 30/70; 20/80; 10/90. Prior to this study also other cumulative concentrations were evaluated. With cumulative concentrations ranging from 50 to 90 mM there were hardly any differences observable. With higher concentrations, like 200 mM, the background noise increased remarkably and resulted in diminished method performance. The desired pH values were best adjusted in the 100 mM buffers of His/MES. Other buffers tested for the measurement showed insufficient characteristics. Phosphate buffers (10 mM) or sodium acetate (4 mM) / acetic acid (10 mM) / methanol: acetonitrile (1:2) showed high background noise and signal detection was therefore not possible. Best sensitivity and suitable background characteristics were obtained for the mixture of 20 mM MES and 80 mM His at pH 6.6. This buffer composition was selected for further use in our study. As it can be seen in Figure 23 the peak shapes deteriorate upon effect of lower pH. [adapted from P1]

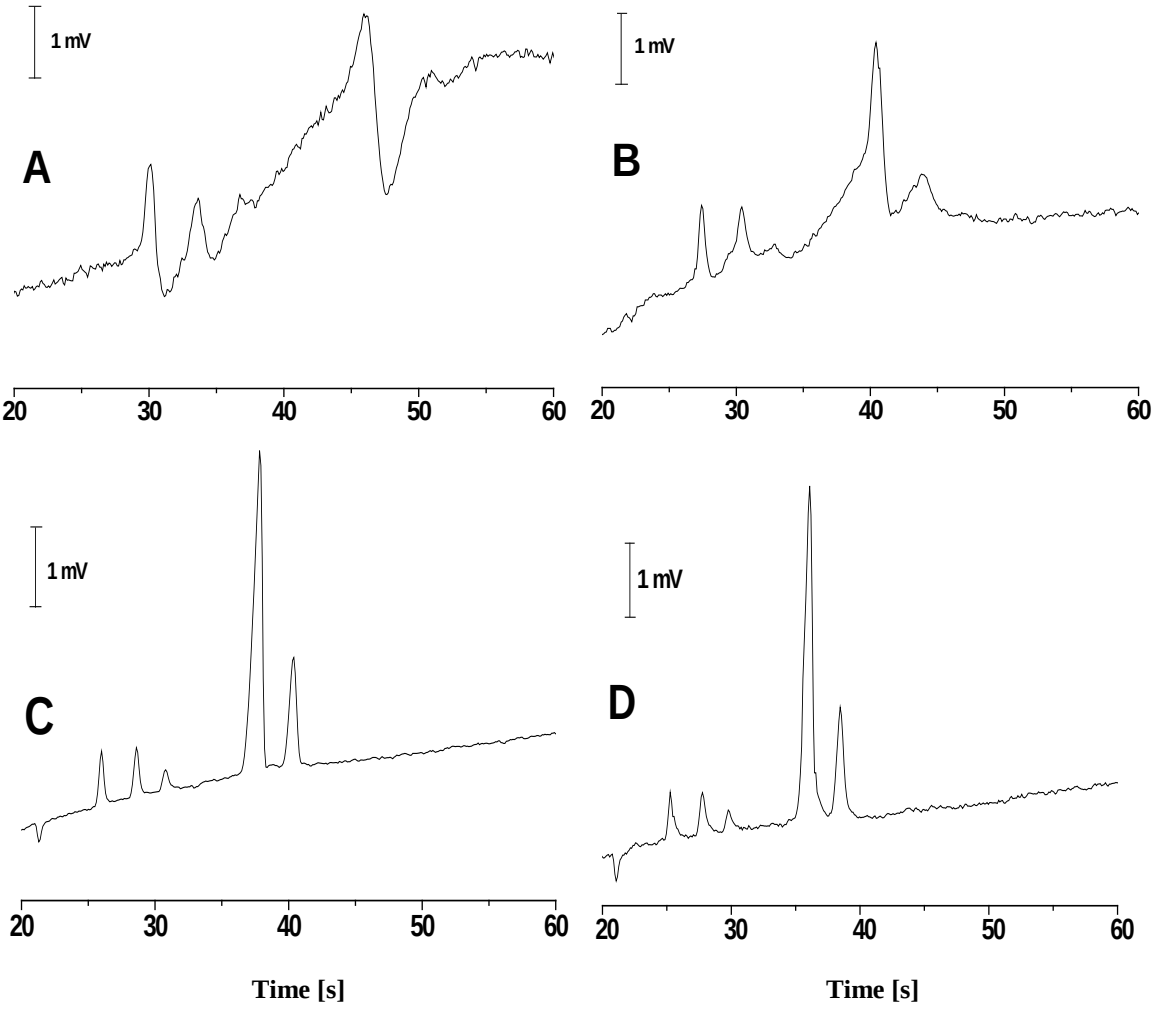

Figure 23. Effect of pH on the separation of methylamine, dimethylamine, trimethylamine, diethylamine and triethylamine (peaks appearing in this order) by microchip electrophoresis. Separation conditions: Separation voltage 3.8 kV, Injection: 0.5 kV for 5s; excitation voltage 5.6 V, His/MES buffer composition (80:20) at different pH-values: (A) pH 5.8; (B) pH 6.38; (C) pH 6.6; (D) pH 6.9. Concentration of all amines used was 0.5 µg/mL.

Optimization of the separation voltage

The maximum separation voltage that can be applied using the microfluidic analysis system is 3.8 kV. The effect of the separation voltage on the performance of separation was studied within a range from 2.5 to 3.8 kV. It turned out that the highest voltage delivered the best results for the separation of the target analytes. The target species are well separated following the order of their increasing size in less than 35 s. However, the reduction of separation voltage only resulted in longer migration times whereas the resolution and separation efficiencies were not improved. Figure 24 shows an electropherogram for the separation of 5 short-chained aliphatic amines. Baseline resolution for all target analytes was achieved.

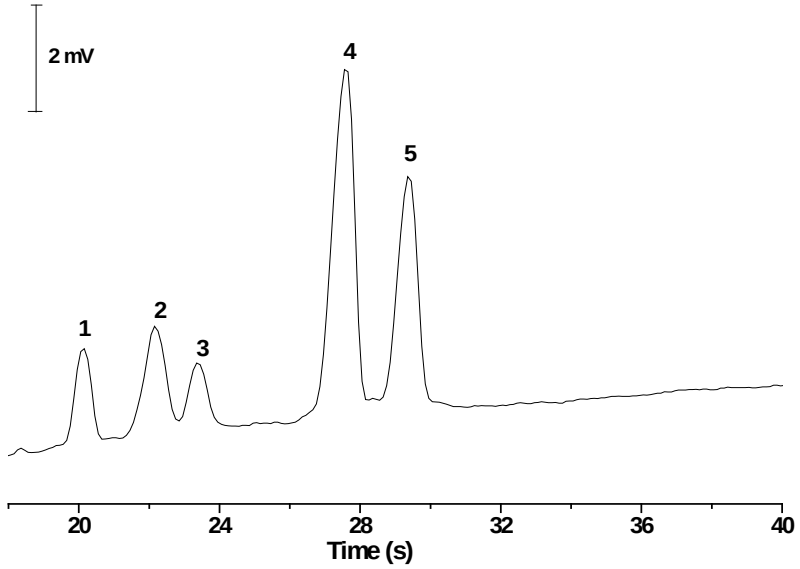

Figure 24. Electropherogram for a mixture of 5 µg/mL of each (1) methylamine, (2) dimethlyamine, (3) trimethylamine, (4) diethylamine and (5) triethylamine in His/MES (80:20 mM) buffer, pH 6.6, at a separation voltage of 3.8 kV using a miniaturized microchip electrophoresis device with contactless conductivity detection. Further conditions: injection: 0.5 kV for 5 s across the injection channel; excitation voltage: 5.6 V.

Optimization of the detector excitation voltage

In order to optimize the signal-to-noise characteristic the effect of the applied excitation voltage was studied. The ChipGenie® edition E allows a variation of the AC excitation voltage between 0 and 12 V. For excitation voltages not higher than 3 V the sensitivity was found to be rather low. Basically, no signal peak from the amines could be identified in this range. Once the excitation voltage amplitude reaches 4 V, the response for the aliphatic amines improves significantly. Changing the excitation voltage from 4 to 5.5 V the signal-to-noise ratio constantly increases and peak areas are growing steadily. Nevertheless, voltages above 5.5 V delivered also peak distortions and a significant baseline drift with higher background signals. Thus, the best response characteristics can be obtained by applying an AC voltage of 5.6 V to the thin-film electrodes. The signal-to-noise ratio was determined as the ratio of signal peak height to peak-to-peak baseline noise height. In Figure 25 the effect of excitation voltage on the signal-to-noise ratio is illustrated.

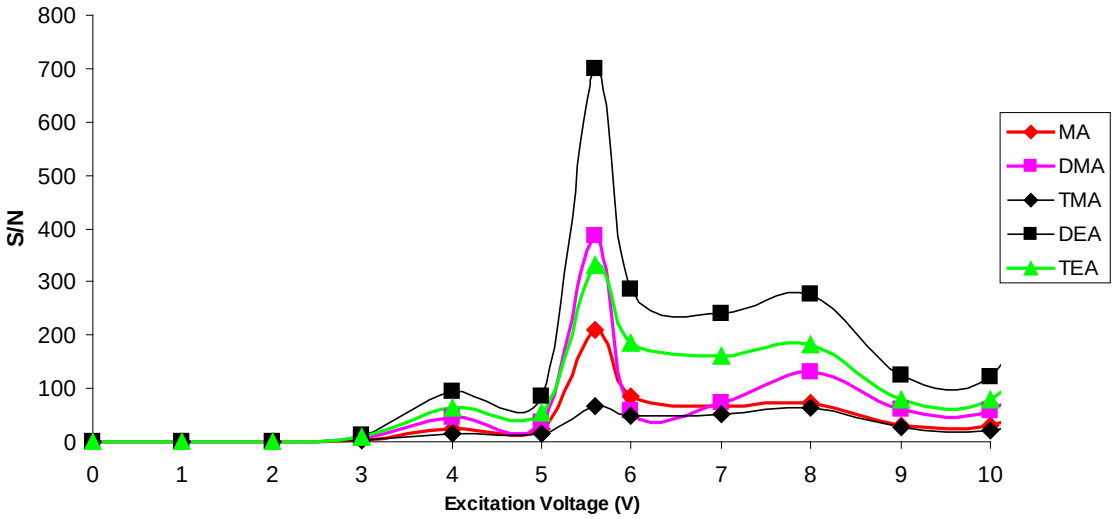

Figure 25. Effect of the excitation voltage applied to the thin-film gold electrodes on the signal-to-noise ratio. A clear maximum at around 5.6 V can be observed for all determined compounds. All measurements were carried out using a His/MES buffer at pH 6.6. Separation voltage applied to the microchip electrophoresis device was 3.8 kV. The analytes studied were methylamine (MA), dimethylamine (DMA), trimethlylamine (TMA), diethylamine (DEA) and triethylamine (TEA), measured at 5 ppm, respectively.

Analytical characteristics

The capacitively coupled contactless conductivity (C^4D) detector based on thin-film gold electrodes displayed well-defined concentration dependence. Figure 26 shows the excellent reproducibility for repetitive separations of the aliphatic amines. Under the optimized conditions, the linear ranges of methylamine, dimethylamine and trimethylamine were all covering the concentration interval from 0.5 to 10 ppm. The linear ranges for diethylamine and triethylamine were ranging from 0.1 to 10 ppm. The limits of detection were all well below 400 ng/mL. Linear correlation was lost upon increase of concentrations over 10 ppm and a plateau is developing towards higher concentrations. The average peak areas from 7 to 10 measurements, without SDME pretreatment, were taken into the evaluation of the calibration results. Table 6 shows the relevant analytical characteristics of the chip electrophoresis – C^4D protocol for aliphatic amine determination.

Table 6. Analytical characteristics for the determination of low aliphatic amines via microchip electrophoresis on a PMMA chip and C^4D

Analyte	MA	DMA	TMA	DEA	TEA
R^2	0.993	0.986	0.992	0.991	0.994
Sensitivity (mV/s) / (µg/mL)	0.252	0.424	0.121	1.053	0.511
Working range (µg/mL)	0.5 - 10	0.5 - 10	0.5 - 10	0.1 - 10	0.1 - 10
LOD [a] (ng/mL) (based on S/N=3)	137.6	85.2	396.5	41.0	99.9
Intra-day RSD[b] (%) (Conc. 1 µg/L)	2.4	3.7	4.8	10.4	8.3
Inter-day RSD [c] (%) (Conc. 1 µg/L)	5.6	5.1	8.3	19.8	15.8

[a] Limit of detection, concentrations corresponding to peak heights exceeding three times the baseline noise
[b] Relative standard deviation for the peak areas for repetitive injections of 1 ppm, n=5
[c] Relative standard deviation for the peak areas for injections of 1 ppm on 4 different days, n=5,

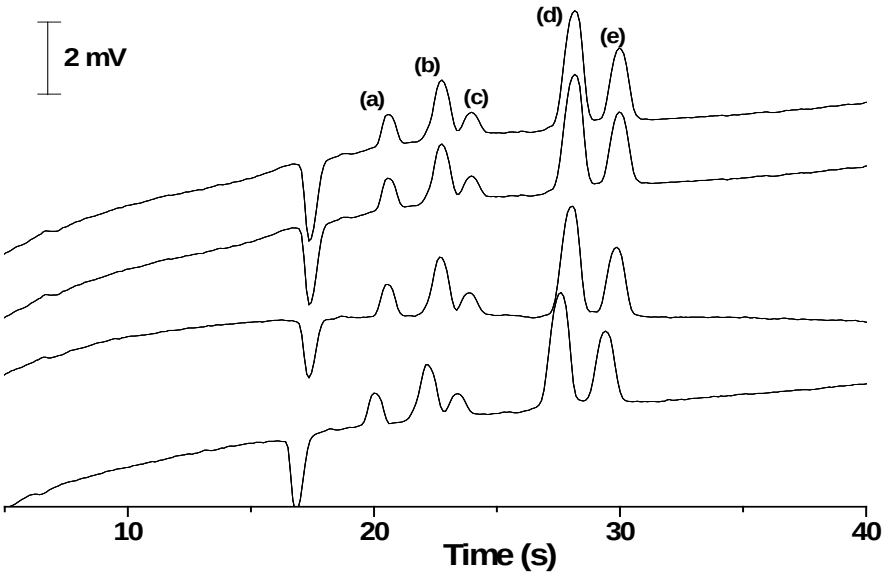

Figure 26. Repetitive electropherograms for the separation of five short-chained aliphatic amines on a microchip electrophoresis device under optimized conditions. Separation conditions as in Figure 24. The signals correspond to the following aliphatic amines (a) methylamine (b) dimethylamine, (c) trimethylamine, (d) diethylamine and (e) triethylamine. The concentration of all amines was 5 µg/mL.

Long-term performance

The thin-film electrodes are not contacting the solution. However, the gold films are exposed to the impact of the spring contacts implemented in the ChipGenie® edition E. This led to a deterioration of the gold surface and after an enhanced number of chip runs the signal response got worse until it died off completely at some point (more than 500 runs). To prevent this problem silver paste was put on the damaged spots of the electrodes. After this, good long-term stability for the chips in use could be obtained. More than 1000

electropherograms could be recorded with one PMMA microchip of this kind. Thus, the PMMA microchips offered enhanced performance stability compared to the often used and easier fabricated PDMS chips. Upon long-term use a shift of the migration times toward longer separation times was observed. For consecutive intraday-runs the reproducibility of the migration times was evaluated together with the corresponding values for interday measurements. For eight consecutive runs (N=8, respective analyte concentration=5 ppm) the RSD%-values for the migration times were for the 5 compounds in a range from 0.41 to 0.66%. For the interday evaluations (N (days) =4, repetitive days) RSD%-values in an interval ranging from 1.11 to 1.55% were obtained. However, the shift towards longer migration times for long-term used chips (more than 500 sample injections) compared to newly manufactured chips is significant. An increase of up to 10 seconds could be observed when comparing a fresh chip with an older one. This result is probably due to adsorption effects to the channel surface. Analyte molecules constantly cover more of the surface of the channel and subsequently measured analytes are thus held back longer on their way to the detection electrodes. [adapted from P1]

5.1.2 Optimization of the HS-SDME parameters

Optimization of extraction time

The effect of the extraction time on the analytical performance was tested. The extraction time was varied in a range from 2 to 16 minutes and the respective resulting peak areas for the analytes were determined. It was found that best results for most of the analytes were obtained for a sonication time of 10 minutes.

Optimization of NaOH addition for extraction

Another parameter that had to be considered was the amount of alkaline solution that is added to the sample solution in order to volatilize the compounds. The addition of different amounts of 50% NaOH solution to the analytes was investigated. The sensitivity of the method increased steadily up to the addition of 1 mL, whereas for higher amounts than 1 mL the performance did not improve further. This effect is explained with the complex shifts in phase equilibrium in the headspace mode upon NaOH addition. The smaller the headspace volume (i.e. less space for analyte molecules), the better is the sensitivity of the method [135]. [adapted from P1]

5.1.3 Application to real world samples

The complex matrices of seafood samples such as shrimp with the presence of a variety of other biogenic amines are a challenge for the selective determination of the volatile degradation products responsible for toxic consequences of tissue decay. Initial tests showed that a direct injection of aqueous shrimp extracts into the microchip system results in a disturbed detection of the target analytes due to the interference of other cationic compounds in the sample which appear at similar or same migration times. An approach to solve this problem is the ultrasound assisted HS-SDME. During the studies the use of SPME fibers with a polydimethylsiloxane (PDMS) and polydimethylsiloxane/divinylbenzene (PDMS/DVB) coating was evaluated. These fibers are comparably expensive and do not deliver any improvements regarding the extraction of the desired target analytes. None of these approaches resulted in suitable outcomes regarding the method performance. Furthermore the desorption of analytes from the extraction fiber into the small sample reservoir of the microchip is a fairly unpractical and more time-consuming process step compared to the SDME procedure. Using the SDME technique instead allows the straightforward transfer from a very complex matrix to an ideal solution matrix that is suitable for the direct injection into the MCE-C^4D system. Extracts from commercially available shrimp, purchased from local grocery stores (Regensburg, Germany), were injected for evaluation of practical application. Samples were crushed and 500 mg were diluted with 1 mL of running buffer and 1 mL of NaOH in a septum vial. After preconcentration in the 5 µL buffer drop the solutions were diluted 10-fold and injected into the miniaturized Chip-CE-C^4D system. For injection-to-injection reproducibility (of peak areas) for 7 consecutive measurements of a shrimp sample relative standard deviations of 4.7 (DMA) and 6.4% (TMA) resulted. A standard addition determination of DMA in a fresh shrimp sample was studied and additions of 0.5, 1 and 1.5 µg/mL were applied. A concentration of 7.2 mg/kg DMA in the shrimp originating from the Pacific Ocean was calculated. Furthermore, the enhanced biodegradation due to improper storage was monitored with our method. The shrimp samples were kept aerated at room temperature and thus the progress of amine development with time could be observed. In Figure 27 the rise in ammonia, dimethylamine and trimethylamine upon decay of the tissue is illustrated. In case of trimethylamine a 6-fold increase in concentration was measured over the turn of one week of improper storage of the shrimp tissue. [adapted from P1]

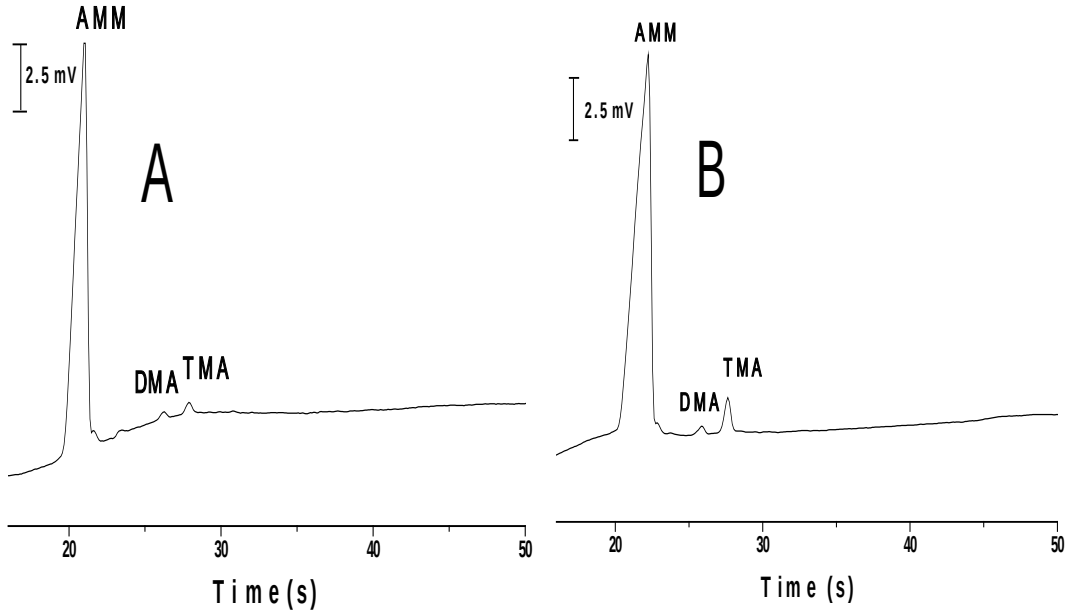

Figure 27. Electropherograms of the determination of ammonia (AMM), dimethylamine (DMA) and trimethylamine (TMA) in fresh shrimp. **A** sample taken from a just opened, refrigerated shrimp package **B** rotten shrimp kept unrefrigerated and aerated at room temperature for 7 days.

5.1.4. Conclusion

In the course of this study we established the method protocols for the quick and reliable determinations of aliphatic amine compounds (MA, DMA, TMA, DEA and TEA) using a combination of SDME and MCE on a newly developed portable device based on microchip electrophoresis with contactless conductivity detection. A quick and reliable separation of the target analytes could be achieved in less than 40 s. It could be proven that the procedure can be applied to the determination of volatile amines in shrimp tissue. The contactless conductivity detection makes the method even more attractive, as it provides good sensitivity, easy implementation, is a low-cost method and prevents electrode fouling as the analytes never contact the measuring electrodes. The use of HS-SDME was found to be an effective means for interfacing chip electrophoresis with real world samples. In this way, the presented approach offers great potential for the monitoring of important processes in quality control, environmental settings and metabolism studies. In comparison to conventionally used lab-based systems the miniaturized setup offers the advantages of high speed, efficiency, portability and the consumption of low sample and reagent amounts. Thus, this approach promises to result in a truly total microanalytical system. [adapted from P1]

5.2 Comparison of the performance characteristics of two tubular contactless conductivity detectors

5.2.1 Calibration dependence

Principal analytical parameters were determined from the detector responses to the KCl solutions under non-separation conditions. A typical calibration curve for the detector with cell 1 is shown in Figure 28 (the calibration dependence for the detector with cell 2 is similar); nonlinear calibration dependences for wide concentration ranges are commonly encountered for C^4D due to the complex character of the measured signal. The calibration curve can be split into two linear segments. The regression equations and the respective conductivity intervals of each segment are listed in Table 8. The LOD for detector alignment with cell 1 and 2 were determined from the triple baseline noise value (see inset in Figure 28) and the respective regression equation (Table 7) and amounted to 0.4 μM KCl (5.7×10^{-6} S m^{-1}) and 0.2 μM KCl (3.2×10^{-6} S m^{-1}), respectively. The inset in Figure 28 also illustrates the objectivity of the LOD values estimated. The analytical characteristics for detection of KCl obtained in this work and those published in the literature are compared in Table 8. It is evident that the parameters differ not significantly for various cell geometries and C^4D operational parameters. These results are in good agreement with previous work that studied this aspect of C^4D detection [87, 134]. [adapted from P2]

Table 7. Calibration parameters for the tested detectors with tubular cell (y, detector response, κ, specific conductivity)

Conductivity interval, [Sm^{-1}]	Regression equation, y [V], κ [Sm^{-1}]	Coefficient of determination, r^2
Cell 1		
$1 \times 10^{-4} - 1.5 \times 10^{-3}$	$y = -0.29 \pm 0.10 + (3721 \pm 126)\ \kappa$	0.994
$1.5 \times 10^{-5} - 1 \times 10^{-4}$	$y^* = (1582 \pm 93)\ \kappa$	0.990
Cell 2		
$1.5 \times 10^{-4} - 1.5 \times 10^{-3}$	$y = -0.26 \pm 0.11 + (4212 \pm 127)\ \kappa$	0.996
$7.5 \times 10^{-5} - 1.5 \times 10^{-4}$	$y^* = (2832 \pm 140)\ \kappa$	0.998

*) Intercept zero value lies within reliability interval.

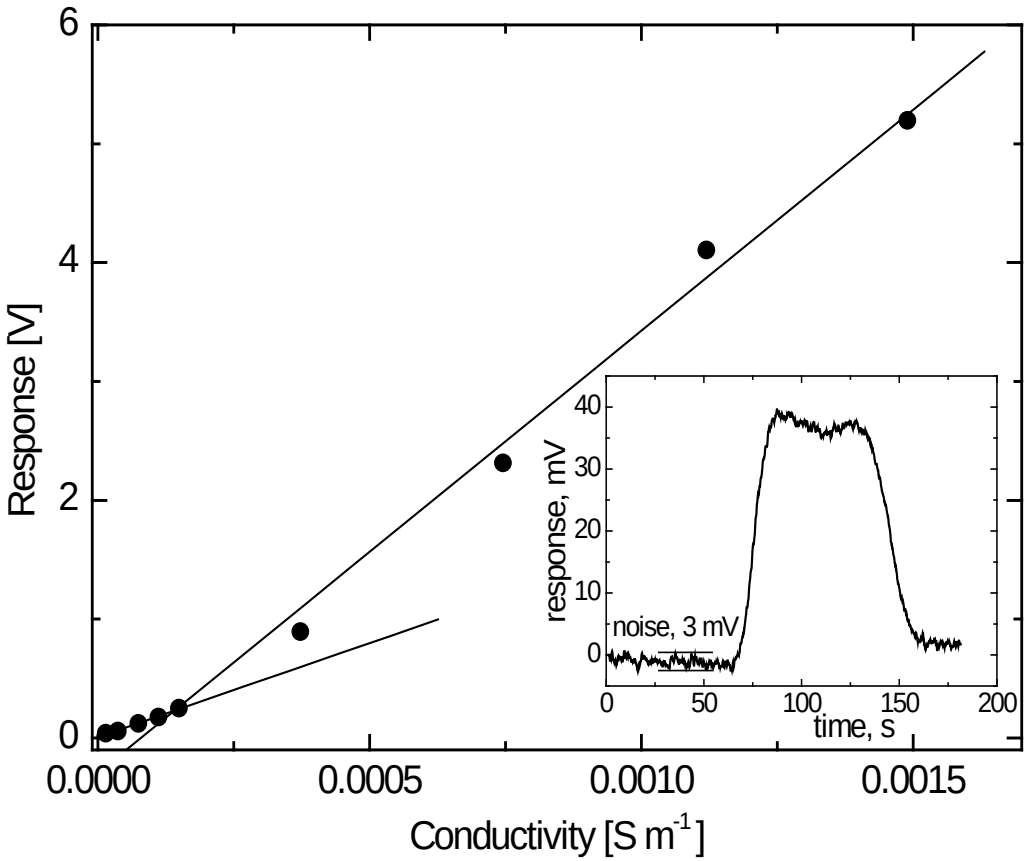

Figure 28. Dependence of the response of the detector with cell 1 on the solution conductivity. The points are medians of three measurements (RSD 0.3–6%). Measurements were done under steady-state conditions injecting 500 μL of KCl solutions. Inset: example of the response to the solution with the lowest tested conductance, 1.5 x 10^{-5} S m^{-1} (1 μM KCl)

Table 8. Comparison of analytical characteristics for the contactless conductometric detection of KCl in the liquid chromatography arrangement obtained in this work with values published in the literature

Detection cell	C^4D parameters	Linear dynamic range, μM	Limit of detection, μM	Ref.
Thin-layer	100 kHz/10 V	0.5 – 1000	0.2	[129]
Tubular	150 kHz/50 V	8 – 80	0.6	[137]
Tubular	290 kHz/20 V	2 – 100	0.6	[139]
Tubular, cell 1	100 kHz/10 V	1 – 10 5 – 100*	0.4	This work
Tubular, cell 2	100 kHz/10 V	5 – 10 5 – 100*	0.2	This work

*) Calibration dependence with two linear segments, maximum tested concentration, 100 μM KCl

5.2.2 Comparison of the experimental calibration dependence with a theoretical model

The current flowing through the detection cell is determined by the cell impedance, *Z*, which can be described by equation (1) (for the details see [129, 139]; all parameters in the equations below are specified in Table 1 and Figure 11):

$$Z = \frac{\left[R - \frac{2i}{\omega C}\right]\frac{-i}{\omega C_X}}{R - \frac{2i}{\omega C} - \frac{i}{\omega C_X}} \tag{1}$$

where $\omega = 2\pi f$ is the angular velocity. *R* is the cell resistance and *C* is the capacitance of the tubular capacitors calculated from the respective equations:

$$R = \frac{1}{\kappa}\frac{L}{a} \tag{2}$$

and

$$C = \frac{\pi \varepsilon_r \varepsilon_0 w}{\ln\frac{\rho}{r}}. \tag{3}$$

The signal passing through the cell is alternating current, *I*, which depends on the input AC voltage amplitude and the cell impedance. The difference of the current, ΔI, is registered

$$\Delta I = \frac{U}{|Z(\mathrm{KCl})|} - \frac{U}{|Z(\mathrm{H_2O})|} \tag{4}$$

where *Z* (KCl) and $Z(H_2O)$ are the cell impedances containing a KCl solution and pure water, respectively. Based on these equations, the calibration dependence can be modelled. The equivalent circuit of the cell used for model calculations is very simplified, therefore the absolute values of the calculated dependence usually differ significantly from the experimental values. For meaningful comparison of at least the course of the computed and experimental calibration curves, these two are compared in normalized form, i.e., the individual response values are divided by the largest value.

The electrode width, *w*, which influences both principal parameters characterizing a detection cell, namely the capacitance *C* and the resistance *R* (where the geometric cell length, $L=2w + d$), plays a decisive role. Reasonable agreement between the experimental and the modelled calibration dependence could not be obtained, when the geometric electrode width was taken into computation. In case the value of the electrode width was lowered in the computation,

satisfactory agreement between experimental and modelled course of the calibration curves for cell 1 was obtained for the electrode width of 1.4 mm (see Figure 29). The relatively strong effect of the electrode width on the modelled calibration dependence is illustrated also for another two different values in Figure 29. Similar calculations can be applied to cell 2. [adapted from P2]

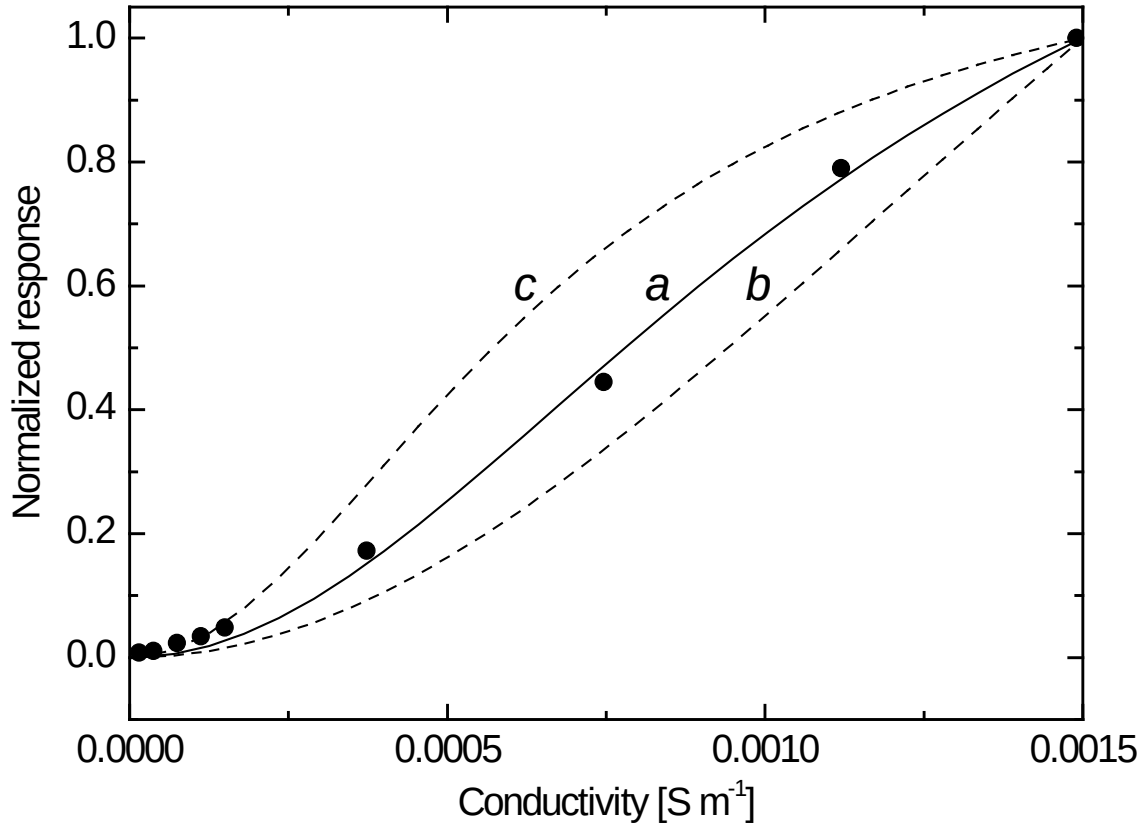

Figure 29. Comparison of the experimental (points) and the modelled (lines) dependences of the detector response on the solution conductivity for cell 1. Curve *a*, the best fit for the effective electrode width of 1.4 mm, curve *b* and *c* for the electrode width 2.0 and 1.0 mm, respectively.

The effect of the electrode width on the detector signal stems from the dependence of the cell impedance *Z* on the electrode width. As shown in Figure 30, the dependence passes through the minimum for a certain electrode width. The current signal follows a trajectory characterized by the lowest impedance on passage through the cell. Consequently, the signal does not pass through the whole geometric electrode width, *w*, but only through a specific part, the effective width, w_{eff} [132, 139]. The effective electrode width varies, among other aspects, with the cell geometry and with the conductivity of the solution in the cell, see inset in Figure 30. Therefore, the estimated effective electrode width, 1.4 mm, for which the calibration curve was calculated, is in an acceptable agreement with the experiment. The result is not far from the values calculated on the basis of the simple model. This value represents a certain average value of the effective electrode width within the conductivity

range tested. For the thinner tube wall and the greater tube opening, the impedance of the cell 2 is lower than that of the cell 1, which is also evident from Figure 30.

The theory with regard to the electrode effective width has a significant practical consequence. In designing C^4D cells, the electrode geometric width and thus the geometric detection volume is not a critical parameter; the small influence of the geometric electrode width on the magnitude of the signal measured and on the width of the analyte zones has been found also in CZE [140]. The effective detector volume, $V_{eff} = (2 \times w_{eff} + d)\ \pi r^2$ varies with the solution conductivity and for the value of w_{eff} = 1.4 mm (used in the model calculations, see above) equals 0.2 μL, i.e., the effective detection volume of the cell 1 is three times smaller then the geometric one. The best fit of the theoretical and modelled concentration dependence for cell 2 was obtained for w_{eff} = 1.6 mm; using this value, the effective volume of the cell 2 is 0.9 μL. It must be realized that the electrode effective width is also significantly dependent on the frequency of the AC voltage used. The higher the frequency, the shorter is the electrode effective width. The electrode effective widths used in the model calculations were computed for the 100 kHz frequency applied in the measurements [adpated from P2].

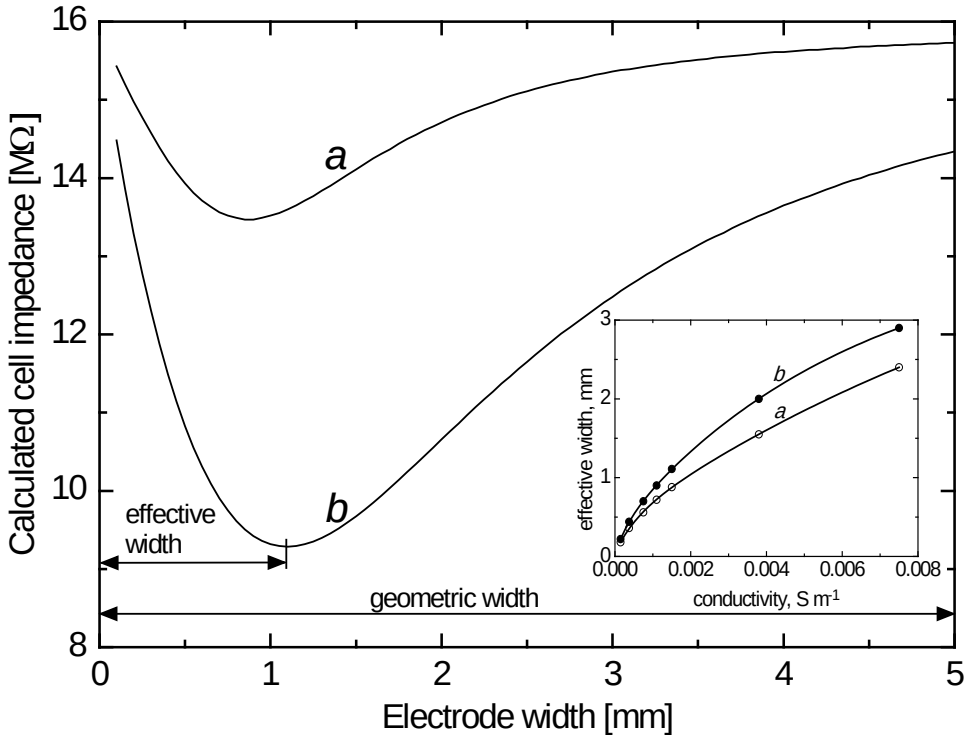

Figure 30. Calculated dependence of the cell impedance on the electrode width for cell 1 (*a*) and cell 2 (*b*) for a solution with a conductivity of 1.5 x 10^{-3} S m^{-1} (100 μM KCl). Inset: calculated dependence of the effective electrode width on the solution conductivity, cell 1 (*a*), cell 2 (*b*)

5.2.3 Application of the tubular C^4D cells in conjunction with HPLC

In this study the same model system as selected in [129] was used to enable the comparison of the performance characteristics. The model compounds were benzoic acid, sodium capronate, lactic acid and octanesulfonic acid. Except benzoic acid, the utilized organic acids are hardly detectable by conventional UV-absorption detection. In contrast, all four organic acids can easily be detected by the C^4D method; Figure 31 shows the chromatograms obtained using the respective C^4D cells. The chromatograms are comparable; not all the peaks are resolved to the baseline because no thorough optimization of the separation conditions was carried out for the purpose of our tests. Table 9 summarizes the dependences of the C^4D response on the tested analyte concentrations when using the detection cells 1 and 2. The detector responses with both detection cells are linear for all four analytes over the entire concentration range investigated. The zero intercept values lie within the confidential intervals for all the calibration equations except for that of benzoic acid in detection cell 2.

The coefficients of determination consistently limit to 1.0 and the limits of detection (determined as the three times baseline noise (S/N=3)) were found to range between the values of 0.7 and 9.9 μM for both tubular detection cells. Contrary to the model computations and the results obtained for KCl under steady-state conditions, in the chromatographic configuration the detector with cell 1 gives a higher sensitivity compared to that of the detector with cell 2; see the respective slopes of the regression equations in Table 9. One possible explanation for this behaviour might be that under chromatographic conditions the zone is not wide enough to establish a stationary analyte concentration in the detection cell. The zone is thus diluted by the mobile phase and this dilution is more pronounced in the cell with greater geometric volume (cell 2). The signal measured is apparently affected more by the dilution effects than by the thickness of the detection cell wall. For this reason, cell 2 yields a lower signal in the chromatographic system, even if its wall is thinner than that of cell 1. The respective limits of detection are lower for all compounds using the detector with cell 1 compared to detection with cell 2 and reaching a minimum LOD of 0.7 μM for octanesulphonic acid. In overall comparison to the planar arrangement, both tubular cells show higher sensitivity and lower LOD's (see Table 9). Furthermore, the tubular cells show a significant (5-fold) better separation efficiency and increased resolution (regarding peaks 3 and 4) compared with the thin-layer alignment. The two tubular cells show no significant differences regarding separation efficiency with plate heights equal to 0.22 mm for sodium capronate in both cell 1 and 2. For these relatively low separation efficiencies it is reasonable

to assume, that the slightly larger sample zone dilution in cell 2, which observably has influenced the sensitivity, has almost no impact on separation efficiency. [adapted from P2]

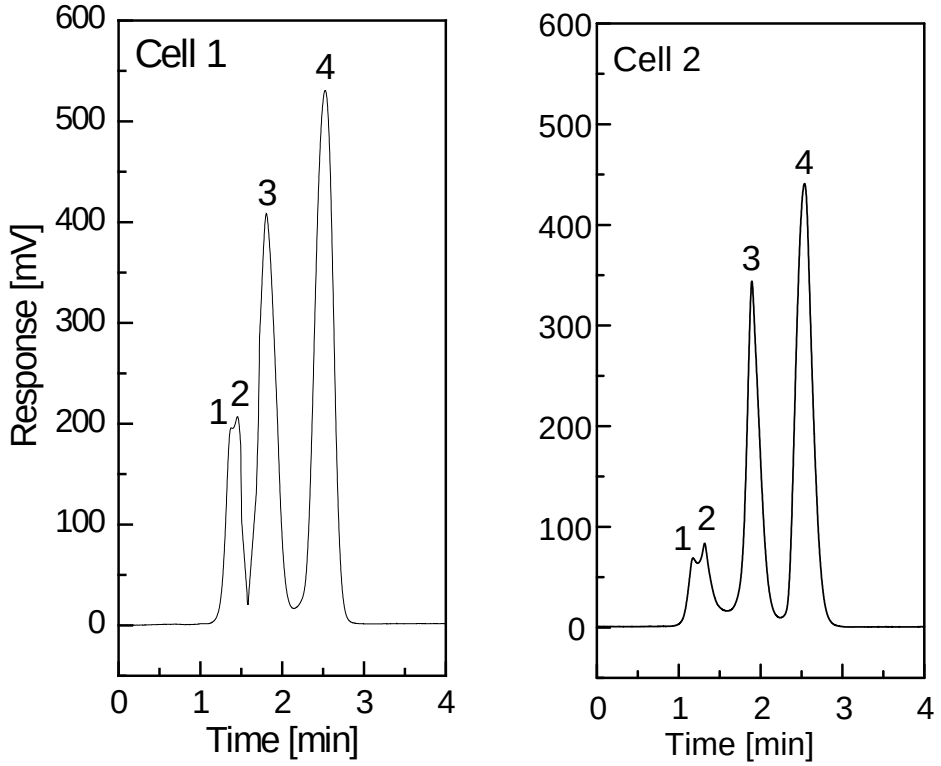

Figure 31. Chromatograms of the test mixture measured on the tubular C^4D with cell 1 and cell 2. Peak identification with the analyte concentrations (mM) in parentheses: (1) octanesulfonic acid (0.3); (2) lactic acid (0.4); (3) benzoic acid (2.0); (4) sodium capronate (8.0). The mobile phase was 60% acetonitrile/40% water (v/v), a flow rate of 0.8 mL min^{-1} and an injection volume of 10 µL were used

Table 9. Calibration results for the tested organic compounds in the concentration range from 0.01 to 1 mM, obtained according to single-substance determinations with tubular cell detectors (number of experimental points, 8, y, detector response, *c*, concentration).

Analyte	Regression equation, *y* [mV], *c* [mM]	Coefficient of determination	Limit of detection [μM]
Cell 1			
Sodium capronate	$y = (514.9 \pm 9.0)\ c$	0.998	5.8
Benzoic acid	$y = (1222.1 \pm 17.9)\ c$	0.998	2.5
Lactic acid	$y = (1547.8 \pm 13.0)\ c$	0.999	1.9
Octanesulfonic acid	$y = (4334.8 \pm 51.5)\ c$	0.999	0.7
Cell 2			
Sodium capronate	$y = (303.4 \pm 5.5)\ c$	0.998	9.9
Benzoic acid	$y = -9.7 \pm 3.8 + (710.6 \pm 7.9)\ c$	0.999	4.2
Lactic acid	$y = (1040.7 \pm 12.3)\ c$	0.999	2.9
Octanesulfonic acid	$y = (2790.7 \pm 31.7)\ c$	0.999	1.1
Thin layer cell [27]			
Sodium capronate	$y = (32.7 \pm 3.1)\ c$	0.991	27.0
Benzoic acid	$y = (-0.7 \pm 0.5) + (125.4 \pm 1.0)\ c$	0.999	7.2
Lactic acid	$y = (4.6 \pm 1.9) + (284.1 \pm 4.7)\ c$	0.999	3.1
Octanesulfonic acid	$y = (622.3 \pm 9.8)\ c$	0.999	1.6

5.2.4 Conclusion

The two tubular cells, differing in their geometric parameters, were tested for contactless conductivity detection in LC and their characteristics were compared with those of a previously studied thin-layer cell. The cells were tested under non-separation conditions with model solutions of KCl and the applicability to detection in LC was tested using a set of ionic organic compounds. It was found (see Tables 8 and 9) that the analytical characteristics are similar for both tubular cell configurations. Calibration dependence for the steady-state response can be described acceptably by the simple theoretical model provided that the electrode effective width concept is employed. In summary it can be concluded that both detection cell designs are applicable for C^4D in LC. However, in comparison with the thin-layer cell, the tubular cells are substantially simpler and their fabrication is much easier. Above that, it was found that the tubular cells are outperforming the thin-layer cell in terms of the main analytical parameters. From this point of view, detectors with the tubular cells are more suitable for contactless conductivity detection with HPLC. [adapted from P2]

5.3 Very fast capillary electrophoresis with electrochemical detection for high-throughput analysis using short, vertically aligned capillaries

5.3.1 Choice of model compounds, detection parameters and buffer system

FcMTMA acetate, basic violet 16 as well as basic green 1 form cationic species in the used NACE buffer. Ferrocene was used as neutral EOF marker in some instances. The non-aqueous buffer system consisted of 1 M acetic acid and 10 mM ammonium acetate in pure ACN (acetonitrile). This kind of background buffer has a number of advantages: favorable electroosmotic and electrochemical properties, low viscosity of ACN is beneficial to measurements in small ID capillaries and the high ratio of dielectric constant to viscosity aids in speeding up the separations. For all model substances a suitable amperometric response signal was obtained. The FcMTMAA is oxidized at much lower potential (0.4 V) as compared to the two dye substances (redox potentials at around 1.0 – 1.1V vs. Ag/AgCl). The Pt microdisk electrodes offer very good stability of amperometric response characteristics in nonaqueous media. An important aspect in end-column CE-AD measurements is the detection potential shift due to the electrophoretic current. Hence, the AD characteristics were studied under the influence of a moderate separation voltage. Hydrodynamic voltammograms (HDV) for all three substances were therefore generated for an electric field strength of 1 kV/cm. The respective HDVs were recorded in a range from +0.5 V to +1.7 V at a 50 µm platinum microdisk working electrode. Current plateaus were reached at 1.0 V for FcMTMAA and at 1.5 V for the other two substances under the above mentioned HV separation conditions. Hence, a voltage of 1.3 V was chosen for most experiments, as the signal-to-noise ratios become unfavourable at higher detection potentials for all substances.

5.3.2 Effect of the applied voltage and injection conditions

The effect of applied separation voltage on the observed separation efficiency was investigated in a range from 3.5 kV (corresponding to field strength of about 0.5 kV/cm) to 22 kV (3.0 kV/cm) using a 7 cm short capillary with 15 µm ID capillary. The respective migration times of the analytes were shortened significantly along with a trend towards sharpening of the peak shape (depending on capillary ID). For larger ID (>25µm) capillaries increased field strengths resulted in substantial background noise and peak broadening due to increased Joule heating and potential shifts that disabled the detection of the two textile dyes.

Furthermore, with smaller ID capillaries like the 10 µm ID capillary it was possible to separate the three cationic species at field strengths of about 3 kV/cm. It was found that for a detection potential of 1.3 V, current signals decrease with higher field strengths due to the increased potential shift (Figure 32). This observation is confirmed by the observation that the FcMTMAA (the compound with the lowest oxidation potential) peak height remains at a similar level for field strengths from 1.0 kV/cm to 2.0 kV/cm, whereas dyes with higher oxidation potential show significantly reduced peak height with increasing field strength due to the potential shift effects.

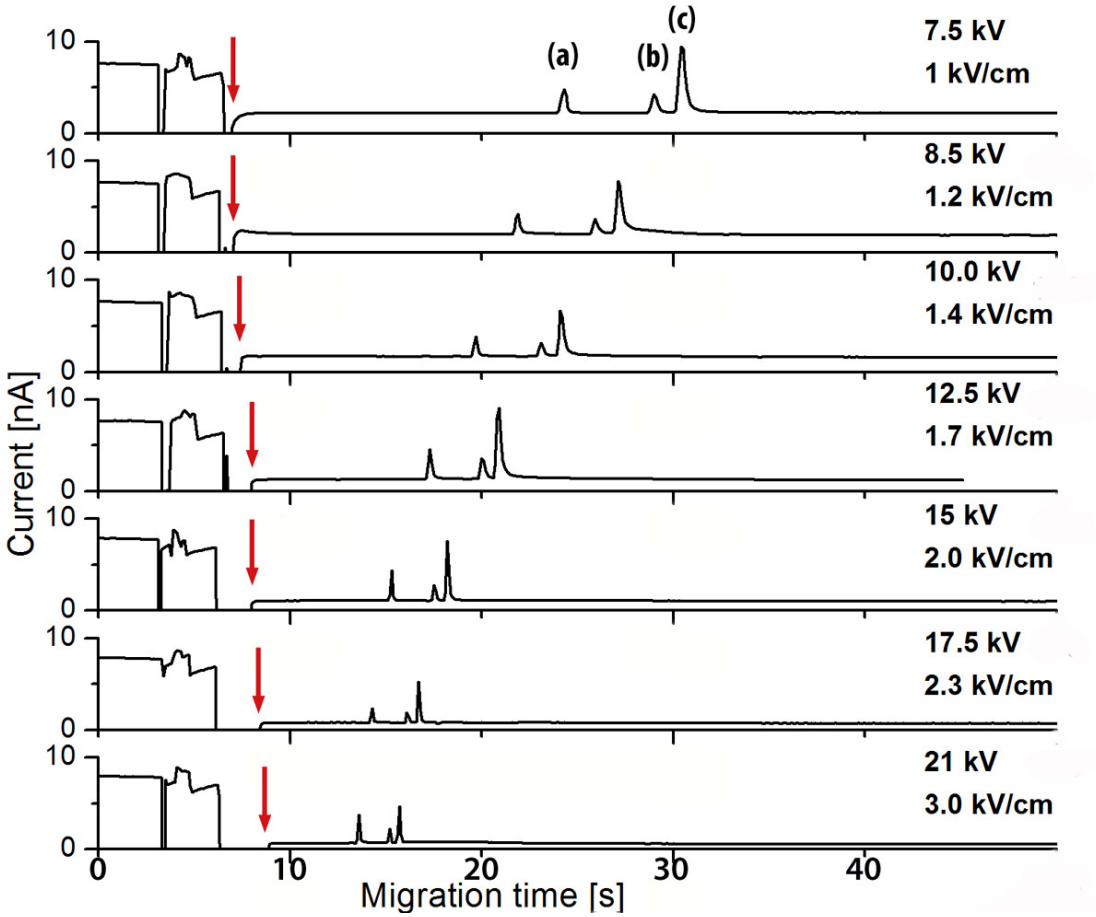

Figure 32. CE-AD investigations of the three model substances FcMTMAA (a), basic violet 16 (b) and basic green 1 (c) at different electric field strengths. Individual runs started at the points indicated by the arrows, respectively. Separation capillaries: 10 µm ID, 7 cm length; analyte concentrations: 10 µM; buffer: non-aqueous buffer system consisting of acetonitrile, 1 M acetic acid and 10 mM ammonium acetate; detection potential 1.3V.

The effects of (electrokinetic) injection time and injection voltage were examined for injection times ranging from 0.1 s to 1.0 s at different voltages of 5 to 10 kV. The responses were investigated with special regard to the peak broadening and the signal intensity. Even though amperometric signals increase more or less linearly with the injection times at

different voltages it was observed, that for the band broadening a dramatic increase occurs from 0.5 s onwards. The 0.1 s injection results in very low current signals which is probably just the effect of spontaneous injection [141] and as both 0.1 s and 0.2 s injections showed to be less reproducible than 0.3 s injections, we settled with 0.3 s as the best suited injection time.

5.3.3 Optimization of capillary inner diameter

With the use of shorter capillaries comes the need to reduce more and more the injection volume in order to keep band broadening at a minimum. The easiest approach to do this is the reduction of capillary inner diameters. Use of smaller diameters offers further advantages in CE-AD: first Joule heating is reduced, secondly the influence of the HV electrical field on the detection electrode potential is decreasing with decreased capillary ID. In turn, lower electrophoretic currents enable a wider spectrum of background electrolytes. Figure 33 shows the different electropherograms for separations of the model mix in vertically aligned 7 cm-long capillaries with ID ranging from 50 to 5 µm. The alignment of capillary-to-electrode was done by a digital microscope and adjusted in a manner that the distance was equal (± 5µm) to the inner diameter of the respective capillary.

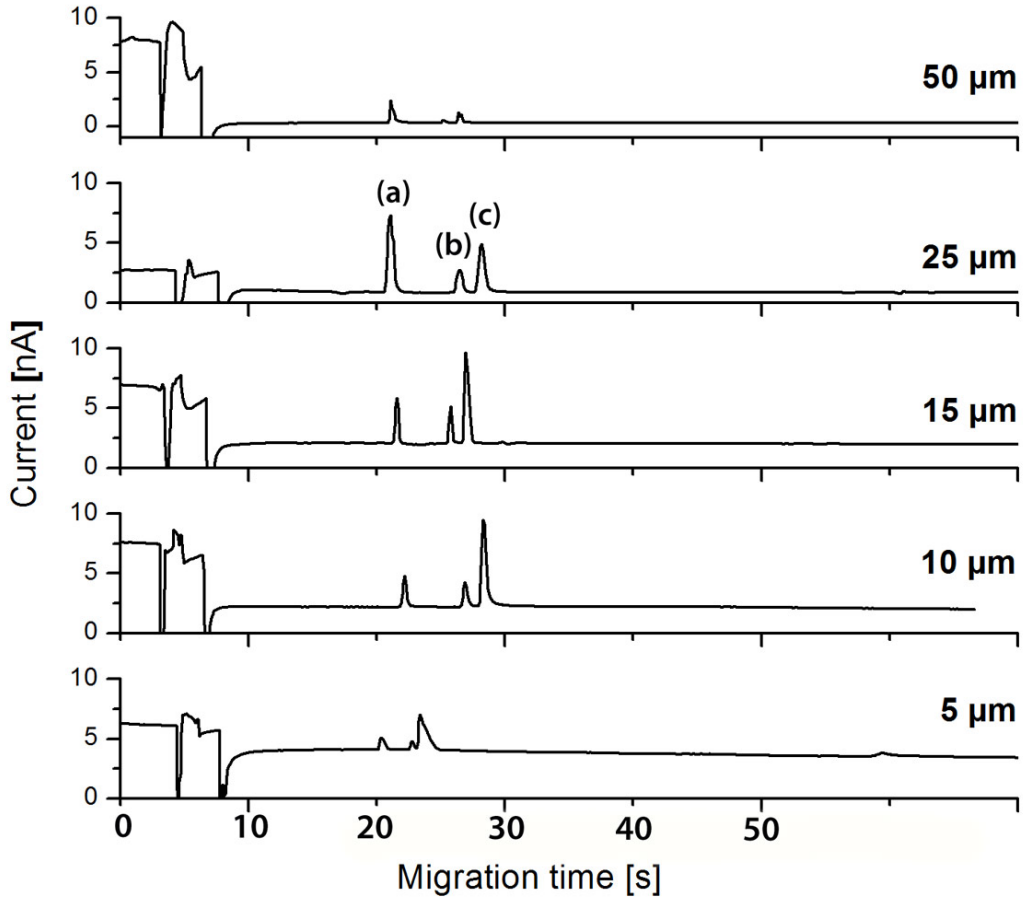

Figure 33. Comparison of the effect of capillary ID on the separation of cationic compounds FcMTMAA (a), basic violet 16 (b) and basic green 1 (c) (all at 100 µM concentration) using short capillary pathways. Separation capillaries: 7 cm length. Separation voltage: 7.5 kV. Other conditions as in Figure 32.

In case of vertically aligned CE-AD a number of counteracting effects have to be kept in mind. The direct opposition to gravity flow worsens laminar flow in the capillary and obviously favours decreasing inner diameter capillaries. For the 50 µm capillary the EOF seems to be too low (relative to the gravity flow) to carry the analytes over the 50 µm gap to the electrode in sufficient amounts. Furthermore, the effect of potential shift has to be kept in mind, as with increasing IDs higher electrophoretic currents are associated, the actual detection potential is shifting to less positive potential [142, 143]. This leads to the observed shift in ratios of FcMTMAA peak heights to BV16/BG1 peak heights. For FcMTMAA the expected decrease in signal height with lower capillary ID can be observed. However, in case of the other two compounds with much higher oxidation potentials (1.0 and 1.2 V in contrast to 0.4 V for FCMTMAA) the current signals are growing or stay at the same level with decreasing IDs. This can be attributed to the above mentioned shifts of the actual detection potential observed for the larger diameter capillaries (50 and 25 µm). In case of lower ID capillaries the currents and the potential shift are drastically reduced and the maximum peak height for the two dyes can be observed. In addition to that, it was found that band

broadening is reduced by using narrow bore capillaries. Even though all the aforementioned reasons would lead to the conclusion that the 5 µm capillary might be the best suitable one, practical considerations speak against the lowest tested inner diameter. The handling and polishing is complicated and a reproducible capillary preparation process is difficult to achieve with the 5 µm capillary. Frequent clogging during the polishing process and poorly reproducible results led us to the conclusion that 10 and 15 µm inner diameter capillaries are the best choice for the presented system.

5.3.4 Analytical performance of the automated short-capillary CE-system

Under optimized conditions the CE-setup with electrochemical detection was used for the separation of a mixture of model substances, consisting of FcMTMAA, basic violet 16 and basic green 1. Good peak height precisions expressed as RSD in the range of 2.7 to 4.5% for the 3 compounds were obtained (n=11). The corresponding RSD values for the migration times were in the range from 0.7 to 1.0% (n=11). The limits of detection (S/N=3) were found to be 0.16 µM for FcMTMAA, 0.57 µM for basic green 1 and 0.82 µM for basic violet 16. The precision of the method is illustrated in terms of 11 consecutive separations shown in Figure 34.

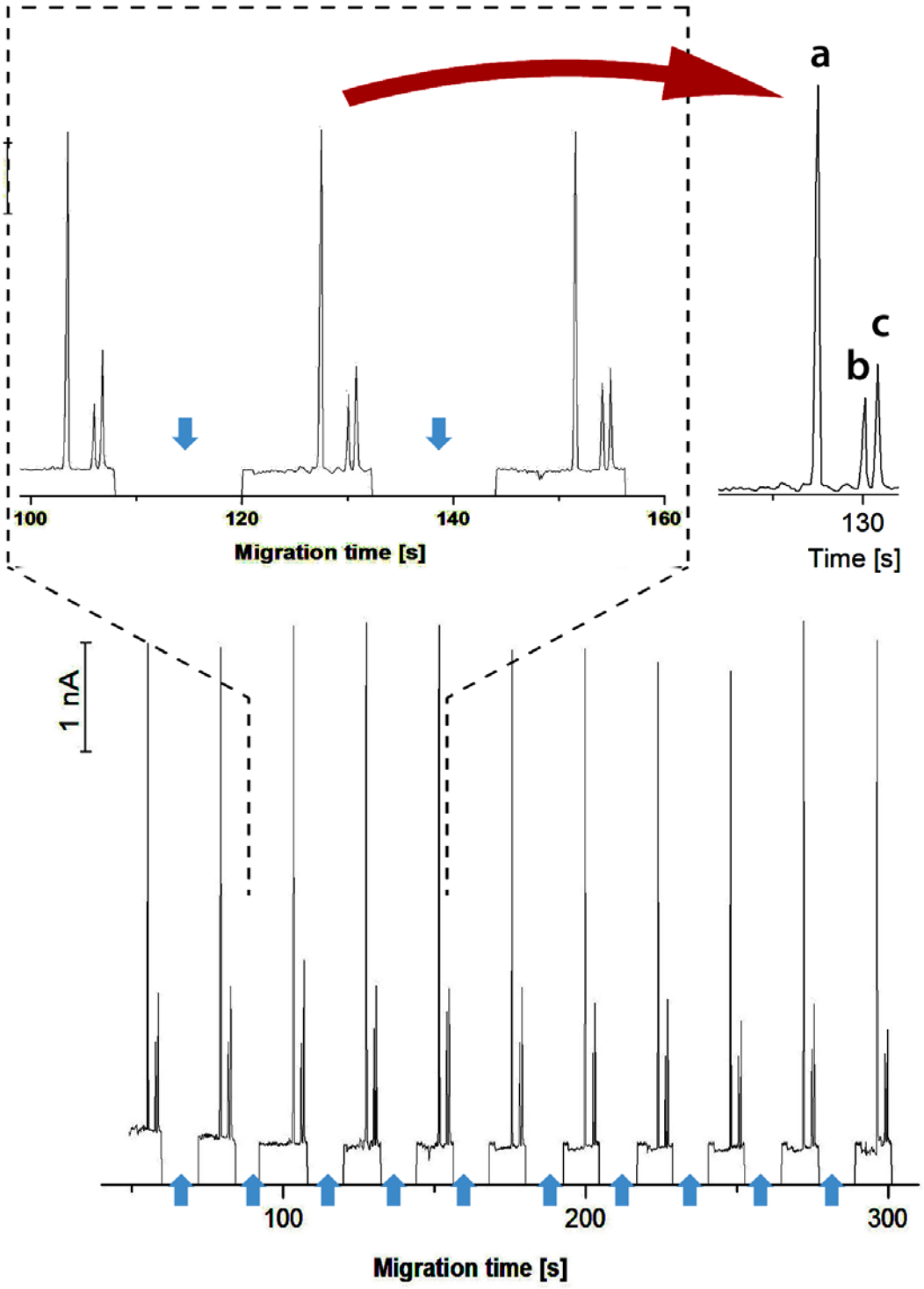

Figure 34. Excerpts from 11 consecutive separations of (a) FcMTMAA, (b) basic violet 16 and (c) basic green 1 (all 10 µM). On the bottom: 11 separations; above it: cut-out of three measurements in more detail. On the upper right side: detailed look of one measurement. The arrows indicate the segments where the disturbance deriving from the transfer between sample and buffer vials was truncated for better illustration. The runs were carried out with a separation voltage of 15 kV in a 7 cm x 15 µm capillary. Electrokinetic injection: 12 kV/0.3s.

5.3.5 Testing the limits of the system

Based on the optimised conditions and by applying high electric field strength (2.5 kV/cm) to a 4 cm short capillary (10 µm ID), very fast CE-AD measurements were carried out. In Figure 35 it is demonstrated how two of the model substances were determined at a concentration of 10^{-6} M within a separation time of 3 s. With half peak widths of just about 0.15 s the resulting peaks are very narrow. It takes about 2.5 s to establish baseline stabilization and hence the FcMTMAA is too fast to be detected, whereas the BV16 and the BG1 can be separated in about 3 s.

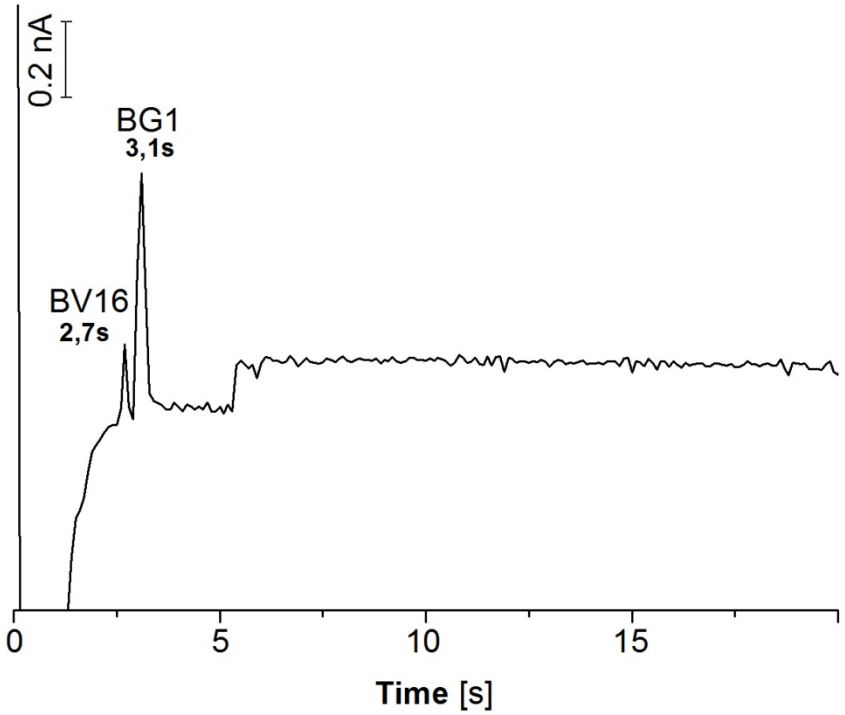

Figure 35. Separation of a 10^{-6} M mix of the three model compounds FcMTMAA (migrates within the rising part of baseline), basic violet 16 and basic green on a 4 cm long capillary with 10 µm ID. Separation voltage, 10 kV; electrokinetic injection, 7.5 kV/0.3 s; separation buffer, 10 mM ammonium acetate and 1 M acetic acid in acetonitrile.

5.3.6 Small sample volumes

Measurements from small vials ranging from 5 µL down to 500 nL were carried out. To prevent evaporation from the small sample volumes PVC/PE-foils are put over the small cavities for the samples. Tapered capillaries etched with hydrofluoric (HF) acid, were used to perform the injection through the foil (see figure 36).

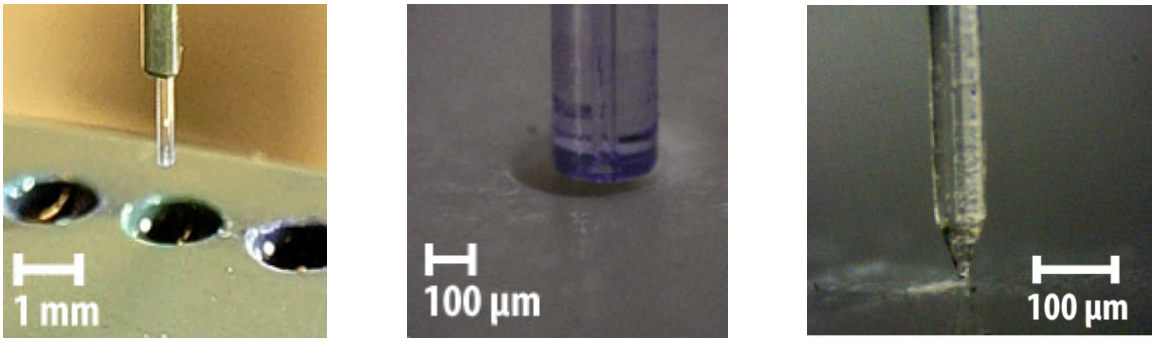

Figure 36. A injection from 1 µl sample vials. For illustrative purposes the capillary is exposed a little further from underneath the high-voltage electrode as it usually is. **B** 50 µm capillary in a vial that fits just the capillary. **C** to prevent evaporation from the small sample vials a PVC/PE foil is put over the holes and stitched with specially etched capillaries.

5.3.7 Application to real-world samples

In order to test the practical suitability of the system to real life applications it was applied to the determination of dyes in overhead projector pens and markers. Different-color (green, blue and red) overhead projector pens from Faber-Castell were investigated for their content in methylene blue, basic green 1 and basic red 28. In order to do this, lines of certain length and width were drawn on a glass plate and then dissolved in 1 mL of the non-aqueous buffer solution. Furthermore, the high-throughput capability for real samples was evaluated. A number of different lines were drawn on the glass plates and then dissolved in the buffer. Such determinations are useful for forensic applications or crime scene investigations. The results of the application can be seen in Figure 37.

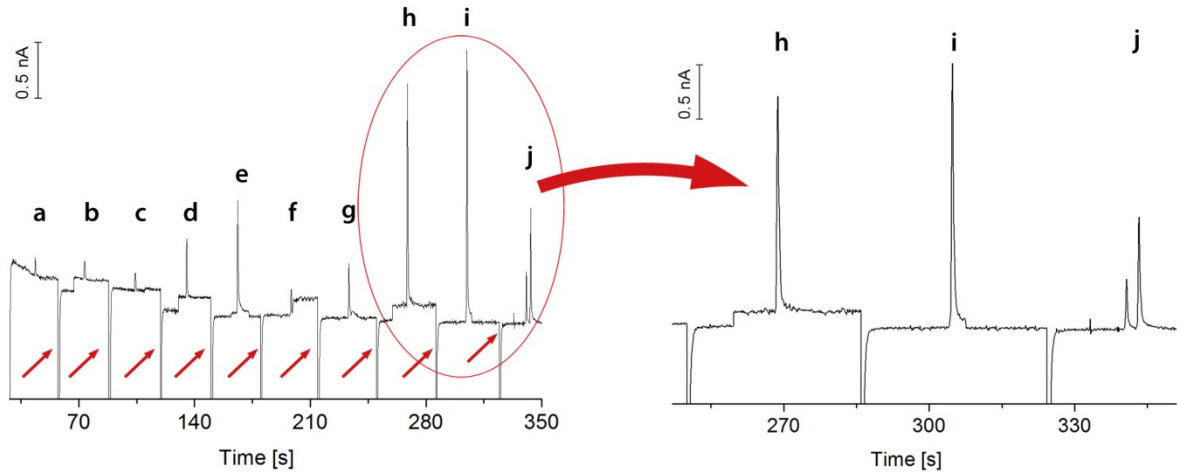

Figure 37. Left side: Application of the method to the determination of dyes in commercial overhead projector pens. (a-e) green pen (basic green 1 peak is obtained) (f-i) blue pen (methlyene blue peak is obtained) and (j) mix of both. Right side: Close-up of the last three measurements. The transfer spikes resulting from transfer of the capillaries between the sample and buffer vials are truncated for better illustration. Individual measurements were started at the points indicated with an arrow i.e. where the baseline was re-equilibrating, respectively. The signals correspond to the following line segments: (a, f) 10x2 mm, (b, g) 10x4 mm, (c) 10x6 mm, (d, h) 10x8 mm, (e, i) 10x10 mm dissolved in 1mL non-aqueous CE buffer. Experimental conditions: capillary length, 7cm with ID 15 µm; separation voltage, 10 kV; injection, 7.5 kV/0.3 s; 50 µm Pt-electrode; detection potential, 1.4 V

5.3.8 Conclusion

Fast separations from complex sample matrices are of high relevance for a number of research fields (reaction kinetics, screening applications and metabolomics). The presented CE-AD system with vertically aligned short capillary pathway is capable of achieving fast and efficient separations for high-throughput analysis of electrochemically active analytes. However, it is not restricted to amperometric detection, as further detection strategies like contactless conductivity detection (C^4D) or time-of-flight mass spectrometry (TOF-MS) can be implemented easily. Some benefits of this system include the use of easy-to-handle and low-cost fused silica capillaries as compared to expensive and complex chip-based systems. Although chip based systems offer similar separation times, the overall analytical protocol including sample change is much faster with the described system. Using vertically aligned capillaries high separation efficiencies can be achieved. Furthermore, the described system offers the potential to work with very small sample volumes and hence with increased injection efficiency (ratio of actually introduced sample volume and total sample volume necessary to manage injection). Future developments deriving from this strategy include a portable low-cost CE-device with dual electrochemical detection (AD, C^4D) and combination with TOF-MS. [section 5.3 is mostly adapted from P4]

5.4 Automated CE-MS

5.4.1 Precision of the automated method compared to previous manual schemes

Measurements were evaluated for peak heights, peak areas and migration times. The respective relative standard deviations (RSD) were compared to previously performed manual injections [19]. The results obtained for peak heights are shown in Table 10.

Table 10. Variation of HV (25 kV and 30 kV) and positions of the injection vials in the autosampling unit**.** For all measurements: n=5, meaning that for "Same vial" 5 repeated injections from the same vial were performed and for "Sequence" 5 consecutive measurements from different injection vials containing aliquots of the same mix were done.

	25kV		**30 kV**	
Compound	**Sequence**	**Same vial**	**Sequence**	**Same vial**
Histidine	4.4	4.4	3.0	6.4
Adrenaline	2.3	7.3	2.0	3.5
Noradrenaline	6.7	5.2	5.4	0.7

Comparing the obtained values with the ones for manual measurements, a significant improvement could be recognized. The automated method delivers RSD values for the peak heights (n=5) of 1 to 7%, whereas the manual mode lies at 10 to 16% with n=4. [19]. Comparable results were also obtained for peak areas (2 to 8%), however no comparison values for the manual mode are available. It was a further goal, to show the applicability of the system to true high-throughput applications. Therefore, a number of consecutive measurements from varying injection vials was run. A measurement cycle of 15 separations each at 30 kV with electrokinetic injection (1s / 10 kV) was carried out and evaluated. The chromatogram of this determination is shown in Figure 38. For better illustration just the noradrenalin mass trace is illustrated.

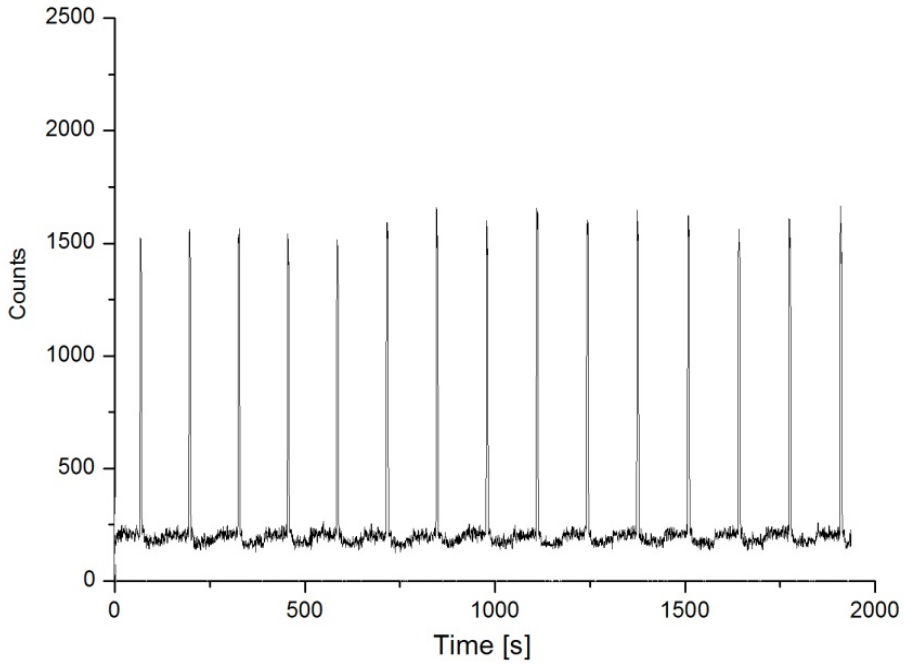

Figure 38. Extracted mass trace of noradrenaline for 15 consecutive measurements at 30 kV separation voltage in a 30 cm x 25 µm capillary. Injection: 1s / 10 kV for individual measurement. Concentration of noradrenaline: 100 µM. CE background electrolyte used was 0.1 M formic acid (pH 3).

It could be shown, that for n=15 the RSD values for peak height ranged from 2 to 4% (for the different compounds). Peak areas were in an acceptable range of 5.6 to 7.6%. These results show the high-throughput capability of short pathway CE-MS measurements. This stands in contrast to the often doubted long-term instability of the ESI spray and the discussion about the danger of possible bubble introduction into the separation capillary after repeated injections.

5.5 Microanalytical study of sub-nanoliter sample volumes

5.5.1 Injection parameters and influence of tip shape

The utilized injection protocol for the CBI-CE-MS method is shown in Table 11. This cycle can be repeated automatically after one injection is finished.

Table 11 Overview of an optimized injection protocol for very small sample volumes

Step	Description	Parameters	Instrument
1	Align inj. capillary into funnelled sep. capillary	manually	Microscope camera
2	Take up sample solution	1 to 100 nL	Microcontrolled syringe
3	Move to sample position in x and z-directions	x-&z-sample pos.	x- & z-motors
4	1st cool down of Peltier element	-2 to -5 °C	Peltier controller &element
5	Placing drop onto Peltier surface	~500 pL to 50 nL	Microcontrolled syringe
6	2nd cool down to -20°C	-20°C	Peltier controller
7	Flushing injection capillary	100 – 250 nL	Syringe pump
8	Move to water reservoir	go to *x*-position 1	*x*-motor
9	Take in water and reverse plunger	-100nL, 20 nL/s	Syringe pump
10	Move back to sample position	x-&z-sample pos.	x- & z-motors
11	Carefully guide capillary on top of frozen drop	on demand	z-motor
12	Reduce cooling to 0°C	0°C	Peltier controller
13	Guide capillary further into drop	on demand	z-motor
14	Switch of cooling	>10°C	Peltier controller
15	Withdraw (simultaneously with 13) sample	varying	Syringe pump
16	Reverse plunger direction	35 nL, 20 nL/s	Syringe pump
17	Go to position “up”		z-motor
18	Go to injection position in x and z-direction		x- and z-motors
19	Expel sample	varying	Syringe pump
20	Start of separation and data acquisition	30 kV	HV-source / TOF-MS
21	Move inj. capillary out of cell	“Up”-position	z-motor

After capillary alignment in x and y direction the z-axis injection position needs to be defined. This is done just once right after assembling of the system. Special caution is necessary for introduction of the tapered tip into the funnelled separation capillary. Next the sample solution is dropped on the hydrophobized glass slide on the already pre-cooled Peltier element (about -2°C). It was found beneficial to hydrophobize the capillary tip with octylsilane (just the outer part!). The reason is that with normal fused silica capillaries the small drops tend to creep up on the sidewalls of the tips and thus placement of ultrasmall volumes onto the cold surface is impossible. In this study, one microcontrolled syringe pump was available and sample drops were placed with the actual injection capillary. In addition to that, “larger” (>10 nL) volumes could be easily placed with a 0.5 µL microsyringe onto the

surface. Simultaneously to drop placement, the surface temperature was set at -20°C, to assure that no evaporation losses occurred. Problems at this point were the possible sticking, i.e. freezing of the drop to the capillary end. In Figure 39 the process of sample uptake with a tapered 15 µm ID capillary from a previously placed and frozen 500 pL drop is illustrated. The drop size was calculated in this case from the dimensions extracted from the microphotographs. It has to be kept in mind that such a volume would be evaporated within a second under normal CE injection conditions. The capillary, with an OD at the tip smaller than a human hair, was guided in z direction on top of the frozen drop (Figure 39 A, B) and the freezing was stopped, the drop unfroze quickly (C) and sample was sucked into the capillary until the totally available sample was inside the capillary (D, E).

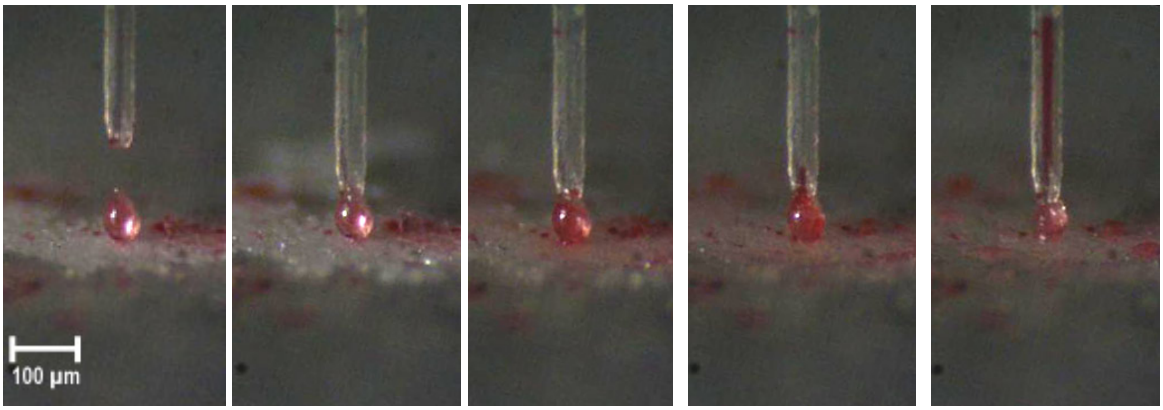

Figure 39. 4 Microphotographs of the uptake of an initially frozen 500 pL drop with a tapered 15 µm ID capillary which was etched to about 20 µm OD. **A** frozen drop **B** capillary placed on top of it **C** unfreezing begins **D** drop is liquified **E** injection of the complete drop.

5.5.2 Fast CE-MS determinations from very small sample volumes

One intrinsic benefit of utilizing CBI is that the spatially fixed separation capillary allows the use of short separation pathways in conjunction with ESI-TOF-MS. The ESI-interface requires 12 cm in length and only another 3 cm are needed for coupling to the injection cell, so that work with capillaries of 15 cm length is possible. In this work 26 cm capillaries were used in order to assure full separation of the 3 close-migrating cyclic nucleotides at 30 kV separation voltage (more than 1.2 kV/cm field strength). In order to reduce detrimental effects of increased Joule heating 25 µm ID capillaries were used for separation. A buffer of 25 mM ammonium acetate (pH 9.25) was found suitable for separation of the closely migrating cyclic nucleotides. In Figure 40, separation of 4 cyclic and acyclic nucleotides from a drop smaller than 1 nL was carried out in a 26 cm x 25 µm capillary in 65 seconds. Highly efficient separation of the anionic compounds with peak widths at half height from 0.2 to 0.4 s was achieved.

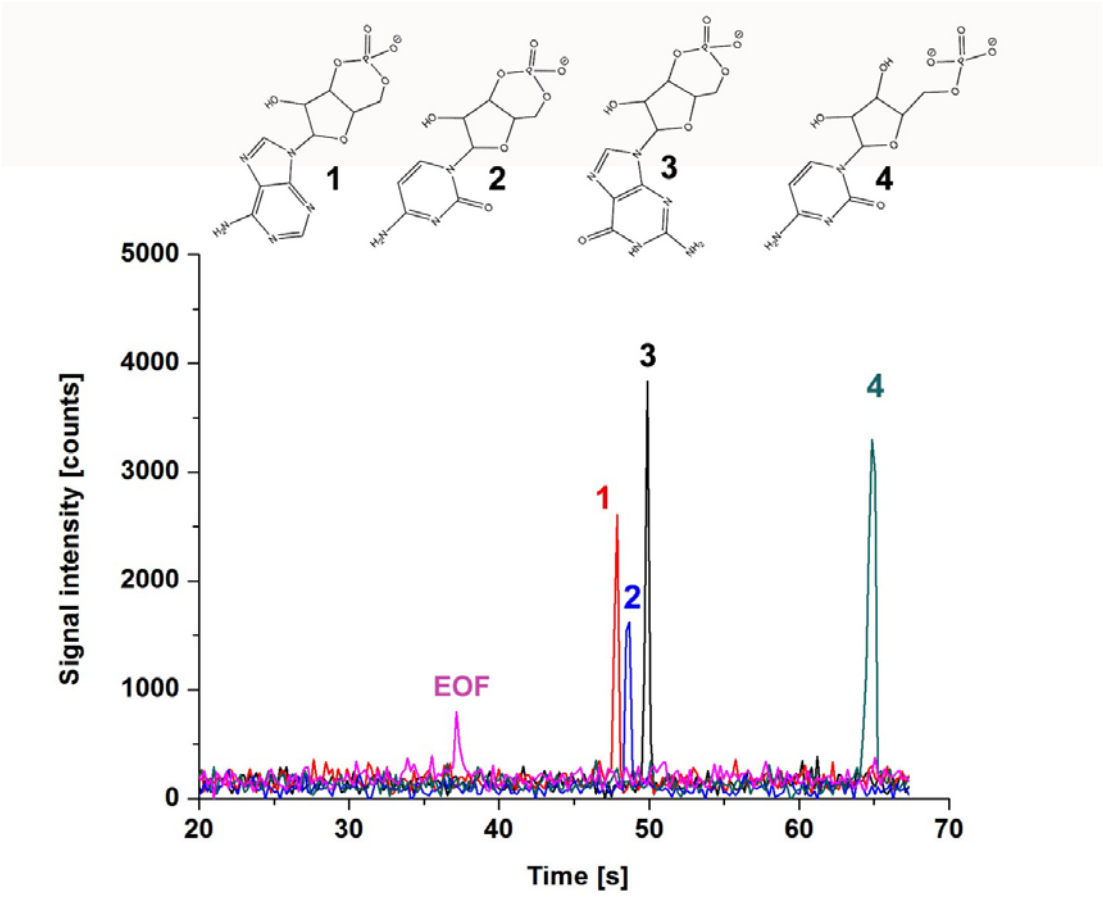

Figure 40. Fast CE-MS separation of 3 cyclic nucleotides (cAMP, cGMP and cCMP) and CMP (all substances at a concentration of 50 µM) via CBI-CE-TOF-MS. DMSO was used as EOF marker. Separation at 30 kV in a 20 x 25 µm capillary filled with 25 mM ammonium acetate (pH 9.25) as BGE. Extracted ion traces for DMSO and the analytes (1) cAMP (2) cCMP (3) cGMP (4) CMP are illustrated. A 500 pL drop was injected 100% efficiently into the separation capillary. On top, the structures of the analytes in their charged states at pH 9.25 are shown.

5.5.3 100% Injection efficiency

Sample uptake from small volumes would not be desirable if afterwards a significant amount of sample would be lost during the transfer from the injection capillary into the separation capillary. In the case of limited available sample amounts, it is essential to transfer the full amount into the separation capillary. A concept to enable nearly 100% injection efficiency for the case of normal, flat-polished 360 µm OD capillaries has been developed [19]. A PDMS-seal ring was carefully placed on top of the separation capillary. Guiding the injection capillary directly onto this seal ring allowed to close off the insides of both capillaries from their surroundings. However, tight sealing only worked efficiently if both capillaries still possessed the comparatively strong capillary wall. As it was shown, introduction of very small sample volumes is only possible with tapered capillaries. Therefore, a different approach specifically designed for small outer diameters of the injection capillary was developed (see Figure 41).

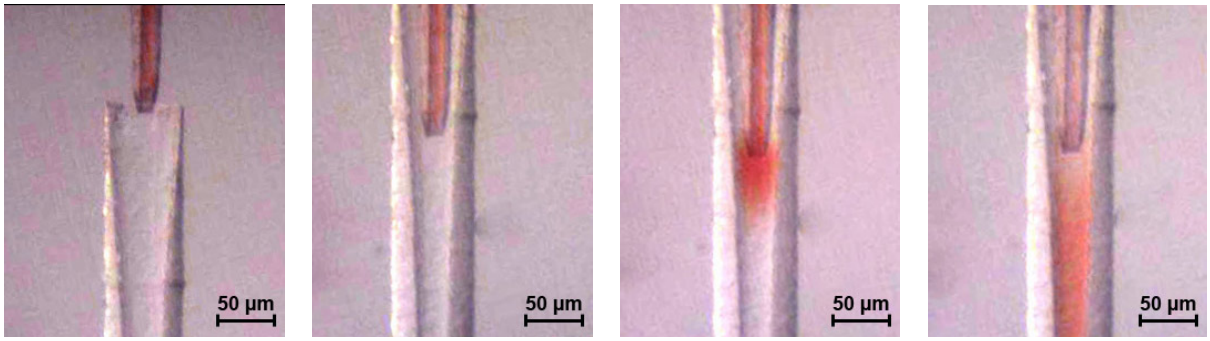

Figure 41. Microphotographs of a 100% efficient injection process. The steps are: **A** funnelled separation capillary (lower capillary) opposed to tapered injection capillary **B** injection capillary is guided into the separation capillary until the insides are firmly closed against the environment. **C** the sample volume (colored red for illustrative purposes) is expelled **D** application of the high voltage

The concept was studied using a tapered injection capillary opposed either to a "normal" 360 µm OD separation capillary or introduced into a funnelled capillary. As shown in Figure 42 (top right), for the former case the sample is diluted and a cloud of the colored (for illustrative purposes) sample solution spreads out around the separation capillary, resulting in reduced sensitivity. Signal intensities for the use of the tapered-to-funnelled approach are about 2 to 3 times higher (see Figure 42, lower electropherogram).

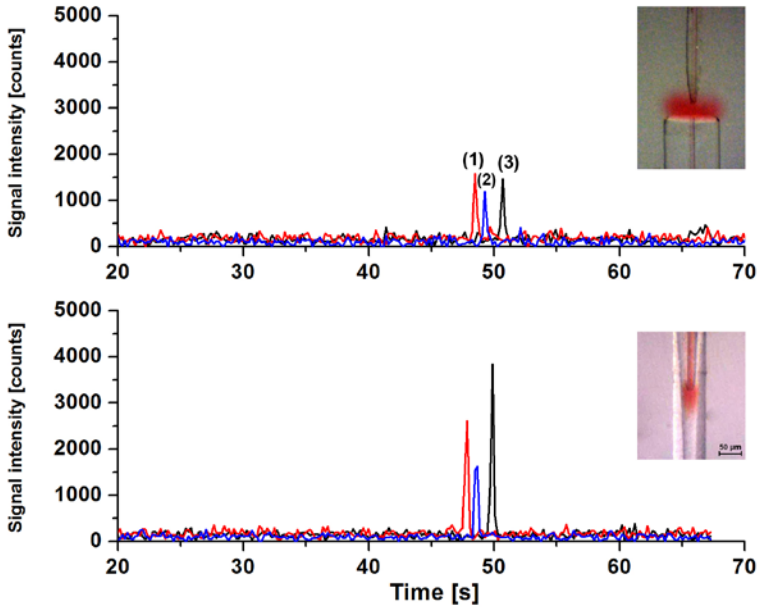

Figure 42. Comparison of CE-MS separations in a 20 cm x 25 µm capillary without (top) a funnelled separation capillary and with (bottom) introduction of sample from a tapered injection capillary into a funnelled 25 µm separation capillary. Extracted ion traces for the analytes (1) cAMP, (2) cGMP and (3) cCMP (concentrations were 50 µM in all cases) are shown. The samples were colored with basic red 28 textile dye for illustrative purposes. Other conditions as in Figure 40.

5.5.4 Analytical characteristics and high-throughput potential

Refrigerated surfaces enable conservation of multiple drops for repetitive measurements without the risk of erroneous results deriving from evaporation losses. The application of the described method to a number of colored (again for illustrative purposes only) 500 nL sample drops of a cyclic nucleotide mixture is shown in Figure 43. The initial separation was started (according to Table 11) and after this run the high voltage of 30 kV was kept switched on permanently (resulting in more introduced sample) during subsequent injections. This latter point explains the higher signal intensities for the 2^{nd}, 3^{rd} and 4^{th} separation. In the meantime of a progressing separation, the injection capillary could already take up the next drop. The RSD (n=3) of the peak heights of cGMP was found to be 1.9%**.** The findings indicate the potential of the system for titer plate like applications in the smallest dimensions seen so far for CE determinations. In conventional CE operation titer plates require a volume of at least 5 µL to perform high-throughput measurements whereas in our setup densely arranged drops of 500 nL pose no challenge. For even smaller volumes the high-throughput handling is more delicate but possible.

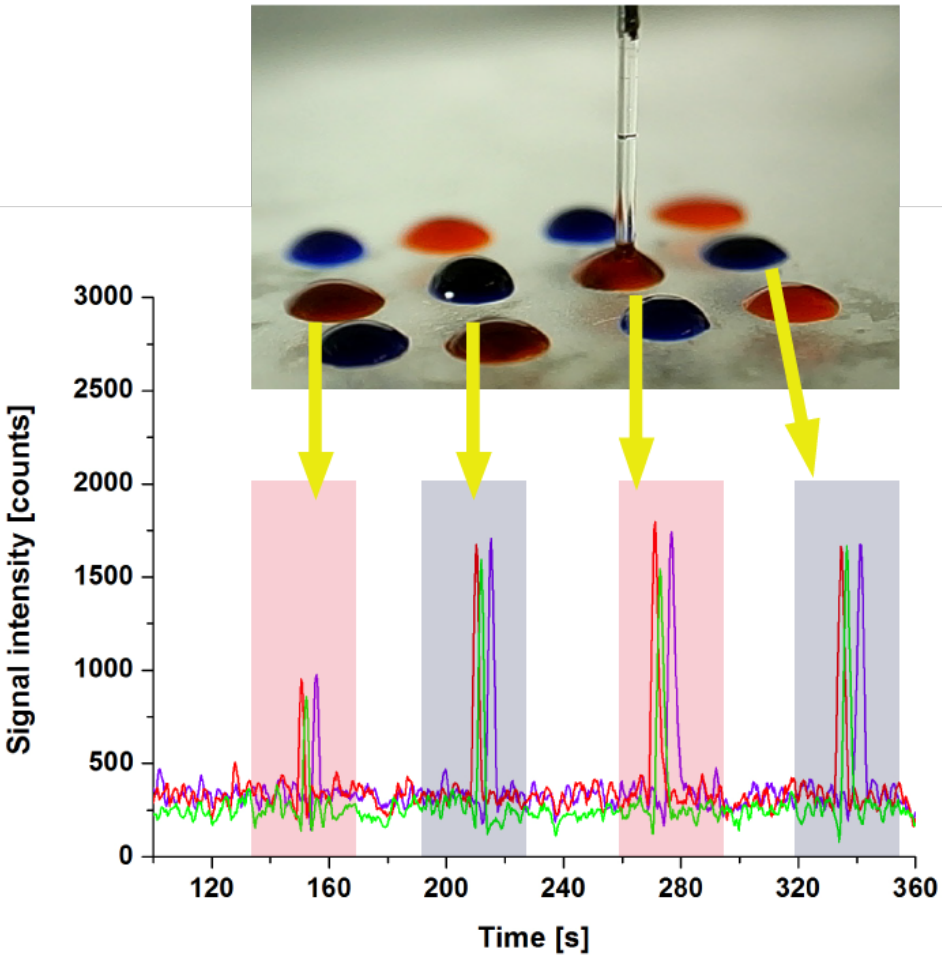

Figure 43. Consecutive measurements from 4 different 500 nL drops on a cooled Peltier surface. The model system consists of 3 cyclic nucleotides (cAMP, cCMP and cGMP, concentration of 25 µM). For illustrative purposes the drops were colored differently with red and blue dyes. Other conditions as in Figure 40.

The analytical performance of the system was also evaluated in terms of precision of a sequence of measurements from the same drop. Precision of the tapered-to-funnel CBI injections were found to be in a comparable range (RSD (n=5) of peak heights: 6-8%) to previous studies with the setup and better than with a manual injection procedure (RSD (n=7): 8.3% and 10%, respectively) [77]. Relative detection limits (S/N=3) of the CE-TOF-MS method were found to be 4.5 µM, 8.5 µM and 9.8 µM for cGMP, cAMP and cCMP, respectively, when determined under the conditions shown in Figure 40. Considering the extremely small and completely injected sample volume of 500 pL used in this approach, the absolute limits of detection were 2.2 x 10^{-15} mol, 4.2 x 10^{-15} mol and 4.9 x 10^{-15} mol for cGMP, cAMP and cCMP, respectively.

5.5.5 Preconcentration by evaporation of solvent

Liquid volumes of about 20 µL of a model system were evaporated to final sample volumes of ca. 200 nL. Under utilization of a microbalance it was possible to precisely quantitate the respective drop sizes and to calculate the corresponding increase in concentration. In the example shown in Figure 44 the first measurement was done with a 20.40 µg drop containing the analytes at an initial concentration of 500 nM. No signals for the model analytes could be detected as the concentrations were below the limits of detection. After injection into the separation capillary the injection capillary was brought back to the remaining sample drop and sample uptake at a weight of 0.21 µg was done. The results showed that for a model system (cAMP, cCMP and cGMP) reduction of two orders of magnitude in volume led to a corresponding 100-fold increase in concentration with signal intensities suitable for quantitative evaluations. This procedure could be repeated with satisfactory precision for peak heights with RSD of 13% (n=4).

The concept worked well in case of model solutions prepared in distilled water. However, it has to be noted, that such a dramatic reduction in volume could cause problems for many real-world applications due to matrix problems. All interferents and matrix components would also be preconcentrated and thus would often deteriorate the analytical determination.

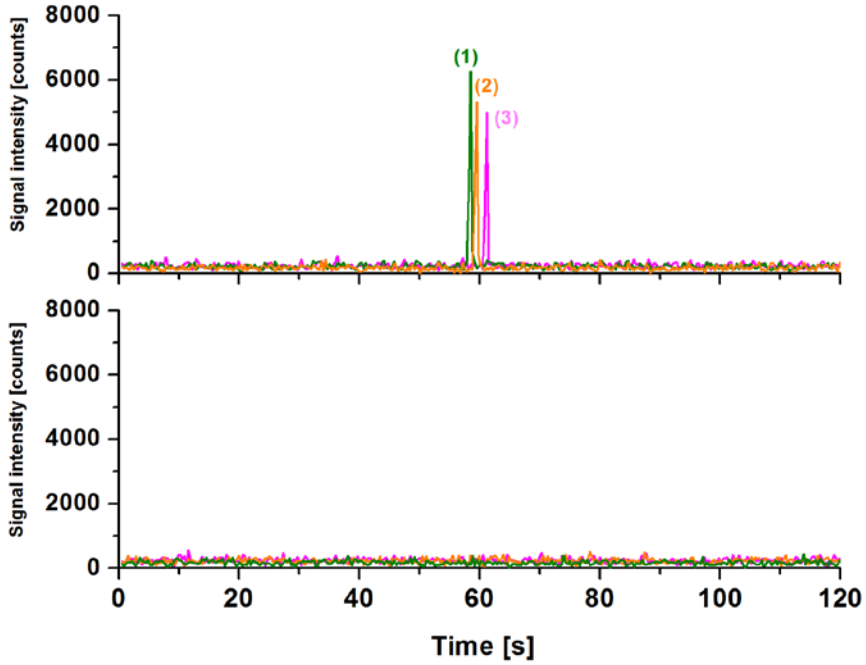

Figure 44. Results of preconcentration by evaporation from a drop of 20.40 µL (bottom electropherogram) reduced to 210 nL (top electropherogram) for a model system of (1) cAMP (2) cCMP (3) cGMP. The bottom electropherogram shows the extracted ion traces of the model analytes with initial concentrations of 500 nM (below the LOD). The upper ion traces correspond to a preconcentration protocol with an increase of concentrations of about two orders of magnitudes. Separation conditions as in Figure 40.

5.5.6 Application of the preconcentration to determination of cyclic nucleotides in human urine

Therefore, it was tried to apply the above preconcentration strategy to human urine in combination with a solid phase extraction (SPE) protocol (adapted from [56]) to remove interferents. In untreated urine, the determination of nucleotides (as an example the sample was spiked with cGMP) was massively disturbed by interfering compounds and high salt content. Consequently, the direct preconcentration (5-fold, from 0.00533 g to 0.00112 g) of urine spiked with 10 µM cGMP resulted in a very poor signal in the extracted ion trace for cGMP (see Figure 45 (A)). The implementation of a SPE protocol (see Experimental section) led to good preconcentration factors of 5 to 7 (see Figure 45 (B)). In the example shown, urine spiked with 10 µM of cGMP was subjected to the SPE procedure and the pretreated sample was evaporated from 0.00546 g to 0.00084 g (concentration increase about 6.5) and subsequently injected. The signal intensity compared well to a reference measurement of about 70 µM cGMP in pure water. However, higher preconcentration factors (PFs) could not be achieved due to similar disturbances as found in untreated urine (Figure 45 (A)).

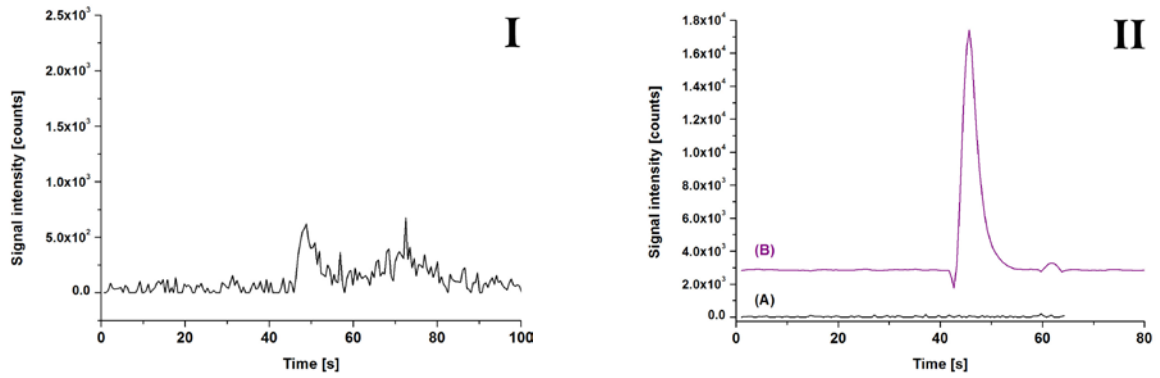

Figure 45. Application of the preconcentration approach to cGMP spiked into human urine. In (A) a 5-fold preconcentration of 10 µM cGMP in original matrix is illustrated. In (B), a previous SPE protocol removes some of the interfering compounds and a 7-fold preconcentration shows a signal for cGMP. For separation conditions see Figure 40.

5.5.7 Conclusion

This work demonstrated the capability of capillary batch injection (CBI) for the sample uptake and 100% efficient injection of sample volumes smaller than 1 nL. A strategy for reduction of actually needed sample volumes to perform CE injections was found by utilizing a setup integrating capillary-based sample uptake and CBI components in combination with fast CE-MS. Based on the CBI injection technique an efficient strategy to transfer small sample volumes to CE-ESI-TOF-MS was developed. An optimization of all parameters regarding controlled drop freezing / unfreezing, injection, sample transfer and CE separation led to a robust and reliable system. The highly efficient separation of the cyclic nucleotides could be done in a 25 µm x 20 cm long capillary in less than 1 minute. Furthermore it could be shown that evaporation of solvent can be exploited for preconcentrating analytes in small sample volumes of only 500 nL. However, one challenge associated with this approach is that matrix constituents are also preconcentrated. Consequently, suitable microanalytical sample pretreatment strategies have to be applied to face this problem. It was shown that a suitable concept is a two-step protocol (with prior SPE) applied to bioanalytically relevant sample matrices like urine. [section 5.5 mostly adapted from P5]

5.6 Novel 2-Dimensional on-line coupling of IC and CE-MS (IC x CE-MS)

In this section the results obtained with the novel mode of comprehensive 2-D separation are presented. It was the first comprehensive on-line coupling of IC and CE. The goal of the study was to provide a device and a method for an improved separation of ionic species, which has increased peak capacity, is more cost-effective and less error-prone than the methods known and used conventionally. Hence, the two most important instrumental methods to separate ionic species were brought together in an orthogonal on-line system. Whereas IC separates ions based on their affinity to ion exchanging stationary phases, in CE the mobility (depends on charge and hydrodynamic radii) of ions in an electrical field is responsible for separation. Within this work the process development and the way towards solving the technical problems of the coupling are described. Furthermore, the first IC x CE-MS measurements for a "*proof-of-principle*" were elaborated.

5.6.1 Optimization of system design and measurement procedure

Although two-dimensional systems were known, a combination of ion exchange chromatography methods and electrophoresis based methods was not contemplated in the past for various reasons. In particular, the relatively slow separation speed of conventional CE based on the use of long capillaries was deemed to exclude the construction of a corresponding two-dimensional separation system. A difference between the usage of the outlet capillary coming from the IC device for injection (in the following called IC mode) when using 2-Dimensional IC-CE and the CBI injection capillary used for conventional CBI (called CBI mode) are the fundamentally different flow characteristics that develop in the injection cell. The reason is that in IC mode a previous IC separation is happening and a constant flow of distilled water (after suppression) through the outlet capillary is present and pushes analyte zones toward the CE separation capillary. In CBI mode the fluid remains stationary in the injection capillary and small sample portions are expelled on demand onto the separation capillary. The different flow characteristic from the IC outlet capillary has important implications for the 2D system and its crucial step: the transfer of analyte zones from the IC into the CE capillary. These implications and the factors governing the injection process for IC x CE are discussed in the following sections.

IC-flow-rate. In order to enable a reasonably fast overall determination of analytes and prevent excessive band broadening for the IC zones and to not significantly prolong the

overall analysis protocol, the actual flow rate in the IC outflow capillary should not be too low. However, initial tests showed that rather high flow rates (> 10 µL/min) lead to a locally, highly diluted aqueous zone around the inlet of the separation capillary and, subsequently, to the interruption of the electrophoretic current. As a first step, the visualization of the (distilled, i.e. low-conductive) water effluent from the IC capillary under application of different flow rates was of interest. This was accomplished by mixing a blue-color dye into the IC eluent stream. It could be demonstrated, how the cloud of substance distributes around the separation capillary under different conditions (for an example see Figure 46).

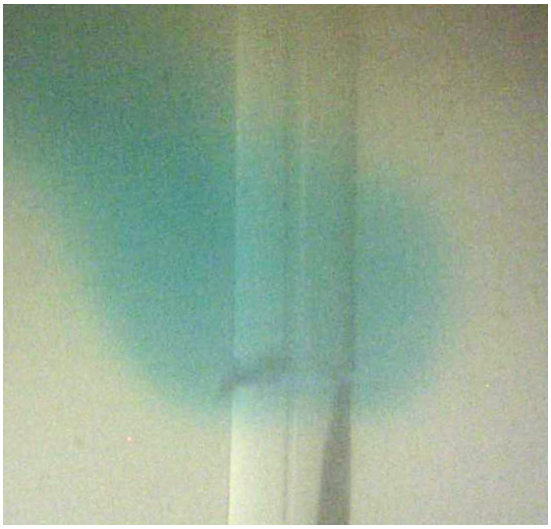

Figure 46. Distribution of IC flow (from upper capillary) around the CE separation capillary (lower capillary) in injection position at a flow rate of 10 µL / min. The IC eluent was coloured blue with a dye for this experiment.

The local dilution around the separation capillary lead to a current breakdown even at low flow rates. Furthermore, peak resolution and separation efficiency in CE deteriorated when a too long sample zone was introduced into the CE separation capillary. Hence, a protocol of repeated up-and-down cycling of the IC capillary was applied. This meant that the IC capillary had to be withdrawn for certain time periods and brought back in close proximity (injection position) to the CE capillary. This allowed for the introduction of distinct sample zones in the CE separation. After testing flow rates ranging from 2 to 10 µL/ min, it was found that a flow rate of 5 µL / min provided the best stability of the electrophoretic current and reasonable IC separation times for the model systems investigated.

Capillary distance. The critical part of the method is the transfer of the IC effluent to the CE system. Thus, an evaluation of the proper distance between the two capillaries in axial z-direction was necessary. The focus was put first on the results of direct contact measurements. The capillary ends were guided carefully right on top of each other and

subsequently IC x CE measurements were done. It was found that significant current fluctuations occurred as compared to measurements with a small gap in z-direction between the capillaries. The reason is most likely the large amount of distilled water that enters the separation capillary in this alignment. Therefore a distance of about 25 to 50 µm for the initial proof-of-concept investigations was chosen.

Injection protocol. Next the focus was put on the protocol for the microprocessor-controlled *up-and-down* cycling of the IC capillary. From the previously made observations it was clear that a constant injection leads to local dilution and subsequent current problems. On the other side, short injection times can lead to reduced sensitivity, especially under conditions of low IC flow rate. In the course of this study a protocol of 2 s in injection position and 15 s in preinjection position was found to be best suited for the specific model system. Preinjection means that the end of the IC capillary remains in the BGE, but far enough away from the separation capillary inlet to assure that no IC outflow enters the CE capillary; typically at least 200 µm. In the *z*-injection position a segment of the IC sample zone is introduced into the CE capillary by laminar flow caused by the ESI-interface and electrokinetically via the HV that is constantly applied throughout a measurement cycle. A further advantage of the axial injection movement was found: the movement causes an additional convection in the buffer solution and dilutes the emerging IC carrier flow and thus minimizing the influence of the IC carrier flow on the electrophoretic current stability. This allows using the system without a mechanical stirring unit. For IC x CE, the time during which the IC capillary is in front of the separation capillary, the voltage applied, the flow rate into the CE capillary and the IC flow rate determines the amount of sample injected. In tables 12 and 13 the optimized parameters and the steps to carry out a full measurement are listed.

Table 12. Overview of parameters used for first successful 2-dimensional IC x CE coupling via CBI modulator

Parameter	**Value**
Injection distance	25 to 50 µm
Injection protocol	2 s inj. position, 15 s preinj, position
Stirring	2 s
IC flow rate	5 µL/min
IC capillary	75 µm ID x 60 cm
CE capillary	25 µm ID x 20.5 cm
Separation voltage	22.5 kV (corresponds to 1 kV/cm)

Table 13. Overview of steps to perform an IC x CE-MS measurement

Step	Instrument	Description
1	Ion chromatograph (IC)	Load sample
2	IC	Detection with the conductivity detector
3	x-motor	go to position “inject”
4	HV-source, TOF-MS	Switch on HV-source, start data acquisition with TOF-MS
5	z-motor	Go into position “Injection”, remain 2 s
6	Stirrer	Stir for 2s simultaneously with step 8
7	z-motor	Go into position “Preinjection”, remain 15 s
8	z-motor	Repeat steps 5,6 & 7 over and over until measurement is over
9	HV-source	Switch off HV

5.6.2 First 2-Dimensional IC-CE measurements

The appeal of IC x CE measurements lies first of all in the possibility to separate substances that co-elute in IC via the complementary CE principle and vice versa to resolve CE’s co-migrating peaks beforehand in the IC. Therefore, a model system that shows the potential for solution of both problems was chosen. The rate of injection steps or the timely sequence of volume segments depends on the separation speed of the CE. This means that as short as possible separation capillaries and high voltages are desirable. However, with capillaries reaching 20 cm in length the previously (section 5.5) shown cyclic nucleotides cCMP and cGMP are not completely baseline resolved anymore. On IC-side the separation time would have to be very high to split up the peaks of cCMP and CMP and cAMP and AMP, respectively. In CE, however, these anionic species can be separated in less than 35 seconds and thus a fast IC-CE protocol is enabled. The first successful IC x CE measurement was a separation of the IC-co-eluting cAMP and AMP. A mix of the two substances was loaded onto the IC device, run through its system and the outflow transferred into the CE capillary under utilization of the optimized parameters. One further advantage of the IC x CE setup is that the effluent from the IC comprises a solution having low background conductivity with the analytes separated therein. This causes a “stacking” effect, due to differences in conductivity of electrophoresis buffer and injected sample solution, which results in a sharpening of the injected zones and in signal magnification. The results of this first measurement can be seen in Figure 47 on the next page.

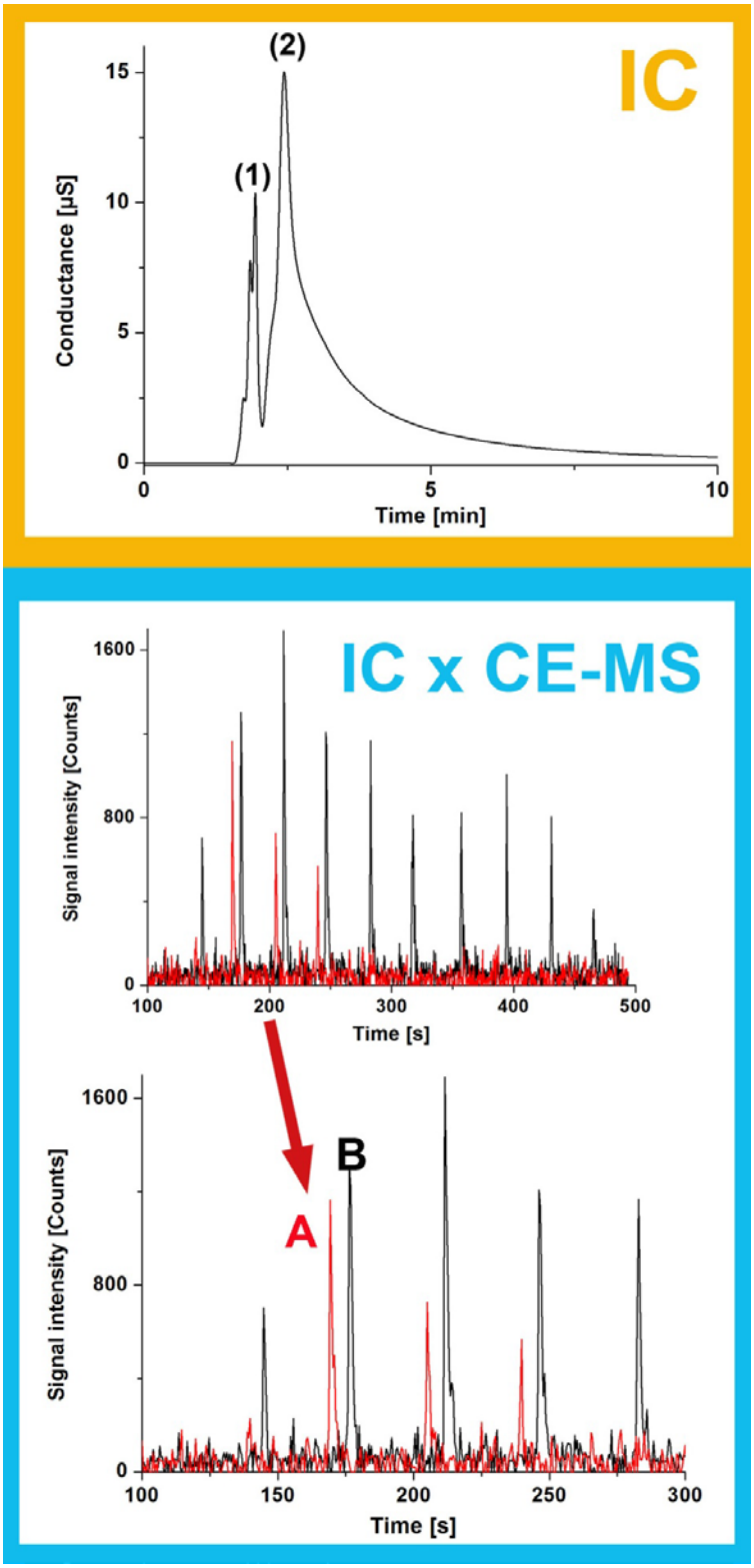

Figure 47. Results for the first successful IC x CE-TOF-MS measurement with lab-built modulator. In the upper chromatogram (orange box) the IC co-elution of a mixture of cAMP and AMP (each at 300 µM) is shown. Peak (1) is the phosphate (not visible in MS) that is present in the solution and in Peak (2) the two compounds co-elute and do not separate. The blue box below shows the 2-Dimensional IC x CE-TOF-MS measurement of the model mixture. Separation conditions IC: IonSwift MAX-200 anion column; eluent: 40 mM KOH; injection volume: 0.4 µL, flow-rate: 5 µL/min; transfer capillary: 60 cm length / 75 µM inner diameter. CE separation conditions: 25 mM NH_4Ac / NH_3 buffer (pH 9.15); capillary: 20.5 cm x 25 µm ID; injection time: 2 s; preinjection time: 15 s.

However, under the technical circumstances used for this determination it was only possible to work with high starting concentrations (high µM to mM range). The reason was that an injection valve in a continuous switching mode was used. This resulted in a loss of analyte (up to 60%). To improve sensitivity a change to a direct inlet system was made. After solving this problem, it was proceeded to the mixture of 6 nucleotide compounds to show the capabilities of IC x CE-MS for simultaneous separation of co-migrating analytes in CE via IC and the resolution of co-eluting IC peaks via CE. In Figure 48 on the next page the two individual separations via CE and IC of target species are illustrated in the upper part. It can be seen that the IC does not resolve cAMP and AMP as well as it does not separate cCMP and CMP. On the upper right side a CE run is illustrated in which cGMP and cCMP are not separated properly on a short CE capillary. However, by combining the two methods via the 2-D HPIC-CD-CBI-CE-ESI-TOF-MS setup the simultaneous solution of both problems can be achieved and peak capacity is significantly enhanced even for this comparatively simple model system. It was found that using the optimized parameters presented in Table 15 all peaks appear in a baseline-resolved manner in the CE-MS chromatoelectropherogram. The peak distribution of the individual peaks relating to a substance represent the form and shape of their corresponding IC peaks. This is illustrated for the peaks of cGMP (peak 4 in the IC chromatogram and peaks (e) in the IC x CE electropherograms) and GMP (peak 5 in IC; (f) in IC x CE) in the zoom-in in bottom right corner of Figure 48.

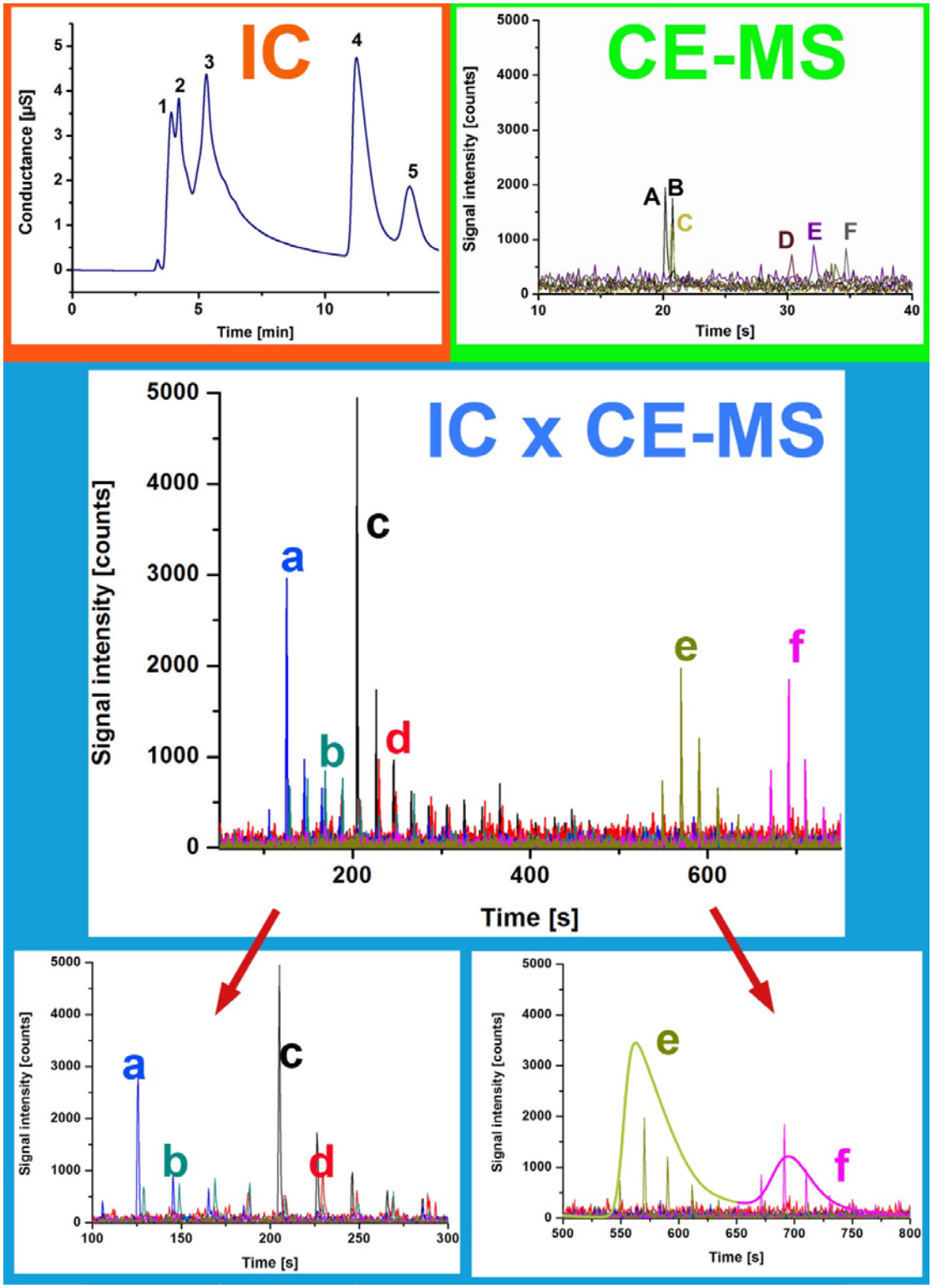

Figure 48. Results of IC x CE-MS measurements. In the orange box (top left) an individual IC run. The peaks are as follows: (1) Phosphate (not relevant for IC x CE) (2) Unresolved and co-eluting cCMP and CMP (3) Co-eluting cAMP and AMP (4) cGMP (5) GMP. On the right, in the green box, a CE-MS separation of (A) cAMP (B) cCMP (C) cGMP (D) CMP (E) ADP (F) ATP in less than 40 s at 25 kV in a 20.5 cm x 25 µm capillary. In the blue box a 2-dimensional IC x CE-MS chromatoelectropherogram that shows the separation of the co-migrating compounds in the CE electropherogram and the co-eluting analytes in the IC chromatogram. Peaks in the IC x CE-MS chromatoelectropherogram: (a) cCMP (100 µM) (b) CMP (300 µM) (c) cAMP (100 µM) (d) AMP (300 µM) (e) cGMP (100 µM) (f) GMP (300 µM). The respective zoom-ins are shown at the bottom. In the right zoom-in, the peaks (e) and (f) are shown with their corresponding IC curve for illustration. Conditions Ion Swift MAX-200 anion column; IC-flow 5µL/min; IC eluent: 40 mM KOH, IC capillary: 75µm ID x 60 cm; CE sep. capillary: 25 µm ID x 20.5 cm; 25 mM NH_4OAc / NH_3 buffer (pH 9.15), separation voltage: 22.5 kV, injection time: 2 seconds; preinjection time: 17 seconds

5.6.3 Conclusion

In summary, the presented system demonstrated for the first time the coupling of IC with CE via a novel microprocessor-controlled modulator. The system brought a powerful methodology on the scene of 2-dimensional liquid phase separation techniques. Basically, the two most important techniques for ion separation are coupled via an interface and the complementary nature of their principles can be used to achieve separation of complex bioanalytical or environmental samples. Enhanced overall speed and powerful detection and sensitivity in combination with MS are one of many advantages this system has to offer. Besides that, the coupling to MS was accomplished by already established introduction of the CE capillary into an ESI-interface. This is an advantage in contrast to the novel and so far unusual coupling of IC and MS. A further benefit of the overall setup is the fact, that besides the extracted mass traces generated by the TOF-MS detection also the conductivity detection signals from the IC can be used for analytical evaluation. Sample comprising nucleotides and cyclic nucleotides were subjected to the system and it could be shown that IC x CE delivers highly efficient separations in cases where the individual separation methods failed to resolve the compounds. All in all the combination resulted in a strong increase in peak capacity due to the high separation efficiency of CE and due to the orthogonality of IC and CE. [parts of section 5.6 are adapted from P6]

6. Summary

Fast capillary electrophoresis (CE) coupled to either electrochemical detection modes or mass spectrometry is a powerful tool for applications like metabolomics or monitoring of fast rate reaction kinetics. Mostly microchip electrophoresis (MCE) has dominated the research on rapid electrophoretic separations since the technique emerged in the early 1990's. However, the use of short pathway conventional capillaries is starting to gain more interest. The well-characterized fused silica capillaries can add unique features to the field of fast rate CE separations. In the first part of this thesis the capabilities of both conventional CE and MCE for conducting fast and efficient electromigrative separations have been evaluated first hand with either commercially available devices or lab-developed setups offering novel and unique properties.

Firstly, the coupling of MCE with the microextraction technique headspace-single drop microextraction (HS-SDME) was used to monitor the biodegradation process of seafood samples. Five volatile, short-chained aliphatic amines were determined using a His/MES buffer (His/MES ratio of 80:20 at pH 6.6) as background electrolyte (BGE). The separation of the analytes was carried out in a 8.7 cm long separation channel of a PMMA microchip integrating thin-film gold electrodes for capacitively coupled contactless conductivity detection (C^4D). A number of characteristics of extraction and determination of target species were optimized and applied to shrimp samples. The compounds were separated within less than 30 s at a field strength of 0.4 kV/cm. The proposed method is simple, quick, presents low levels of waste, works with small sample quantities and is suitable to quantify aliphatic amines in seafood samples like shrimp or fish from where they are naturally developing upon biodegradation.

Secondly, it was an aim to investigate the comparably new CE detection technique of capacitively coupled contactless conductivity detection (C^4D). It is an emerging and increasingly mature detection mode for CE or MCE. C^4D offers nearly universal detection for charged species and, as the name suggests, no contact with the solutions occurs and hence electrode fouling or unwanted electrode reactions are a minor issue. Apart from the practical experiences gained with MCE-C^4D in the previously mentioned project a deeper understanding of C^4D was strived for. Two tubular C^4D cells with varying proportions have been investigated under focus on their principal analytical features under non-separation and

separation conditions in conjunction with liquid chromatography (LC). Furthermore, the properties of the tubular cells were compared to the characteristics of a previously tested thin-layer detection cell. Using a theoretical model, the experimental findings were set in comparison to calculated values. This allowed to a certain degree the modelling of the complex behaviour of C^4D detection in combination with LC. Furthermore, the tubular cells were used for the HPLC separation of a model system of organic acids. In comparison to the thin-layer cell, the tubular cells are superior regarding the determined analytical characteristics.

In the next part of the work, the possibilities of achieving highly efficient and very fast (less than 10 s) CE separations on vertically aligned short pathway capillaries with amperometric detection (AD) were investigated. Utilizing a homemade experimental setup it was possible to separate electroactive substances in a non-aqueous BGE in 3s. Extraordinarily high field strengths of up to 3 kV/cm and capillaries of varying inner diameter (ID, ranging from 5 to 50 µm) as short as 4 cm were essential for achieving very fast separations. Furthermore, all parameters regarding the optimal use of AD in this system were investigated and successfully optimized. The vertical alignment allows for construction of titer-plate based devices for true high through-put applications. A sample throughput of theoretically up to 200 separations/hour could be shown.

Based on the experiences with CE on short pathway capillaries and the work with a portable MCE device a novel portable CE device with corresponding control software was developed and constructed. The device features very small overall dimensions (12 x 12 x 24 cm), light-weight (5 kg) and full portability for *in-field* operation. Furthermore, it enables dual electrochemical detection (ECD) and can be easily coupled to a mass spectrometer. A miniaturized high-voltage source delivers voltages for electrokinetic injection and separation of up to 8 kV. The vertically aligned separation capillaries can be varied in length from 4 to 15 cm and hence application of field strengths as high as 2.6 kV/cm is possible. The autosampling injection unit allows for a high throughput of samples. The power needed to run the device can be drawn completely from 12 V battery packs or a car battery.

In the second part of the thesis, the goal was investigate the CE injection technique of capillary-batch-injection (CBI). So far, the injection efficiency, meaning the ratio of injected sample to actually needed sample volume to perform an injection, in CE is rather poor (10^{-3}

to 10^{-6}). Therefore, an optimized method to carry out fast capillary electrophoresis (CE) with ultrasmall sample volumes (less than 10 nL) was developed. Furthermore, a protocol for quantitative preconcentration of trace compounds in small sample volumes by evaporation of solvent was elaborated and applied to complex sample matrices.

Extremely small sample drops (500 pL) were used to perform a CE injection. An experimental setup comprising a thermoelectric element with cooling unit and a corresponding temperature control device that enables freezing and unfreezing of very small sample volumes was developed. Using sharp-tapered injection capillaries and the precise positioning motors of the CBI-setup, the sample uptake and almost 100% efficient injection of ultrasmall samples into funnelled separation capillaries was successfully achieved. Highly efficient CE-TOF-MS separations of a model system consisting of cyclic nucleotides and nucleotides were done in 23 cm short capillaries (25 µm ID) in less than 50 seconds.

Lastly, a novel way to perform comprehensive 2-D separations was developed by coupling high performance ion chromatography (HPIC) and CE via a modulator unit. The presented system showed for the first time the coupling of IC with CE via a novel microprocessor-controlled modulator. Basically, the two most important techniques for ion separation are coupled via an interface and the complementary nature of their principles can be used to achieve separation of complex bioanalytical or environmental samples. Enhanced overall speed and powerful detection and sensitivity in combination with MS are one of many advantages this system has to offer. Samples comprising nucleotides and cyclic nucleotides were subjected to the system and it could be shown that IC x CE delivers highly efficient separations in cases where the individual separation methods failed to resolve the compounds. All in all, the combination resulted in a strong increase in peak capacity due to the high separation efficiency of CE and due to the orthogonality of IC and CE.

7.Zusammenfassung

Die Kopplung von schneller Kapillarelektrophorese (CE) mit elektrochemischer Detektion (ECD) oder Massenspektrometrie ist ein interessantes analytisches Instrument, beispielsweise zur kinetischen Charakterisierung von schnellen Reaktionen oder für *Metabolomics*-Anwendungen. Die Mikrochipelektrophorese (MCE) hat seit ihrer Einführung zu Beginn der 90er Jahre des letzten Jahrhunderts die Forschung rund um schnelle elektrophoretische Trennungen beherrscht. Jedoch rückte der Einsatz von kurzen Segmenten klassischer Quarzglaskapillaren kürzlich wieder mehr in den Fokus. Die vollumfänglich charakterisierten Quarzglaskapillaren verfügen über einizigartige Eigenschaften die sehr nützlich für schnelle elektrophoretische Trennungen sind. Der erste Teil dieser Arbeit widmet sich den Möglichkeiten zur Erlangung schneller elektromigrativer Trennungen mittels CE oder MCE mit entweder kommerziell verfügbaren Apparaturen oder selbst entwickelten Geräten, welche über neue und besondere Merkmale verfügen.

Zuerst wurde die Kopplung von MCE mit der miniaturisierten Probenvorbereitungstechnik *headspace-single drop microextraction* (HS-SDME) zur Verfolgung von biologischen Zerfallsprozessen von Meeresfrüchten untersucht. Fünf leichtflüchtige, kurzkettige aliphatische Amine wurden unter Verwendung einer His/MES-Lösung (im Verhältnis 80:20, pH 6.6) als Hintergrundelektrolyt bestimmt. Die Trennung erfolgte in einem 8.7 cm langen Trennkanal eines PMMA-Mikrofluidik-Chips mit integrierten Dünnschicht-Goldelektroden für die kapazitiv gekoppelte kontaktlose Leitfähigkeitsdetektion (C^4D). Eine optimierte Methode zur Trennung wurde entwickelt und schließlich auf Shrimp-Proben angewandt. Die Analyten konnten in weniger als 30 s bei Feldstärken von 0.4 kV/cm getrennt werden. Die vorgeschlagene Methode ist einfach, schnell, erzeugt wenig Abfall, kommt mit geringen Probenmengen aus und ist geeignet um quantitativ aliphatische Amine in Meereserzeugnissen wie Fisch oder Shrimp zu bestimmen.

Zweitens, war es ein erklärtes Ziel die vergleichsweise junge CE-Detektionstechnik der kapazitiv gekoppelten Leitfähigkeitsdetektion (C^4D) genauer zu untersuchen. Es handelt sich um einen aufstrebenden und zunehmend ausgereiften Detektionsmodus für CE oder MCE. C^4D ermöglicht die nahezu universelle Detektion geladener Spezies und wie der Name schon sagt, erfolgt kein Kontakt mit den Lösungen im Trennkanal. Dies hat den Vorteil, dass Probleme wie Elektrodenabnutzung, Gasblasenentwicklung an der Elektrodenoberfläche oder

unvorteilhafte Elektrodenreaktionen eine untergeordnete Rolle spielen. Neben den praktischen Erfahrungen, die während der Arbeit mit MCE-C^4D im bereits erwähnten Projekt gewonnen werden konnten wurde ein tieferes Verständnis der Detektionstechnik angestrebt. Zwei zylinderförmige C^4D-Zellen mit unterschiedlichen geometrischen Charakteristiken wurden untersucht. Besonderes Augenmerk wurde dabei auf ihre vorrangigen analytischen Merkmale unter Nicht-Trenn- und Trennbedingungen in Kombination mit Flüssig-Chromatographie (LC) gelegt. Darüber hinaus, wurden die beiden zylinderförmigen Zellen mit einer bereits zuvor charakterisierten Dünnschicht-Detektionszelle verglichen. Mit Hilfe eines theoretischen Modells konnten die gefundenen, experimentellen Werte mit berechneten Werten verglichen werden. Dies erlaubte zu einem gewissen Grade die Modellierung des komplexen Verhaltens der C^4D-Detektion in Verbindung mit Flüssigchromatographie. Zudem wurden die zylinderförmigen Zellen zur HPLC-Trennung von organischen Säuren eingesetzt. Es konnte gezeigt werden, dass die zylinderförmigen Zellen hinsichtlich ihrer analytischen Merkmale der Dünnschicht-Zelle überlegen sind.

Im nächsten Teil der Arbeit wurden die Möglichkeiten zur Erlangung von sehr schnellen (in weniger als 10 s) und hocheffizienten Trennungen in vertikal angeordneten, kurzen Kapillarsegmenten in Kombination mit amperometrischer Detektion (AD) untersucht. Unter Benutzung eines selbstgebauten experimentellen Aufbaus war es möglich elektroaktive Substanzen in 3 s zu trennen. Außerordentlich hohe Feldstärken von bis zu 3 kV/cm und gerade einmal 4 cm lange Kapillaren verschiedener Innendurchmesser (5 bis 50 µm ID) waren entscheidend für die Erreichung besonders schneller Trennungen. Zudem wurden alle Parameter die Einfluss auf den optimalen Gebrauch der amperometrischen Detektion in diesem System hatten untersucht und erfolgreich optimiert. Die platzsparende, vertikale Anordnung erlaubt die Entwicklung von *titer-plate* basierten Vorrichtungen zur Durchführung von wahren Hochdurchsatz-Anwendungen. Ein Probendurchsatz von theoretischerweise bis zu 200 Proben/Stunde konnte implementiert werden.

Aufbauend auf den Erfahrungen mit CE in kurzen Kapillarstücken und der Arbeit mit dem portablen MCE Gerät wurde ein eigener, neuer tragbarer CE-Apparat mit zugehöriger Kontrollsoftware entwickelt und gebaut. Das Gerät besitzt geringe Gesamtausmaße (12 x 12 x 24 cm), ist besonders leicht (5 kg) und ist für *vor-Ort* Einsätze geeignet. Zudem verfügt es über doppelte elektrochemische Detektion und kann auch ganz einfach mit der Massenspektrometrie (im Labor) gekoppelt werden. Eine miniaturisierte

Hochspannungsquelle liefert Hochspannungen von bis zu 8 kV sowohl für elektrokinetische Injektion als auch die Trennung. Die vertikal angeordneten Trennkapillaren können in ihrer Länge von 4 bis 15 cm variiert werden und somit können Feldstärken bis zu 2.6 kV/cm erreicht werden. Die automatisierte Injektionsvorrichtung ermöglicht hohen Probendurchsatz auf kleinem Raum. Das Gerät bezieht die benötigte Laufleistung entweder aus 12 V Akkupacks, einer Autobatterie oder durch einen 12 V Adapter aus dem Stromnetz.

Im zweiten Teil der Arbeit wurde das Ziel verfolgt die Anwendungsbreite der neuen CE-Injektionsstrategie Kapillar-Batch-Injektion (CBI) zu erweitern und diese Technik noch genauer zu untersuchen. Dies erfolgte mittels eines, in unserer Gruppe gebauten, automatisierten CBI-Aufbaus. Bisher ist die Injektionseffizienz, definiert als Verhältnis von tatsächlich injizierter Probe zur benötigen Probenmenge um eine Injektion durchzuführen, eher unvorteilhaft (im Bereich von 10^{-3} bis 10^{-6}). Daher wurde eine optimierte Methode zur Durchführung von schnellen Kapillarelektrophorese-Trennungen mit extrem kleinen zur Verfügung stehenden Probenvolumina entwickelt. Zudem wurde eine Methodik zur quantitativen Aufkonzentrierung von Spurensubstanzen in kleinsten Probenvolumina durch Verdampfung des umliegenden Lösungsmittels entwickelt und auf komplexe Probenumgebungen angewandt.

Extrem kleine Probentropfen (500 pL) konnten für CE Injektionen verwendet werden. Unter Normalbedingungen verdampfen diese kleinen Probemengen sehr schnell. Aus diesem Grunde wurde ein Aufbau bestehend aus thermoelektrischem Element mit zughöriger Kühleinheit und entsprechender Temperaturkontrolleinheit entwickelt und gebaut, welcher es ermöglicht kleinste Probentropfen im CBI-Setup einzufrieren und wieder nach Bedarf aufzutauen. Unter Einsatz von scharf-zugeätzten Injektionskapillaren und mit Hilfe der präzisen Positioniermotoren des CBI-Aufbaus, war es möglich die 100% effiziente Injektion von nL- oder pL-großen Proben in trichterförmig geätzte CE Trennkapillaren durchzuführen. Hocheffiziente CE-TOF-MS Trennungen eines Modellsystems von zyklischen und nicht-zyklischen Nukleotiden in einer 23 cm langen (25 µm ID) in weniger als 50 s konnten durchgeführt werden.

Außerdem wurde ein neuartiger Weg zur Durchführung von 2-dimensionalen Trennungen mittels Kopplung von Ionenchromatographie (HP-IC) und CE entwickelt und evaluiert. Das entwickelte System ermöglichte zum ersten Mal die Kopplung von Ionenchromatographie

und Kapillarelektrophorese mittels eines geeigneten und von einem Mikroprozessor gesteuerten Modulators. Die beiden wichtigsten Techniken zur Trennung von Ionen wurden gekoppelt und ihre sich gegenseitig ergänzenden Trennprinzipien konnten ausgenutzt werden um komplizierte bioanalytische Proben zu analysieren. Erhöhte Geschwindigkeit und leistungsstarke Detektion und Empfindlichkeit in Verbindung mit dem Massenspektrometer sind Beispiele für die Vorzüge die dieses System zu bieten hat. Verschiedene Proben von Nukleotiden und zyklischen Nukleotiden wurden mit dem System untersucht und es konnte gezeigt werden, dass IC x CE genau dort sehr effiziente Trennungen liefert, wo die Einzel-Methoden scheitern. Alles in allem ermöglicht die Methodik aufgrund ihrer hohen Trennleistung und der hohen Orthogonalität von IC und CE eine deutliche Steigerung der *peak-capacity* (verglichen zu den individuellen Trenntechniken).

8. References

1 West J, Becker M, Tombrink S, Manz A (2008) Anal Chem 80:4403-4420

2 Woods LA, Roddy TP, Ewing AG (2004) Electrophoresis 25:1181-1187

3 Scanlan C, Lapainis T, Sweedler JV, Landers JP (Ed.) (2008) Handbook of Capillary and Microchip Electrophoresis and Associated Microtechniques. CRC Press, Boca Raton

4 Becker H, Mühlberger H, Hoffmann W, Clemens T, Klemm R, Gärtner C (2008) Proc SPIE 6886: 68860C/1–68860C/7

5 Mühlberger H, Wonhee J, Guber AE, Saile V, Hoffmann W (2008) IEEE Sensors 8:572-579

6 Ryvolova M, Preisler J, Brabazon D, Macka M (2010) TrAC 29:339-353

7 Lewis AP, Cranny A, Harris NR, Green NG, Wharton JA, Wood RJK, Stokes KR (2013) Meas Sci Technol 24:1-20

8 Kuban P, Hauser PC (2009) Electrophoresis 30:176-188

9 Coltro WKT, Lima RS, Segato TP, Carrilho E, de Jesus DP, do Lago CL, da Silva JAF (2012) Anal Methods 4:25-33

10 Landers JP (Ed.) (1994) Handbook of Capillary electrophoresis. CRC Press, Boca Raton

11 Weinberger R (2000) Practical capillary electrophoresis. Academic Press, San Diego

12 Bergholdt AB, Lehmann SV (1998) Chirality 10:699-705

13 Chu Q, Fu L, Guan Y, Ye J (2005) J Sep Sci 28:234-238

14 Wuersig A, Kuban P, Khaloo SS, Hauser PC (2006) Analyst 131**:**944-949

15 Opekar F, Coufal P, Stulik K (2009) Chem Rev 109:4487-4499

16 Henchoz Y, Schappler J, Geiser L, Prat J, Carrupt PA, Veuthe JL (2007) Anal Bioanal Chem 389:1869-1878

17 Matysik FM, Neusüß C, Pelzing M (2008) Analyst 133**:**1764-1766

18 Breadmore MC (2012) J Chromatogr A 1221:42-55

19 Grundmann M, Matysik FM (2012) Anal Bioanal Chem 404:1713-1721

20 Zhang T, Fang Q, Du WB, Fu JL (2009) Anal Chem 81:3693-3698

21 Matysik FM (2000) Anal Chem 72:2581-2586

22 Riekkola ML (2002) Electrophoresis 23:3865-3883

23 Engelhardt H, Beck W, Schmitt T (1994) Kapillarelektrophorese. Vieweg, Braunschweig

24 Lauer HH, Rozing GP (2009) High performance Capillary Electrophoresis. Agilent Technologies, Waldbronn

25 Kopplin PS (2008) Capillary electrophoresis: Methods and Protocols. Humana Press, New Jersey

26 Manz A, Graber N, Widmer HM (1990) Sens Actuators B 1:244-248

27 Manz A, Harrison D, Verpoorte E, Fettinger J, Paulus A, Lüdi H, Widmer HM (1992) J Chromatogr A 593: 253-258

28 Henry CS (ed) (2006) Microchip Capillary Electrophoresis. Methods and Protocols. Humana Press, New Jersey

29 Rios A, Escarpa A, Simonet B (2009) Miniaturization of Analytical Systems. Wiley, Chichester

30 Castaño-Álvarez M, Fernandez-Abedul M, Costa-Garcia A, Agirregabiria M, Fernandez LJ, Ruano-Lopez JM, Barredo-Presa B (2009) Talanta 80:24-30

31 Lunte SM, Hulvey MK, Fischer DJ, Kuhnline CD (2010) Encyclopedia of Analytical Chemistry, Wiley, Chichester

32 Escarpa A, González MC, López Gil MA, Crevillén AG, Hervás M, García M (2008) Electrophoresis 29:4852-4861

33 Arora A, Simone G, Salieb-Beugelaar GB, Kim JT, Manz A (2010) Anal Chem 82:4830-4847

34 Lacher NA, Garrison KE, Martin RS, Lunte SM (2001) Electrophoresis 22:2526-2536

35 Jorgenson JW, Lukacs KD (1981) Anal Chem 53:1298-1302

36 Matysik FM (2010) Anal Bioanal Chem 397:961-965

37 Vandaveer WR, Pasas SA, Martin RS, Lunte SM (2002) Electrophoresis 23:3667-3677

38 Nyholm L (2005) Analyst 130:599-605

39 Zhong M, Lunte SM (1996) Anal Chem 68:203-207

40 Fu CG, Fang ZL (2000) Anal Chim Acta 422:71-79

41 Cao X, Fang Q, Fang ZL (2004) Anal Chim Acta 513:473-479

42 Wang W, Zhou F, Wu W (2009) Microchim Acta 166:35-39

43 Seiman A, Jaanus M, Vaher M, Kaljurand M (2009) Electrophoresis 30:507-514

44 Kappes T, Hauser PC (1998) Anal Commun 35:325-329

45 Kappes T, Schnierle P, Hauser PC (1999) Anal Chim Acta 393:77-82

46 Kappes T, Galliker B, Schwarz MA, Hauser PC (2001) TrAC 20:133-139

47 Opekar F, Stulik K (2011) Electrophoresis 32:795-810

48 Hutchinson JP, Johns C, Breadmore MC, Hilder EF, Guijt RM, Lennard C, Dicinoski G, Haddad PR (2008) Electrophoresis 29:4593-4602
49 Lee M, Cho K, Yoon D, Yoe DJ, Kang SH (2010) Electrophoresis 31:2787-2795
50 Kaigala GV, Bercovici M, Behnam M, Elliot D, Santiago JG, Backhouse CJ (2010) Lab Chip 10:2242-2250
51 Kohler I, Schappler J, Rudaz S (2012) Anal Bioanal Chem 405:125-141
52 Kataoka H (2005) Curr Pharm Anal 1:65-84
53 do Rosario PM, Nogueira JM (2006) Electrophoresis 27:4694-4702
54 Ashri NY, Abdel-Rehim M (2011) Bioanalysis 3:2003-2018
55 Abdel-Rehim M (2010) J Chromatogr A 1217:2569-2580
56 Morales-Cid G, Cárdenas S, Simonet BM, Valcárcel M (2009) Electrophoresis 30:1684-1691
57 Morales-Cid G, Cárdenas S, Simonet BM, Valcárcel M (2009) Anal Chem 81:3188-3193
58 Jooß K, Sommer J, Bunz S, Neusüß C (2013) Electrophoresis 35:1236-1243
59 Hernandez E, Benavente F, Sanz-Nebot V, Barbosa J (2007) Electrophoresis 28:3957-3965
60 Medina-Casanellas S, Benavente F, Barbosa J, Sanz-Nebot V (2012) Anal Chim Acta 717:134-142
61 Pedersen-Bjergaard S, Rasmussen KE (1999) Anal Chem 71:2650-2656
62 Bjorhovde A, Halvorsen TG, Pedersen-Bjergaard S, Rasmussen KE (2003) Anal Chim Acta 491:155-161
63 Jiang X, Basheer C, Zhang J, Lee HK (2005) J Chromatogr A 1087:289-294
64 He Y, Lee HK (1997) Anal Chem 69:4634-4640
65 Jeannot MA, Cantwell FF (1997) Anal Chem 69:235-239
66 Theis AL, Waldack AJ, Hansen SM, Jeannot MA (2001) Anal Chem 73:5651-5658
67 Jermak S, Pranaityte B, Padarauskas A (2006) Electrophoresis 27:4538-4544
68 Kumar A, Burns J, Hoffmann W, Demattio H, Malik AK, Matysik FM (2011) Electrophoresis 32:920-925
69 Choi K, Kim J, Jang YO, Chung DS (2009) Electrophoresis 30:2905-2911
70 Yangcheng L, Quan L, Guangsheng L, Youyuan D (2006) Anal Chim Acta 566:259-264
71 Choi J, Choi K, Kim J, Ahmed AY, Al-Othman ZA, Chung DS (2011) J Chromatogr A 1218:7227-7233

72 Kuldvee R, Kaljurand M (1999) Critical Rev in Anal Chem 29:29-68
73 Kulp M, Vaher M, Kaljurand M (2005) J Chromatogr A 1100:126-129
74 Woods LA, Powell PR, Paxon TL, Ewing AG (2005) Electroanalysis 17:1192-1197
75 Matysik FM (2006) Electrochem Comm 8:1011-1015
76 Backofen U, Hoffmann W, Matysik FM (1998) Anal Chim Acta 362:213-220
77 Backofen U, Matysik FM, Hoffmann W, Ache HJ (1997) Chemical and Biological Sensors and Analytical Electrochemical Methods. The Electrochemic Soc, Pennington
78 Malik AK, Grundmann M, Matysik FM (2013) Talanta 116:559-562
79 Grundmann M, Rothenhöfer M, Bernhardt G, Buschauer A, Matysik FM (2012) Anal Bioanal Chem 402:2617-2623
80 Gross JH (2011) Mass spectrometry. A textbook. Springer, Heidelberg, Germany
81 Smith RD, Olivares JA, Nguyen NT, Udseth HR (1998) Anal Chem 60:436-441
82 Bonvin G, Schappler J, Rudaz S (2012) J Chromatogr A 1267:17-31
83 Kolch W, Neusüß C, Pelzing M, Mischak H (2005) Mass Spectrom Rev 24:959-977
84 Rabilloud T, Chevalle M, Luche S, Lelong C (2010) J Proteomics 73:2064-2077
85 Kler PA, Posch TN, Pattky M, Tiggelaar RM, Huhn C (2013) J Chromatogr A 1297:204-212
86 Mellors JS, Black WA, Chambers AG, Starkey JA, Lacher NA, Ramsey JM (2013) Anal Chem 85:4100-4106
87 Dallüge J (2003) Multidimensionality in capillary gas chromatography. Leipzig, Germany
88 Wallingford RA, Ewing AG (1987) Anal Chem 59:1762-1766
89 Matysik FM (2008) Microchim Acta 160:1-14
90 Wang J, Chen G, Chatrathi MP, Wang M, Rinehart R, Muck A (2008) Electroanalysis 20:2416-2421
91 Quaiserová-Mocko V, Novotny M, Schaefer LS, Fink GD, Swain GM (2008) Electrophoresis 29:441-447
92 Mukherjee J, Kirchhoff JR (2009) Anal Chem 81:6996-7002
93 Pelaez-Cid A, Blasco-Sancho S, Matysik FM (2008) Talanta 75:1362-1368
94 Chu Q, Jiang L, Tian X, Ye J (2008) Anal Chim Acta 606:246-251
95 Martin LG, Jongwana LT, Crouch AM (2010) Electrochim Acta 55:4303-4308
96 Zheng L, Zhang L, Tong P, Zheng X, Chi Y, Chen G (2010) Talanta 81:1288-1294
97 Li X, Zhu D, You T (2011) Electrophoresis 32:2139-2145

98 Zhang ZX, Zhang XW, Zhang SS (2009) Anal Biochem 387:171-177
99 Yuan B, Zheng C, Teng H, You T (2010) J Chrom A 1217:171-174
100 Yang Z, Wang H, Zhang W, Wang Q, He P, Fang Y (2012) Chromatographia 75:297-304
101 Yang Z, Li Z, Zhu J, Wang Q, He P, Fang Y (2010) J of Sep Science 33:1312-1317
102 Hulvey MK, Frankenfeld CN, Lunte SM (2010) Anal Chem 82:1608-1611
103 Vazquez M, Frankenfeld C, Coltro WKT, Carrilho E, Diamond D, Lunte SM (2010) Analyst 135:96-103
104 Omiatek DM, Santillo MF, Heien ML, Ewing AG (2009) Anal Chem 81:2294-2302
105 Bowen AL, Martin SR (2009) Electrophoresis 30:3347-3354
106 Li X, Pan J, Yang F (2011) Microchim Acta 174:123-130
107 Lin KW, Huang Y, Su H, Hsieh Y (2008) Anal Chim Acta 619:115-121
108 Kovachev N, Canals A, Escarpa A (2010) Anal Chem 82:2925-2931
109 Piccin E, Dossi N, Cagan A, Carrilho E, Wang J (2009) Analyst 134:528-532
110 Kuban P, Hauser PC (2008) Anal Chim Acta 607:15-29
111 Mori M, Kaseda M, Yamamoto T, Yamada S, Itabashi H (2012) Anal Bioanal Chem 402:2425-2430
112 Doan TKO, Kuban P, Kiplagat IK, Bocek P (2011) Electrophoresis 32:464-470
113 Duska F, Tuma P, Mokrejs P, Kubena A, Andel A (2007) Clin Nutrition 26:552-558
114 Belin GK, Krähenbühl S, Hauser PC (2007) Journal of Chrom B 847:205-209
115 Epple R, Blanes L, Beavis A, Roux C, Doble P (2010) Electrophoresis 31:2608-2613
116 Mantim T, Nacapricha D, Wilairat P, Hauser PC (2012) Electrophoresis 33:388-394
117 Strieglerova L, Kuban P, Bocek P (2011) J Chromatogr A 1218:6248-6254
118 Tuma P, Malkova K, Samcova E, Stulik K (2011) Anal Chim Acta 698:1-5
119 Petru K, Jac P, Luzova V, Kunes J, Polasek M (2011) Electrophoresis 32:890-895
120 Mai TD, Schmid S, Müller B, Hauser PC (2010) Anal Chim Acta 665:1-6
121 Petru K, Jac P, Sindelkova M, Polasek M (2011) J Sep Science 34:1174-1179
122 El-Attug MN, Hoogmartens J, Adams E, Van Schepdael A (2012) J Pharmaceutical Biomedical Analysis 58:49-57
123 El-Attug MN, Adams E, Hoogmartens J, Van Schepdael A (2011) J Sep Science 34:2448-2454
124 Schuchert-Shi A, Hauser PC (2008) Anal Biochem 376:262-267

125 Kuban P, Hauser PC (2008) Lab Chip 8:1829-1836
126 Mahabadi KA, Rodriguez I, Lim CY, Maurya DK, Hauser PC, de Rooij NF (2010) Electrophoresis 31:1063-1070
127 Zhao J, Chen Z, Li X, Pan J (2011) Talanta 85:2614-2620
128 Ding Y, Rogers K (2010) Electrophoresis 31:2602-2607
129 Míka J, Opekar F, Coufal P, Štulík K (2009) Anal Chim Acta 650:189–194
130 Brito-Neto JGA, da Silva JAF, Blanes L, do Lago CL (2005) Electroanalysis 17:1198-1206
131 Kubáň P, Hauser PC (2004) Electrophoresis 25:3387–3394
132 da Silva JAF, do Lago CL (1998) Anal Chem 70:4339–4343
133 Mendoca KJ, do Lago CL (2009) Electrophoresis 30:3458-3464
134 MicroTOF user manual Version 1.1, Bruker Daltonik GmBH, Bremen
135 Jeannot MA, Przyjazny A, Kokosa JM (2010) J Chromatogr A 1217:2326-2336
136 Opekar F, Štulík K (2006) Electroanalysis 18:1282–1288
137 Kubáň P, Müri MA, Hauser PC (2004) Analyst 129:82–86
138 Kubáň P, Pelcová P, Kubáň V, Klakurková L, Dasgupta PK (2008) J Sep Sci 31:2745–2753
139 Tůma P, Opekar F, Štulík K (2002) Electrophoresis 23:3718–3724
140 Zemann AJ, Schnell E, Volgger D, Bonn GK (1998) Anal Chem 70:563–567
141 Fishman HA, Nabeel MA, Lee TT, Scheller RH, Zare RN (1994) Anal Chem 66:2318-2329
142 Wallenborg SR, Nyholm L, Lunte CE (1999) Anal Chem 71:544-549
143 Matysik FM (1998) Electrochim Acta 43:3475-3482

9. Appendix

9.1. Development of a portable CE device

From the experiences gained with the lab-built automated system with vertically aligned capillaries it was possible to construct an own miniaturized and portable CE system.

9.1.1 Instrumental development

Overall setup

The device is comprised of a micromachined head part integrating the electrochemical cell for amperometric detection, the C^4D detector, the drilled holes for camera alignment and the HV-voltage ground lead. In the middle part are the up-and-down-moveable sample tray and the HV-electrode in the moveable sampling arm. The HV-supply was integrated into the sidewall and safely packed into a PVC-housing. The lower part consists of the electronics and the motors for the autosampling tray and the HV-source controls. The base of the device was formed by a 12 x 12 x 1 cm machined piece of PVC. The rear wall and side walls (also made from PVC) were fitted to the ground plate with Nylon screws. The 26 cm high and 5 kg light device enables the use of a minimum capillary length of 3 cm and a maximum of 15 cm. The front of the device is covered with a Plexiglas board and equipped with a magnetic safety interlock. The fused silica capillaries with IDs ranging from 2 to 100 µm (Polymicro, Phoenix, AZ) were easily cut to the appropriate lengths with a ceramic blade knife. The mini-USB module UM2012 (ELV, Leer, Germany) was used for connection to computers. For galvanic separation an ADUM4160 module from AnalogDevices (Norwood, MA, USA) was used. The device can be powered from the mains power supply with a 12 V / 1 A mains adapter or via respective adapter pieces from either a 12 V battery pack or a 12 V car battery.

High-voltage

A miniaturized HV module EMCO C80 that enabled application of maximum 8 kV of each polarity was obtained from EMCO HighVoltage Corporation (Sutter Creek, CA, USA). It was tightly screwed into a milled cavity in the center of the sidewall. Through microdrilled channels in the wall the wires for the HV-application run to the head part (ground connection of the cell) and the injection arm. At the injection end the capillary was guided through a stainless steel needle which acts as high voltage electrode. The platinum HV ground electrode of the electrochemical cell was connected via a copper coil spring contact.

Detection

The amperometric detection was carried out with the electrochemical cell (EC) described in section 4.3.1. For data acquisition a µStat 200 bipotentiostat from Metrohm (Herisau, Switzerland) was used. The interval time of current measurements for amperometric recording was 0.05 s. The pretreatment of the electrode before each run was done by applying a 3 s cathodic pulse of -1.0 V and a 3 s anodic pulse of +2.0 V. The working electrodes used were as described in section 4.5.3. The EC was inserted into a micromachined cavity in the detection block. The C^4D unit (see section 4.2.4) was placed into a cavity in the detection block right underneath the EC. The tip of the WE, the separation capillary and the insertion hole of the C^4D detector were vertically in line. The detection block was furthermore furnished with two holes fitting the tube of the purpose-made microscope camera (DNT, Dietzenbach, Germany). Thus, the alignment of electrode-to-capillary in the EC could easily be carried out without need for additional clamps or fittings. A light source inserted to the respective hole where the camera is not situated enabled sufficient illumination for the alignment process.

Sampling and controls

The injection system consisted of a stepper motor (Reichelt, Sande, Germany) and a servomotor (model ES-07, Conrad Electronics, Wernberg, Germany) which were both controlled via PSOC3 firmware. The control of the stepper motor was accomplished with an iSMT module from ELV (Leer, Germany). The motors were moving a purpose-built sampling tray of 10 cm OD with 18 vials of 100 µL capacity. The stepper motor moved the round-tray radially whereas the servomotor lifted it up and down towards or away from the inlet of the separation capillary. The sampling tray was set into a PVC-board which could be manually moved up and down in *z*-direction, according to the respectively used capillary length. On top of this PVC-board was the injection arm fixed. It could be moved to the side in cases where TOF-MS measurements with especially short capillaries were desired. For ECD applications it acted as holder for HV-electrode and capillary. Also attached to this board were the motors. Underneath the motors were the purpose-made conductor boards for control of sampling tray, HV source and detection units. The power supply was also regulated from there.

9.1.2 Microsampler Control Software for Portable CE-device

The portable CE was computer-controlled via a graphical user interface, enabling total control of all device components and measurement parameters. The software was designed and developed with LabView 2009. Its details and utilization are described in this section.

User interface

The software user interface for complete control of the portable CE device is shown in Figure A1**.** An overview of the run sequence is given in the top section of the interface (A). The tabs (B) for sequence or machine control allow entering of the respective run sequences (Sequence control) and for more control over the sampler, starting points and lift height (machine controls) can be set. The actual run table (C) allows adjustment of the desired run parameters. Compared to the autosampling software (section 4.4.2) the parameters for both injection and separation are entered in one single row. An overview of the possible parameters and their description is given in Table A1. The sketched illustration (D) of the total device shows the voltage currently applied and the remaining run time during an individual separation.

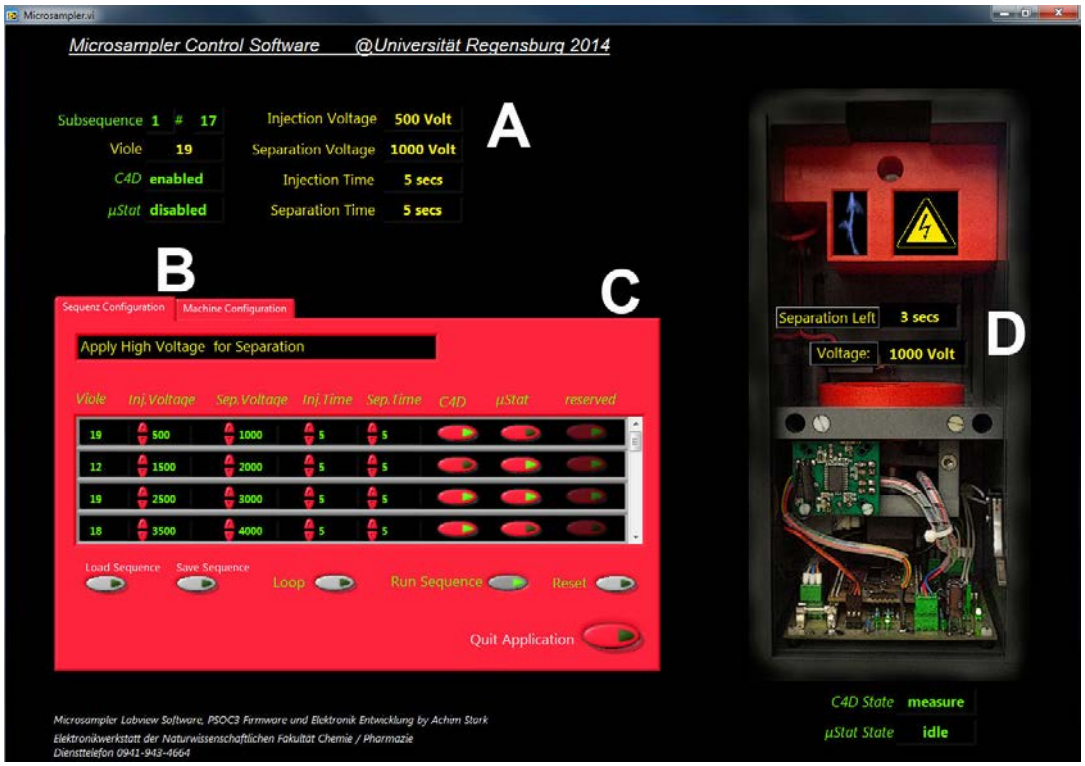

Figure A1. Software MicrosamplerControl user interface **A** Overview of current run sequence details **B** Tabs for sequence or machine configuration **C** Actual sequence table **D** Current run status (time left and applied HV)

Table A1. Functions of the job list's columns

Column	Function
Vial	Position of the respective vial for the executed step
Inj. Voltage	Voltage application for injection (0 to 8000 V)
Sep. voltage	Applicable separation voltage for this sequence (0 to 8000 V)
Inj. time	Chosen length of injection
Sep. time	Time period for application of high voltage
C^4D	Enable / Disable simultaneous triggering of C^4D detection unit with HV sep. start
µStat	Enable / Disable simultaneous triggering of amperometric detection
Reserved	Empty for optional column (potentially as TOF-MS trigger)

9.1.3 Final design and performance

The most important construction goals like light-weight and small overall dimensions were achieved while at the same time integrating various detection schemes into the mobile device. The handling was quite straightforward and the steps to carry out an individual measurement are shown in Table A2. In order to obtain reproducible CE-AD measurements the alignment of capillary-to-detection electrode was essential (step 6).

Table A2. Overview of steps to carry out a measurement with the portable CE device

Step	Description	Parameters	Instrument
1	Fix separation capillary into the EC	-	EC
2	Put C^4D into corresponding cavity	-	C^4D
3	Adjust injection board to capillary length	3 to 15 cm length	P-CE
4	Introduce capillary through detector block and C^4D		EC
5	Make sure capillary end and HV electrode are plane		P-CE
6	Align capillary-to-electrode in x, y & z-direction		Camera
7	Start device		P-CE
8	Initiate software and sampler		PC
9	Fill in buffer and samples		P-CE
10	Enter injection parameters in run table	Inj HV / Inj t	PC
11	Enter run parameters	Sep HV / Sep. time	PC
12	Initiate measurement		PC / P-CE

In the final design, the device appeared as illustrated in Figure A2. The C^4D unit, as well as the amperometric detector, were not fixed to the device and could be easily used otherwise. Potential danger for the user from high-voltage was eliminated by a magnetic safety interlock connected to the Plexiglas-front board. The alignment of capillary and electrode within the device was tested successfully and the whole process is much faster than with previous

setups. The reason was that no additional equipment was necessary to hold the camera or adjust the right distance from window to camera lens.

Figure A2. Front and backside of the lab-developed and –built portable CE device.

The device integrated a lot of functions of a bench-top device in a smaller housing (as it can be seen in the comparison in Figure A3). One important feature was the ability to run the device from batteries or car batteries. This was tested successfully in a remote location with a conventional 12 V car battery and the according adapter pieces.

Figure A3. Comparison of the dimensions of a bench-top CE –device with integrated DAD detector (left) and the portable CE device featuring dual-electrochemical detection.